Innovation, Sciences et Développement économique Canada
Office de la Propriété Intellectuelle du Canada

Innovation, Science and Economic Development Canada
Canadian Intellectual Property Office

CA 3149871 A1 2015/05/28

(21) 3 149 871

(12) DEMANDE DE BREVET CANADIEN
CANADIAN PATENT APPLICATION

(13) A1

(22) Date de dépôt/Filing Date: 2014/11/19

(41) Mise à la disp. pub./Open to Public Insp.: 2015/05/28

(62) Demande originale/Original Application: 2 930 606

(30) Priorités/Priorities: 2013/11/20 (US61/906,738);
2014/11/19 (US14/547,771)

(51) Cl.Int./Int.Cl. *A61K 31/167* (2006.01),
A61P 43/00 (2006.01)

(71) Demandeur/Applicant:
OHIO STATE INNOVATION FOUNDATION, US

(72) Inventeurs/Inventors:
CHEN, CHING-SHIH, US;
BEKAII-SAAB, TANIOS, US;
GUTTRIDGE, DENIS, US;
MARCUCCI, GUIDO, US;
KULP, SAMUEL, US;
TSENG, YU-CHOU, US

(74) Agent: ROBIC

(54) Titre : INHIBITEURS DE HDAC POUR SUPPRIMER LA CACHEXIE LIEE AU CANCER
(54) Title: METHODS FOR SUPPRESSING CANCER-RELATED CACHEXIA

(57) Abrégé/Abstract:
Methods of suppressing cachexia in a mammal with cancer comprising administering HDAC inhibitors are provided. Aspects include methods of administering an HDAC class 1 and 2b inhibitor in an amount effective to substantially maintain the mammal's weight compared to a mammal that does receive the HDAC class 1 and 2b inhibitor.

ABSTRACT

Methods of suppressing cachexia in a mammal with cancer comprising administering HDAC inhibitors are provided. Aspects include methods of administering an HDAC class 1 and 2b inhibitor in an amount effective to substantially maintain the mammal's weight compared to a mammal that does receive the HDAC class 1 and 2b inhibitor.

Date Reçue/Date Received 2022-02-22

METHODS FOR SUPPRESSING CANCER-RELATED CACHEXIA

PRIORITY CLAIM

[0001] Intentionally left blank

BACKGROUND

[0002] Cancer-related cachexia is a debilitating condition associated with loss of muscle mass, fatigue, weakness, and loss of appetite in cancer patients. Cachexia is also associated with severe clinical consequences including muscle weakness which can result in ambulation difficulties, and pulmonary complications. Cachexia is a significant contributing factor in the death of cancer patients.

[0003] Cachexia is characterized by depletion of skeletal muscle mass that is not reversed by conventional nutritional support, leading to pronounced weight loss that severely impacts patient morbidity and mortality. It occurs in more than 80% of patients with gastric, pancreatic, and esophageal cancer; 70% of those with head and neck cancer; and approximately 60% of patients with lung, colorectal, and prostate cancer. See e.g., Muscle (2012) 3, 245-51. Despite cachexia's impact on mortality among cancer patients, no effective therapies have been developed to prevent or impede the progression of cachexia. For example, more than 85% of pancreatic cancer patients, including early stage patients, are estimated to lose an average of 14% of their pre-illness weight. See e.g., BMC Cancer. 2010 Jul 8;10:363. Cachectic pancreatic cancer patients are often weak and fatigued, and have a lower tolerance to therapy and more adverse outcomes to surgery. Consequently, cachexia is the main driver for mortality in pancreas cancer. Sadly, the 5-year survival rate for pancreatic cancer remains at 6% for the last four decades, which is the lowest among all malignancies.

[0004] With the advent of new tools to identify cachectic factors and their effects on skeletal muscle, the field of cachexia has recently made significant advances in understanding the underlying mechanisms that regulate muscle atrophy in cancer and other chronic illnesses. As a result, we now have an appreciation for how cytokines and systemic inflammation regulate muscle atrophy by acting on key signaling pathways that operate from inside the myofiber.

Date Reçue/Date Received 2022-02-22

However, translating these discoveries into effective therapies has been challenging, and, prior to the aspects described herein, an effective treatment for cachexia has been lacking.

[0005] Skeletal muscle mass is regulated, in part, by the relative rate of protein synthesis versus protein degradation. Alamdari, N, et al., Acetylation and deacetylation – novel factors in muscle wasting, Metabolism. Jan 2013; 62(1): 1–11. Loss of skeletal muscle mass occurs when the rate of protein degradation is greater than protein synthesis. Id. Protein acetylation and deacetylation modify transcription factors and gene transcription which may influence muscle mass by rendering proteins more or less susceptible to degradation. Id. Histone acetylases (HATs) and histone deacetylases (HDACs) play a role in regulating protein acetylation and deacetylation.

[0006] However, the effects of these molecules on muscle wasting and cachexia have proven to be contradictory – evidence suggests, for example, that use of HDAC inhibitors (e.g., Trichostatin A (TSA)) results in hyperacetylation which can increase protein degradation leading to increased muscle wasting and cachexia. Contradictory results were found by Narver et. al., (Sustained improvement of spinal muscular atrophy mice treated with trichostatin A plus nutrition. Ann Neurol. 2008; 64:465–70) however, these results have been questioned because treatment with TSA was also accompanied by aggressive nutritional support. Alamdari et al., at 5. Thus, HDAC inhibitors were thought to increase rather than decrease cachexia or their use produced conflicting and contradictory results.

[0007] The development and progression of cancer cachexia is caused by complex, multifactorial pathophysiological responses to tumors in muscle tissues. To date, no FDA-approved therapies are available to prevent or hamper the progression of muscle wasting in cachectic patients. To date, several investigational drugs, which target different aspects of cachexia pathogenesis, have undergone human trials, however, with different clinical outcomes. For example, while Novartis's BYM38 (bimagrumab), a mAb that blocks binding of myostatin and activin to type II activin receptors, received FDA breakthrough therapy designation, GTx's muscle wasting drug enobosarm, a selective androgen receptor modulator, failed in late-stage clinical trials.

[0008] Acetylation of core histones plays an important role in the regulation of gene transcription by controlling nucleosomal packaging of DNA. Deacetylation of histones results in

Date Reçue/Date Received 2022-02-22

tight packing of nucleosomes and transcriptional repression due to limited access of transcription factors to DNA targets. Histone acetylation relaxes nucleosome structures, providing greater access for transcription factors. The balance between histone deacetylation and acetylation is modulated by the histone deacetyl-transferases (HDACs) and histone acetyl-transferases (HAT). An abnormal balance of these factors is correlated with abnormal cell growth and several forms of cancer as discussed in U.S. Patent Number 8,318,808. HDAC inhibitors, in particular, change the balance between acetylation and deacetylation resulting in growth arrest, differentiation, and apoptosis in many tumor cell types. See e.g., U.S. Patent Number 8,318,808.

[0009] 18 HDACs have been identified in humans and are characterized as being zinc dependent or nicotinamide adenine dinucleotide (NAD) dependent (Discov Med 10(54):462-470, November 2010) and are associated with the following classes: class I (HDACs 1, 2, 3, and 8); class II (HDACs 4, 5, 6, 7, 9, and 10; class III (sirtuins 1-7 (SIRT)); and class IV (HDAC 11). Id.

[0010] Of particular interest herein are HDAC inhibitors described in U.S. Patent Number 8,318,808 and are based on, for example, fatty acids coupled with Zn^{2+}-chelating motifs through aromatic Ω-amino acid linkers. In various aspects, the HDAC inhibitors may have the formula:

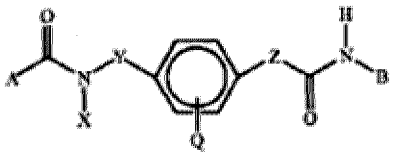

[0011] wherein X is chosen from H andCH3; Y is (CH2)n wherein n is 0-2; Z is chosen from (CH2)m wherein m is 0-3 and (CH)2; A is a hydrocarbyl group; B is o-aminophenyl or hydroxyl group; and Q is a halogen, hydrogen, or methyl. One HDAC inhibitor of particular (N-hydroxy-4-(3-methyl-2-phenyl-butyrylamino)-benzamide) is also known as AR-42. In one aspect, the structure of AR-42 is as follows:

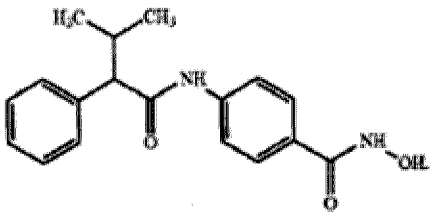

Date Reçue/Date Received 2022-02-22

[0012] AR-42 is a broad-spectrum deacetylase inhibitor of both histone and non-histone proteins with demonstrated greater potency and activity in solid tumors and hematological malignancies when compared to vorinostat (i.e., SAHA). See e.g., Lu YS, et al., Efficacy of a novel histone deacetylase inhibitor in murine models of hepatocellular carcinoma, Hepatology. 2007 Oct;46(4):1119-30; Kulp SK, et al., Antitumor effects of a novel phenylbutyrate-based histone deacetylase inhibitor, (S)-HDAC-42, in prostate cancer, Clin Cancer Res. 2006 Sep 1;12(17):5199-206.

[0013] AR-42 may also possess additional histone-independent mechanisms which contribute to its therapeutic profile. See e.g., Chen MC, et al., Novel mechanism by which histone deacetylase inhibitors facilitate topoisomerase IIα degradation in hepatocellular carcinoma cells, Hepatology. 2011 Jan;53(1):148-59; Chen CS, et al., Histone acetylation-independent effect of histone deacetylase inhibitors on Akt through the reshuffling of protein phosphatase 1 complexes, J Biol Chem. 2005 Nov 18;280(46):38879-87; Yoo CB, et al., Epigenetic therapy of cancer: past, present and future, Nat Rev Drug Discov. 2006 Jan;5(1):37-50.

[0014] AR-42 has a demonstrated inhibitory effect in tumors including, but not limited to, breast, prostate, ovarian, blood cell (e.g., lymphoma, myeloma, and leukemia), liver, and brain. See e.g., Mims A, et. al., Increased anti-leukemic activity of decitabine via AR-42-induced upregulation of miR-29b: a novel epigenetic-targeting approach in acute myeloid leukemia, Leukemia. 2012 Nov 26. doi: 10.1038/leu.2012.342. [Epub ahead of print]; Burns SS, et al., Histone deacetylase inhibitor AR-42 differentially affects cell-cycle transit in meningeal and meningioma cells, potently inhibiting NF2-deficient meningioma growth, Cancer Res. 2013 Jan 15;73(2):792-803; Lu YS, et. al., Radiosensitizing effect of a phenylbutyrate-derived histone deacetylase inhibitor in hepatocellular carcinoma, Int J Radiat Oncol Biol Phys. 2012 Jun 1;83(2); Zimmerman B, et. al., Efficacy of novel histone deacetylase inhibitor, AR42, in a mouse model of, human T-lymphotropic virus type 1 adult T cell lymphoma, Leuk Res. 2011 Nov;35(11):1491-7; Zhang S, et al., The novel histone deacetylase inhibitor, AR-42, inhibits gp130/Stat3 pathway and induces apoptosis and cell cycle arrest in multiple myeloma cells, Int J Cancer. 2011 Jul 1;129(1):204-13.

SUMMARY

Date Reçue/Date Received 2022-02-22

[0015] Aspects described herein provide methods of suppressing cachexia in a mammal with cancer comprising administering a HDAC class 1 and 2b inhibitor to said mammal. One aspect provides a method of suppressing cachexia in a mammal with cancer by administering a HDAC class 1 and 2b inhibitor to said mammal in an amount effective to substantially maintain the mammal's weight compared to a mammal that does not receive the HDAC class 1 and 2b inhibitor. In another aspect, the HDAC class 1 and 2b inhibitor is administered to a mammal with cancer in an amount effective to substantially maintain at least about 90% of said mammal's weight over a period of time of at least fifteen days. In another aspect, the HDAC class 1 and 2b inhibitor is AR-42. In yet another aspect, the mammal with cancer has at least one tumor and the tumor volume is not reduced by more than 6% during about the first fifteen days following treatment with AR-42.

[0016] Other aspects described herein provide methods of suppressing cachexia by administering AR-42 to a mammal with cancer wherein the expression of multiple mediators of muscle atrophy (e.g., pro-cachexia drivers such as IL-6, IL-6Rα, LIF, MuRF1, Atrogin-I) in cancer cachexia is reduced compared to a mammal having cancer that is not treated with AR-42.

[0017] Further aspects provide methods of suppressing cachexia by administering AR-42 to a mammal with cancer wherein cachexia-induced loss of adipose tissue and reduction in skeletal muscle fiber size is substantially restored compared to a mammal that does not receive AR-42.

[0018] Aspects described herein provide methods of maintaining skeletal muscle weight in a mammal having cancer by administering a HDAC class 1 and 2b inhibitor to said mammal in an amount effective to maintain at least about 90% of said mammal's skeletal muscle weight over a period of time of at least fifteen days compared to a mammal that does not receive the HDAC class 1 and 2b inhibitor.

[0019] Further aspects provide methods of prolonging survival of a mammal having cancer by administering a HDAC class 1 and 2b inhibitor to the mammal in an amount effective to substantially prolong survival of the mammal compared to a mammal that does not receive the HDAC class 1 and 2b inhibitor.

[0020] As disclosed herein, AR-42 shows *in vivo* efficacy in suppressing, reducing, or blocking muscle wasting and prolonging survival in animal models of cancer cachexia. In

Date Reçue/Date Received 2022-02-22

addition, the effect of AR-42 on cancer-related cachexia is independent of AR-42's effects on reducing tumor load.

[0020a] In a preferred embodiment, the application provides a histone deacetyl-transferase (HDAC) class 1 and 2b inhibitor for use in prolonging survival of a mammal having cancer, wherein the HDAC is used to substantially prolong survival of the mammal compared to a mammal that does not receive the HDAC class 1 and 2b inhibitor.

[0020b] In another preferred embodiment, the application provides a histone deacetyl-transferase (HDAC) class 1 and 2b inhibitor for use in the manufacture of a medicament in prolonging survival of a mammal having cancer, wherein the medicament is useful to substantially prolong survival of the mammal compared to a mammal that does not receive medicament.

BRIEF DESCRIPTION OF THE FIGURES

[0021] Figure 1A shows exemplary suppression of cancer-induced cachexia in C-26 tumor-bearing mice and depicts changes in total weight (*left*, tumor included) and body weight (*center*, tumor excluded) during the 15-day study in vehicle-treated tumor-free mice (Control) versus tumor-bearing mice treated with vehicle (Vehicle) or oral AR-42 at 50 mg/kg every other day (AR-42). Arrows indicate the times of AR-42 treatment. *Right*, lack of suppressive effect of AR-42 on tumor growth in C-26 tumor-bearing mice. Data are presented as means ± S.D. *P* values: a, 0.045; b, 0.0027; c, 0.049; d, 0.0048;

[0022] Figure 1B shows photographs of representative mice with tumor burdens from each group depicting the therapeutic effect of AR-42 on cancer cachexia;

[0023] Figure 1C shows an exemplary average daily diet consumption among the three treatment groups in the course of study. Data are presented as means ± S.D. (n = 8);

[0024] Figure 1D shows the exemplary effects of AR-42 on the weights of hindlimb muscles, including gastrocnemius, tibialis anterior, and quadriceps (*P* values: a, <0.001; b, 0.0042; c, 0.0046) in both tumor-free and tumor-bearing mice compared to those of vehicle-treated tumor-bearing and tumor-free mice (n = 8);

Date Reçue/Date Received 2022-02-22

[0025] Figure 1E shows the exemplary effects of AR-42 on heart, adipose tissue, and spleen (*P* values: a, <0.001; b, 0.0059; c, 0.001; d, 0.009) in both tumor-free and tumor-bearing mice compared to those of vehicle-treated tumor-bearing and tumor-free mice (n = 8);

[0026] Figure 2A shows exemplary preservation of muscle fiber size in C-26 tumor bearing mice depicting on the left, photomicrographs of H&E-stained sections of gastrocnemius muscles from tumor-free control mice and tumor-bearing mice treated with vehicle or AR-42. Scale bars, 100 μm and on the right, the cross-sectional areas of muscle fibers in gastrocnemius muscles represented as a frequency histogram with a significance of ($P < 0.001$). Data are presented as means ± S.D.;

[0027] Figure 2B shows exemplary Kaplan-Meier survival curves for tumor-bearing mice treated with vehicle, vorinostat (50 mg/kg, p.o., daily), romidepsin (0.6 mg/kg, i.p., twice weekly), or AR-42 (50 mg/kg. p.o., every other day). Survival was defined as the time at which loss of body weight (tumor excluded) reached 20% of starting body weight, which served as a humane endpoint for removal from the study (*, $P < 0.001$, vehicle vs. AR-42; n = 8);

[0028] Figure 2C shows exemplary photographs of representative mice from each group depicting the therapeutic effect of AR-42 versus vorinostat and romidepsin on cancer cachexia in tumor-bearing mice, as manifested by posture, haircoat and body condition;

[0029] Figure 2D shows exemplary relative mRNA expression levels of Atrogin-1//MAFbx and MuRF1 in the skeletal muscles of vehicle-treated tumor-free mice (n = 6) and tumor-bearing mice treated with AR-42 (n = 8), vorinostat (n = 8), or romidepsin (n = 5) compared to that of vehicle-treated tumor-bearing mice (n = 8) at 15 days after tumor cell injection. Data are presented as means ± S.D. *P* values: a, <0.001; b, 0.016; c, 0.0063;

[0030] Figure 3A shows exemplary effects of AR-42 on the levels of intermediates associated with glycolysis and alternative pathways of glucose metabolism;

[0031] Figure 3B shows exemplary effects of AR-42 on glycogen metabolism in gastrocnemius muscles from tumor-free and tumor-bearing mice (n = 8 for each group). Tumor-bearing mice were treated with vehicle or AR-42 (50 mg/kg, p.o., every other day) beginning at day 6 post-tumor cell injection and ending at day 17. Tumor-free control mice were treated with vehicle or AR-42 in parallel. Data are presented in box-and-whisker plots. The bottom and top

Date Reçue/Date Received 2022-02-22

of the box represent the first and third quartiles, and the "+" symbol and the band inside the box denote the mean and median values, respectively. The ends of the whiskers represent the maximum and minimum values in each group;

[0032] Figure 4 shows that AR-42 blocks cachexia-induced changes in the levels of free amino acids and amino acid metabolites involved in regulating neurotransmission, and biomarkers of insulin resistance in the muscles of C-26 tumor-bearing mice. Samples for analysis were generated from the experiment described with respect to Figures 3A and 3B. Data are presented in box-and-whisker plots as described with respect to Figures 3A and 3B;

[0033] Figure 5A shows exemplary (upper) effects of AR-42 on the levels of the pro-cachexia cytokines IL-6 (left) and LIF (right) in the sera of tumor-free versus C-26 tumor-bearing mice and (lower) qPCR analysis of the effects of AR-42 on the mRNA expression of *IL-6Ra* in skeletal muscle of tumor-free versus C-26 tumor-bearing mice. Data are presented as means ± S.D. *P* values: a, <0.001; b, 0.006; c, 0.012 (n = 3). Mice were treated as described with respect to Figure 3;

[0034] Figure 5B shows exemplary principle component analysis of RNA-seq data (left) and Venn diagram (right) showing differentially expressed genes among the four treatment groups. TF, tumor-free; T, tumor-bearing; veh, vehicle-treated; AR, AR-42-treated. Mice were treated as described with respect to Figure 3;

[0035] Figure 5C shows exemplary analysis of the effects of AR-42 on the transcript levels of six key pro-cachexia drivers by RNA-seq (*P* values: a, 0.024; b, 0.028; c, 0.015; d, 0.007; e, 0.024; f, 0.026; g, 0.01; h, 0.012; i, <0.001; j, 0.014; n = 3). Mice were treated as described with respect to Figure 3;

[0036] Figure 5D shows exemplary analysis of the effects of AR-42 on the transcript levels of six key pro-cachexia drivers by qPCR in skeletal muscle of mice in the four treatment groups (*, $P < 0.001$; n = 6). Data are presented as means ± S.D. Mice were treated as described with respect to Figure 3;

[0037] Figure 6A shows suppression of cancer cachexia in C-26 tumor-bearing mice by delaying treatment with AR-42 until late stages of tumor and cachexia. Changes in body weight (tumor excluded) in the course of 18-day study in vehicle-treated tumor-free control mice (T/F,

Date Reçue/Date Received 2022-02-22

Veh) and tumor-bearing mice treated with vehicle (T, Veh) versus those treated with oral AR-42 (shown on the left) starting at day 6 (T, AR42/D6), day 10 (T, AR42/D10), or day 12 (T, AR42/D12). *P* values: a, 0.0015; b, 0.023 (n = 8). Arrows indicate the time points for the start of AR-42 treatment. Data are presented as means. For clarity of presentation, the S.D. bars for each data point are not shown. On the right are results showing the lack of suppressive effect of AR-42 on tumor growth in C-26 tumor-bearing mice in the delayed treatment experiment. Data are presented as means ± S.D. (n = 8);

[0038] Figure 6B shows exemplary photographs depicting the therapeutic effect of AR-42 on cancer cachexia in tumor-bearing mice, despite delayed treatment, as manifested by normal posture, smooth haircoat and better body condition, despite large tumor burdens;

[0039] Figure 6C shows the exemplary effects of AR-42 treatment, initiated at different stages of disease progression as described in Figure 6A, on the weights of hindlimb muscles, including gastrocnemius, tibialis anterior, and quadriceps, in C-26 tumor-bearing mice. Data are presented as means ± S.D. (n = 8; *, $P < 0.001$);

[0040] Figure 6D shows the effects of AR-42 on grip strength of tumor-bearing mice relative to the vehicle-treated tumor-free and tumor-bearing controls at day 15 and day 16. Data are presented as means ± S.D. (n = 8; *P* values: a, 0.01; b, 0.022; c, <0.001; d, 0.0019). N, Newtons;

[0041] Figure 7 shows that AR-42 protects against cancer-induced muscle wasting in the LLC mouse model of cachexia. Exemplary effects of AR-42 versus vehicle on the mass of hindlimb muscles, including gastrocnemius, tibialis anterior, and quadriceps, in both tumor-free and tumor-bearing mice compared to that of vehicle-treated tumor-bearing mice are shown. Mice were treated in the same manner as described in Figure 1A, except that mice were sacrificed at day 20 after tumor cell injection. Data are presented as means ± S.D. (n = 8);

TABLES

Date Reçue/Date Received 2022-02-22

[0041a] Table 1

Supplementary Table 1. Sequences of primers used for real-time RT-PCR

Target	Primer pairs (5' → 3')	
ATGL (*PNPLA2*)	AACACCAGCATCCAGTTCAA	GGTTCAGTAGGCCATTCCTC
Atrogin-1 (*Fbxo32*)	CACATTCTCTCCTGGAAGGGC	TTGATAAAGTCTTGAGGGGAAAGTG
Foxo1	TTCAATTCGCCACAATCTGTCC	GGGTGATTTTCCGCTCTTGC
GAPDH	CATGGCCTTCCGTGTTCCTA	GCGGCACGTCAGATCCA
IL-6Rα	CTCCCGGTGGCCCAGTACCA	TGCACTGGGGCGAGGACACT
Mef2c	GCTGTTCCAGTACGCCAGCAC	AGTGCGTGGGGTGAGTGCATAA
MuRF1 (*Trim63*)	CACGAAGACGAGAAGATCAACATC	AGCCCCAAACACCTTGCA
UCP3	CCAACATCACAAGAAATGC	TACAAACATCATCACGTTCC

Date Reçue/Date Received 2022-02-22

[0041b] Table 2

Table2. IPA of differentially expressed genes (≥4-fold) related to muscle disease or functions between AR-42- and vehicle-treated C-26 tumor-bearing mice (n = 6)

RefSeq ID	Gene ID	Log2 fold change	P value	Description	Disease or function annotation
Upregulated by AR-42					
NM_024291	Ky	4.3	0.0004	Kyphoscoliosis peptidase	Muscle development
NM_010267	Gdapl	4.2	0.0004	Ganglioside-induced differentiation-associated-protein 1	Muscle atrophy; myopathy
NM_013569	Kcnh2	4.1	0.0004	Potassium voltage-gated channel, subfamily H, member 2	Muscle atrophy; myopathy
NM_009608	Actc1	3.9	0.0004	Actin, alpha, cardiac	Muscle development and morphology; myopathy; muscle cell death
NM_183408	Pde4a	3.7	0.0004	Phosphodiesterace 4A, cAMP specific	Myopathy
NM_022322	Tnmd	3.5	0.0004	Tenomodulin	Muscle morphology
NM_013803	Casr	3.5	0.0004	Calcium-sensing receptor	Muscle cell death
NM_008596	Sypl2	3.5	0.0004	Synaptophysin-like 2	Muscle contractility, development, and morphology; skeletal muscle cell size
NM_010518	Igftop5	3.3	0.0004	Insulin-like growth factor binding protein 5	Muscle development; skeletal muscle mass
NM_008876	Pld2	3.2	0.0191	Phospholipase D2	Muscle cell death
NM_080440	Sk8a3	3.2	0.0004	Solute carrier family 8 (sodium/calcium exchanger), member 3	Muscle cell death
NM_198190	Ntf5	3.2	0.0004	Neurotrophin 5	Muscle development
NM_001170537	Mef2c	2.9	0.0004	Myocyte enhancer factor 2C	Muscle contractility and development;
NM_176848	Fbxo2	2.8	0.0004	F-box protein 2	Protein catabolism
NM_022027	Synel	2.7	0.0004	Synaptic nuclear envelope 1	Muscle development function, and morphology; myopathy
NM_009255	Serpine2	2.6	0.0004	Serine (or cysterine) peptidase inhibitor, clade F, member 2	Protein catabolism
NM_001256224	Wnt5a	2.6	0.0011	Wingless-related MMTV integration site 5A	Protein catabolism
NM_134028	Tubg2	2.6	0.0004	Tubulin, gamma 2	Myopathy

Date Reçue/Date Received 2022-02-22

NM_021508	Myox1	2.5	0.0004	Myoxenin 1	Muscle development and morphology, skeletal muscle mass and cell size
NM_110361	Cflar	2.5	0.0004	CASP8 and FADD-like apoptosis regulator	Muscle morphology
NM_178608	Reepl	2.3	0.0004	Receptor accessory protein 1	Myopathy
NM_001252455	Ptprs	2.3	0.0004	Protein tyrosine phosphatase, receptor type, S	Muscle morphology, myopathy
NM_013491	Clcn1	2.3	0.0004	Chloride channel 1	Muscle function
NM_008305	Hspg2	2.3	0.0004	Perlecan (heparan sulfate proteoglycan 2)	Muscle development and morphology
NM_025358	Ndnfa9	2.3	0.0004	NADH dehydrogenase (ubiquinone) 1 alpha subcomplex 9	Myopathy
NM_011436	Sort1	2.3	0.0004	Sortilin-related receptor, LDLR class A repeats-containing	Muscle function
NM_001243009	Col6a3	2.3	0.0004	Collagen, type VI, alpha 3	Muscle development; myopathy
NM_025343	Rmnd1	2.3	0.0200	Required for meiotic nuclear division 1 homolog (S. cerevisiae)	Myopathy
NM_001289762	Rarb	2.2	0.0004	Retinoic acid receptor, beta	Muscle cell death
NM_021355	Fmod	2.1	0.0004	Fibromodulin	Muscle morphology
NM_013645	Pvalb	2.1	0.0004	Parvalbumin	Muscle contractility and development
NM_172259	Myl6b	2.1	0.0004	Myosin, light polypeptide 6B	Muscle development
NM_008551	Mapkapk2	2.1	0.0004	MAP kinase-activated protein kinase 2	Muscle cell death
NM_013712	Itgb1bp2	2.1	0.0004	Integrin beta 1 binding protein 2	Muscle development
NM_021566	Jph2	2.1	0.0004	Junctophilin 2	Muscle development and morphology, myopathy
NM_025823	Pcyox1	2.0	0.0004	Prenylcysteine oxidase 1	Protein catabolism
NM_001013833	Prkg1	2.0	0.0004	Protein kinase, cGMP-dependent, type 1	Muscle contractility and function
NM_019735	Apip	2.0	0.0004	APAF1 interacting protein	Muscle cell death
NM_009022	Aldh1a2	2.0	0.0004	Aldehyde dehydrogenase family 1, subfamily A2	Muscle development and morphology
NM_008524	Lum	2.0	0.0004	Lumican	Muscle morphology

Date Reçue/Date Received 2022-02-22

Downregulated by AR-42

NM_138677	Edem1	-2.0	0.0004	ER degradation enhancer, mannosidase alpha-like 1	Protein catabolism
NM_001163704	Fbxo6	-2.0	0.0004	F-box protein 6	Protein catabolism
NM_011724	Xirp1	-2.1	0.0004	Xin actin-binding repeat containing 1	Muscle, contractility, development, and morphology
NM_001111099	Cdkn1a	-2.1	0.0004	Cyclin-dependent kinase inhibitor 1A (P21)	Muscle development and morphology, skeletal muscle mass and cell size; muscle cell death
NM_001199733	Daxx	-2.1	0.0004	Fas death domain-associated protein	Muscle cell death
NM_001081044	Mylk2	-2.1	0.0004	Myosin, light polypeptide kinase 2, skeletal muscle	Muscle development; myopathy
NM_016736	Nub1	-2.1	0.0004	Negative regulator of ubiquitin-like proteins 1	Protein catabolism
NM_007582	Cacng1	-2.2	0.0004	Calcium channel, voltage-dependent, gamma subunit 1	Muscle development; protein catabolism
NM_020033	Ankrd2	-2.2	0.0004	Ankyrin repeat domain 2 (stretch responsive muscle)	Muscle function and morphology
NM_172845	Adamts4	-2.2	0.0004	A disintegrin-like and metallopeptidase (reprolysin type) with thrombospondin type 1 motif, 4	Muscle development; protein catabolism
NM_009464	Ucp3	-2.2	0.0004	Uncoupling protein 3	Skeletal muscle mass
NM_028142	Pupla2	-2.2	0.0004	Patatin-like phospholipase domain containing 2	Muscle morphology, muscle cell death
NM_104580	Slc8a1	-2.3	0.0004	Solute carrier family 8 (sodium/calcium exchanger), member 1	Muscle development and morphology; muscle cell death; myopathy
NM_008871	Serpine1	-2.3	0.0004	Serine (or cysterine) peptidase inhibitor, clade E, member 1	Muscle development
NM_001081185	Flnc	-2.3	0.0004	Filamin C, gamma (actin binding protein 280)	Muscle development and morphology; myopathy
NM_009238	Sox4	-2.3	0.0004	SRY-box containing gene 4	Muscle development and morphology
NM_001289716	Bcl2l1	-2.4	0.0004	Bcl2-like 1	Muscle cell death; myopathy
NM_001165894	Akt1	-2.4	0.0004	Thymoma viral proto-oncogene 1	Muscle atrophy, development and function; skeletal muscle

Date Reçue/Date Received 2022-02-22

					cell size; myopathy; protein catabolism
NM_007428	Agt	-2.5	0.0004	Angiotensinogen (serpin peptidase inhibitor, clade A, member 8)	Muscle atrophy; smooth muscle mass; muscle cell death; myopathy; protein catabolism
NM_019739	Foxol	-2.5	0.0004	Forkhead box O1	Muscle atrophy and development; skeletal muscle mass; muscle cell death; myopathy
NM_013560	Hspbl	-2.5	0.0004	Heat shock protein 1	Muscle atrophy; muscle cell death; myopathy
NM_026346	Fbxo32	-3.0	0.0004	F-box protein 32	Muscle atrophy; myopathy; protein catabolism
NM_001159324	Gaa	-3.0	0.0004	Glucosidase, alpha, acid	Muscle atrophy, development, function, and morphology; myopathy
NM_008244	Hgs	-3.3	0.0004	HGF-regulated tyrosine kinase substrate	Protein catabolism
NM_013468	Ankrd1	-3.6	0.0004	Ankyrin repeat domain 1 (cardiac muscle)	Muscle development, function, and morphology, muscle cell death
NM_001039048	Trim63	-3.9	0.0004	Tripartite motif-containing 63	Muscle contractility and morphology; skeletal muscle mass and cell size; muscle atrophy; myopathy
NM_008491	Lcn2	-4.9	0.0004	Lipocalin 2	Muscle cell death

Date Reçue/Date Received 2022-02-22

[0041c] Table 3

Table 3. Cytokine profile analysis of serum samples from tumor-free and C-26 tumor-bearing mice treated with vehicle or AR-42 (means ± S.D.; n = 3 for each group)

pg/ml	Tumor-free mice		C-26 tumor-bearing mice	
	Vehicle	AR-42 (n = 3)	Vehicle	AR-42
Eotaxin	677.2 ± 34.2	633.9 ± 84.8	766.8 ± 191.7	636.2 ± 146.0
G-CSF	145.4 ± 27.5	1215 ± 291	2520 ±1533	2284 ± 989
GM-CSF	31.9 ± 18.3	44.7 ± 14.8	36.4 ± 21.1	41.1 ± 23.7
IFNγ	4.7 ± 2.9	1.2 ± 1.7	0.39 ± 0.76	0.89 ± 1.34
IL-1α	293.0 ± 184.7	169.5 ± 130.2	78.7 ± 50.7	25.1 ± 15.7
IL-1β	11.1 ± 17.0	4.7 ± 2.7	2.9 ± 2.3	2.2 ± 1.8
IL-2	3.6 ± 1.1	4.0 ± 1.6	3.8 ± 1.7	1.7 ± 1.3
IL-3	3.0 ± 1.9	1.2 ± 1.4	0.5 ± 0.7	1.7 ± 2.6
IL-4	0.02 ± 0.05	0	0	0.5 ± 0.9
IL-5	3.4 ± 0.6	4.3 ± 1.1	0.76 ± 1.09	25.2 ± 40.6
IL-6	3.0 ± 1.3	5.1 ± 3.6	216.6 ± 108.8	100.6 ± 43.1
IL-7	8.8 ± 2.5	13.0 ± 10.2	10.9 ± 5.2	5.8 ± 2.2
IL-9	38.8 ± 8.7	34.0 ± 13.0	54.4 ± 42.0	11.4 ± 21.2
IL-10	5.6 ± 2.0	6.8 ± 1.0	8.2 ± 3.6	14.9 ± 9.8
IL12 (p40)	57.7 ± 33.1	42.8 ± 44.6	7.3 ± 1.8	7.4 ± 2.8
IL-12 (p70)	4.6 ± 1.5	5.0 ± 1.9	3.8 ± 2.2	15.3 ± 32.0
IL-13	109.9 ± 20.7	63.0 ± 27.6	88.0 ± 24.8	68.3 ± 26.8
IL-15	36.2 ± 13.0	70.7 ± 88.1	94.1 ± 161.3	18.6 ± 8.7
IL-17	5.1 ± 1.1	6.838±3.010	3.293±2.925	3.277±2.774
IP-10	166.2 ± 53.3	135.6 ± 42.4	180.5 ± 59.9	311.5 ± 140.4
KC	89.7 ± 38.2	156.4 ± 62.1	115.1 ± 43.9	1070 ± 1072
LIF	1.7 ± 2.7	5.1 ± 10.247	20.8 ± 13.1	4.7 ± 3.0
LIX	6778 ± 2835	5625 ± 2760	4917 ± 3165	1197 ±1376
MCP-1	41.8 ± 12.1	24.8 ±5.9	35.5 ± 27.3	63.1 ± 17.8
M-CSF	9.5 ± 4.3	5.9 ± 1.7	4.2 ± 2.3	6.6 ± 2.4
MIG	136.5 ± 94.3	66.0 ± 35.1	30.2 ± 18.0	77.4 ± 33.0
MIP-1α	51.3 ± 17.7	42.2 ± 25.0	40.2 ± 24.1	22.9 ± 19.3
MIP-1β	103.7 ± 8.8	89.7 ± 14.7	63.6 ± 17.9	70.2 ± 8.8
MIP-2	81.1 ± 20.9	68.1 ± 20.4	57.4 ± 21.9	49.8 ± 4.0
RANTES	27.9 ± 4.5	21.8 ± 7.3	21.2 ±7.5	20.2 ± 5.5
TNFα	5.5 ± 3.5	0.23 ± 0.52	2.8 ± 3.7	3.2 ± 3.5
VEGF	1.7 ± 0.36	1.5 ± 0.6	1.4 ± 0.5	1.1 ± 0.3

Date Reçue/Date Received 2022-02-22

[0041d] Table 4

Table 4. RNA-seq analysis of differentially expressed genes (> 4-fold) in muscles from AR-42-treated versus vehicle-treated C-26 tumor-bearing mice (n = 3)

RefSeq ID (UCSC)	Gene ID	log2 fold change	*P* value	Description
Upregulated by AR-42				
NM_009700	Aqp4	6.7	0.0004	Aquaporin 4
NM_009867	Cdh4	6.2	0.0004	Cadherin 4
NR_002870	Dnm3os	6.1	0.0004	Dynamin 3, opposite strand
NM_207281.3	4832428D23Rik	6.0	0.0004	RIKEN cDNA 4832428D23 gene
NM_001081116	Arhgef17	5.8	0.0083	Rho guanine nucleotide exchange factor (GEF) 17
NM_008438	Kera	5.8	0.0004	Keratocan
NM_008393	Irx 3	5.6	0.0004	Iroquois related homeobox 3 (Drosophila)
NM_008473	Krt1	5.5	0.0004	Keratin 1
NM_001198886	Dpp6	5.4	0.0004	Dipeptidylpeptidase 6
NM_016749	Mybph	5.1	0.0004	Myosin binding protein H
NM_001162983	Lrrc38	5.0	0.0004	Leucine rich repeat containing 38
NM_001109988.1	D0H4S114	4.9	0.0004	DNA segment, human D4S114
NM_001101475	F830016B08Rik	4.9	0.0382	RIKEN cDNA F830016B08 gene
NR_045431	4933401D09Rik	4.9	0.0004	RIKEN cDNA 4933401D09 gene
NM_001205219	Sorbs2	4.9	0.0436	Sorbin and SH3 domain containing 2
NM_010254	Galr2	4.9	0.0004	Galanin receptor 2
NM_011825	Grem2	4.9	0.0004	Gremlin 2 homolog, cysteine knot superfamily (Xenopus laevis)
NM_001081456	Plcd4	4.8	0.0004	Phospholipase C, delta 4
NM_181664	Crip3	4.7	0.0004	Cysteine-rich protein 3
NM_027948	1700003E16Rik	4.7	0.0004	RIKEN cDNA 1700003E16 gene
NM_028639	Ttc7	4.7	0.0317	Tetratricopeptide repeat domain 7
NR_045491	2310016D03Rik	4.7	0.0004	RIKEN cDNA 2310016D03 gene
NM_025734	Kcng4	4.6	0.0004	Potassium voltage-gated channel, subfamily G, member 4
NM_025290	Rsph1	4.6	0.0004	Radial spoke head 1 homolog (Chlamydomonas)
NM_011506	Sucla2	4.5	0.0014	Succinate-Coenzyme A ligase, ADP-forming beta subunit
NM_001101475	F830016B08Rik	4.5	0.0021	RIKEN cDNA F830016B08 gene
NM_001081052	Nhs	4.5	0.0004	Nance-Horan syndrome (human)
NM_001008533	Adora1	4.4	0.0004	Adenosine A1 receptor
NM_029932	Spns3	4.4	0.0004	Spinster homolog 3 (Drosophila)
NM_001013013	Dhrs7c	4.4	0.0008	Dehydrogenase/reductase (SDR family) member 7C
NM_024291	Ky	4.3	0.0004	Kyphoscoliosis peptidase
NM_010742	Ly6d	4.2	0.0085	Lymphocyte antigen 6 complex, locus D
NM_010267	Gdap1	4.2	0.0004	Ganglioside-induced differentiation-associated-protein 1
NM_013569	Kcnh2	4.1	0.0004	Potassium voltage-gated channel, subfamily 1 (eag related), member 2
NM_176916	Pld5	4.1	0.0004	Phospholipase D family, member 5

Date Reçue/Date Received 2022-02-22

NM_175541	Mum111	2.8	0.0004	Melanoma associated antigen (mutated) 1-like 1
NM_175486	6430571L13Rik	2.8	0.0080	RIKEN cDNA 6430571L13 gene
NM_001025577	Maf	2.8	0.0004	Avian musculoaponcurotic fibrosarcoma (v-maf) AS42 oncogene homolog
NM_133226	Pdzd3	2.8	0.0004	PDZ domain containing 3
NM_008469	Krt15	2.8	0.0004	Keratin 15
NM_029037.4	4930444A02Rik	2.8	0.0004	RIKEN cDNA 4930444A02 gene
NM_029297	Dynlrb2	2.8	0.0112	Dynein light chain roadblock-type 2
n/a	Ercc2,Mir343	2.8	0.0004	Excision repair cross-complementing rodent repair deficiency, complementation group 2
NM_176848	Fbxo2	2.8	0.0004	F-box protein 2
NM_007670	Cdkn2b	2.8	0.0004	Cyclin-dependent kinase inhibitor 2B (p15, inhibits CDK4)
NM_001081416	Fndc1	2.7	0.0336	Fibronectin type III domain containing 1
NM_172794	Zfp454	2.7	0.0004	Zinc finger protein 454
NM_026794	Deb1	2.7	0.0004	Differentially expressed in B16F10 1
NM_177784	Klhl23	1.7	0.0004	Kelch-like 23 (Drosophila)
NM_022027	Syne1	2.7	0.0004	Synaptic nuclear envelope 1
NM_028798	Crct1	2.7	0.0208	Cysteine-rich C-terminal 1
NM_001009951. 1	BC088983	2.7	0.0214	CDNA sequence BC088983
NM_001289450	Kcnab1	2.7	0.0004	Potassium voltage-gated channel shaker-related subfamily, beta member 1
NM_001290825	Co117al	2.7	0.0004	Collagen type XVII, alpha 1
NM_016685	Comp	2.7	0.0004	Cartilage oligomeric matrix protein
NM_177222	Casc1	2.7	0.0166	Cancer susceptibility candidate 1
NM_001290679	Tmem14a	2.7	0.0004	Transmembrane protein 14A
NM_198111	Akap6	2.7	0.0004	A kinase (PRKA) anchor protein 6
NM_020278	Lgi1	2.7	0.0004	Leucine-rich repeat LGI family, member 1
NM_008496	Lgals7	2.7	0.0004	Lectin, galactose binding, soluble 7
NM_025500	Mrp137	2.6	0.0004	Mitochondrial ribosomal protein L37
NM_001290708	Smarcal	2.6	0.0004	SWI/SNF related, matrix associated, actin dependent regulator of chromatin subfamily a, member 1
NM_053166	Trim7	2.6	0.0004	Tripartite motif protein 7
NM_139152	Asb18	2.6	0.0004	Ankyrin repeat and SOCS box-containing 18
NM_009255	Serpine2	2.6	0.0004	Serine (or cysteine) peptidase inhibitor, clade E. member 2
NM_207205	Igsf3	2.6	0.0004	Immunoglobulin superfamily, member 3
NM_023734	Pi16	2.6	0.0206	Peptidase inhibitor 16
NR_045837	9130227L01Rik	2.6	0.0083	RIKEN cDNA 9130227L01 gene
NM_011638	Tfrc	2.6	0.0004	Transferrin receptor
NM_001256224	Wnt5a	2.6	0.0011	Wingless-related MMTV integration site 5A
NM_181541	Caprin2	2.6	0.0004	Caprin family member 2
NM_001077202	Hs6st2	2.6	0.0004	Heparan sulfate 6-O-sulfotransferase 2
NM_010271	Gpd1	2.6	0.0004	Glycerol-3-phosphate dehydrogenase 1 (soluble)
NM_017392	Celsr2	2.6	0.0004	Cadherin EGF LAG seven-pass G-type receptor 2
NM_010576	Itga4	2.6	0.0004	Integrin alpha 4

Date Reçue/Date Received 2022-02-22

NM_011994	Abcd2	2.6	0.0004	ATP-binding cassette, sub-family D(ALD), member 2
n/a	Fabp9	2.6	0.0004	Fatty acid binding protein 9, testis
NM_001030305.2	Pmp2	2.6	0.0004	Peripheral myelin protein 2
NM_001289498	Egflam	2.6	0.0004	Tubulin, gamma 2
NM_134028	Tubg2	2.6	0.0004	EGF-like, fibronectin type III and laminin G domains
n/a	Snora31	2.6	0.0035	Tumor protein, translationally controlled 1
n/a	Tpt1	2.6	0.0035	Tumor protein, translationally controlled 1
NM_001198765	Postn	2.6	0.0004	Periostin, osteoblast specific factor
NM_025998	Nkain1	2.5	0.0004	Na+/K+ transporting ATPase interacting 1
NM_007988	Fasn	2.5	0.0004	Fatty acid synthase
NM_016788	Tnk2	2.5	0.0004	Tyrosine kinase, non-receptor, 2
NM_029761	Dok5	2.5	0.0004	Docking protein 5
NM_133729	2610018G03Rik	2.5	0.0004	RIKEN cDNA 2610018G03 gene
NM_001145887	Tiaml	2.5	0.0004	T-cell lymphoma invasion and metastasis 1
NM_025420	Lce1m	2.5	0.0008	Late cornifield envelope 1M
NM_145134	Spsb4	2.5	0.0004	SplA/ryanodine receptor domain and SOCS box containing 4
NR_040577	1700123M08Rik	2.5	0.0004	RIKEN cDNA 1700123M08 gene
NM_023047	Dpysl5	2.5	0.0004	Dihydropyrimidinase-like 5
NM_139152	Asb18	2.5	0.0004	Ankyrin repeat and SOCS box-containing 18
NM_008409	Itm2a	2.5	0.0004	Integral membrane protein 2A
NM_021508	Myoz1	2.5	0.0004	Myozenin 1
NM_029568	Mfap4	2.5	0.0004	Microfibrillar-assocoated protein 4
NM_026626	Efcab2	2.5	0.0011	EF-hand calcium binding domain 2
NM_172784	Lrp11	2.5	0.0004	CASP8 and FADD-like apoptosis regulator
NR_110361	Cflar	2.5	0.0004	Low density lipoprotein receptor-related protein 11
NM_001291104	Fgf11	2.5	0.0004	Fibroblast growth factor 11
NM_027756	Mfap31	2.5	0.0004	Microfibrillar-assocoated protein 3-like
NM_001111145	Gm514	2.5	0.0004	Gene model 514, (NCBI)
NM_009469	Ulk1	2.5	0.0212	Unc-51 like kinase 1 (C.elegans)
NM_026956	Cd209f	2.5	0.0004	CD209f antigen
NM_019718	Arl3	2.5	0.0004	ADP-ribosylation factor-like 3
NM_026617	Tmbim4	2.4	0.0092	Dopa decarboxylase
NM_016672	Ddc	2.4	0.0004	Transmembrane BAX inhibitor motif containing 4
NM_172899	Dmkn	2.4	0.0004	Dermokine
NM_019563	Cited4	2.4	0.0004	Glu/Asp-rich carboxy-terminal domain, 4
NM_013803	Casr	2.4	0.0119	Cbp/p300-interacting transactivator, with Calcium-sensing receptor
NM_194350	Mafa	2.4	0.0004	V-maf musculoaponeurotic fibrosarcoma oncogene family, protein A (avian)
NM_013933	Vapa	2.4	0.0004	Vesicle-associated membrane protein, associated protein A
NM_025384	Dnajc15	2.4	0.0287	Dnal (hsp40) homolog, subfamily C, member 15
NM_009873	Cdk6	2.4	0.0004	Cyclin-dependent kinase 6
NR_030764	2700097O09Rik	2.4	0.0021	RIKEN cDNA 2700097O09 gene

Date Reçue/Date Received 2022-02-22

NM_153546	Mboat1	2.2	0.0004	Membrane bound O-acyltransferase domain containing 1
NM_001289762	Rarb	2.2	0.0004	Retinoic acid receptor, beta
NM_134079	Adk	2.2	0.0026	Adenosine kinase
NM_010357	Gsta4	2.2	0.0004	Glutathione S-transferase, alpha 4
NM_177073	Relt	2.2	0.0004	RELT tumor necrosis factor receptor
NM_001033131	Krtdap	2.2	0.0011	Keratinocyte differentiation associated protein
NM_175645	Xylt1	2.2	0.0004	Xylosyltransferase 1
NM_007742	Colla1	2.2	0.0004	Collagen, type 1, alpha 1
NR 040577	1700123M08Rik	2.2	0.0004	RIKEN cDNA 1700123M08 gene
NM_016785	Tpmt	2.2	0.0004	Thiopurine methyltransferase
NM_001013771	Gm973	2.2	0.0008	Gene model 973, (NCBI)
NM_021717	Nrip2	2.2	0.0210	Nuclear receptor interaction protein 2
NM_001012450	Ankrd6	2.2	0.0004	Ankyrin repeat domain 6
NM_172600	6720456H20Rik	2.2	0.0057	RIKEN cDNA 6720456H20 gene
NM_145523	Gca	2.2	0.0218	Grancalcin
NM_017378	Pcdh12	2.2	0.0004	Protocadherin 12
NM_153801	Tecr1	2.2	0.0260	n/a
NM_027865	Tmem25	2.2	0.0004	Transmembrane protein 25
NM_177698	Psd3	2.2	0.0218	Pleckstrin and Sec7 domain containing 3
NM_010924	Nnmt	2.2	0.0004	Nicotinamide N-methyltransferase
NM_078479	Mrps21	2.2	0.0112	Mitochondrial ribosomal protein S21
NM_001285849	Paqr7	2.2	0.0004	Progestin and adipoQ receptor family member VII
NM_028132	Pgm2	2.1	0.0004	Phosphoglucomutase 2
NM_172527	Nudt15	2.1	0.0004	Nudix (nucleoside diphosphate linked moiety X)-type motif 15
NM_026732	Mrpl14	2.1	0.0248	Mitochondrial ribosomal protein L14
NM_194060	Foxo6	2.1	0.0004	Forkhead box O6
NR_024619	2610001J05Rik	2.1	0.0216	RIKEN cDNA 2610001J05 gene
NM_021355	Fmod	2.1	0.0004	Fibromodulin
NM_011775	Zp2	2.1	0.0004	Zona pellucida glycoprotein 2
NM_146188	Kctd15	2.1	0.0008	Potassium channel tetramerisation domain containing 15
NM_008571	Mcpt2	2.1	0.0004	Mast cell protease 2
NM_013645	Pvalb	2.1	0.0004	Parvalbumin
NM_001076681	1810012P15Rik	2.1	0.0070	RIKEN cDNA 1810012P15 gene
NM_172259	Myl6b	2.1	0.0004	Myosin, light polypeptide 6B
NR_040577	1700123M08Rik	2.1	0.0470	RIKEN cDNA 1700123M08 gene
NM_012048	Polk	2.1	0.0004	Polymerase (DNA directed), kappa
NM_001168476	Ttc23	2.1	0.0004	Tetratricopeptide repeat domain 23
NM_172522	Megf11	2.1	0.0004	Multiple EGF-like-domains 11
NM_017382	Rab11a	2.1	0.0004	RAB11a, member RAS oncogene family
NM_008609	Mmp15	2.1	0.0004	Matrix metallopeptidase 15
NM_054088	Pnpla3	2.1	0.0004	Patatin-like phospholipase domain containing 3
NM_007590	Calm3	2.1	0.0004	Calmodulin 3
NM_001168471	Dynll2	2.1	0.0355	Dynein light chain LC8-type 2
NM_080856	Asb14	2.1	0.0004	Ankyrin repeat and SOCS box-containing protein 14
NM_198414	Paqr9	2.1	0.0004	Progestin and adipoQ receptor family member IX

Date Reçue/Date Received 2022-02-22

NM_017394	Slc7a10	2.1	0.0321	Solute carrier family 7 (cationic amino acid transporter, y+ system), member 10
NM_001271758	Wnt5b	2.1	0.0393	Wingless-related MMTV integration site 5B
NM_011035	Pak1	2.1	0.0004	P21 (CDKN1A)-activated kinase 1
NM_058212	Dpf3	2.1	0.0014	D4, zinc and double PHD fingers family 3
NM_008832	Phka1	2.1	0.0004	Phosphorylase kinase alpha 1
NM_008551	Mapkapk2	2.1	0.0004	MAP kinase-activated protein kinase 2
NM_013712	Itgb1bp2	2.1	0.0004	Integrin beta 1 binding protein 2
NM_016673	Cntfr	2.1	0.0004	Ciliary neurotrophic factor receptor
NM_021566	Jph2	2.1	0.0004	Junctophilin 2
NM_013415	Atplb2	2.1	0.0004	ATPase, Na+/K+ transporting, beta 2 polypeptide
NM_133687	Cxxc5	2.1	0.0004	CXXC finger 5
NM_011932	Dapp1	2.0	0.0004	Dual adaptor for phosphotyrosine and 3-phosphoinositides 1
NM_153554	Aldh1a2	2.0	0.0004	Aldehyde dehydrogenase 18 family, member A1
NM_001290761	Nmral1	2.0	0.0004	NmrA-like family domain containing 1
NM_146030	Plekhh3	2.0	0.0004	Pleckstrin homology domain containing, family H (with MyTH4 domain) member 3
NM_025823	Pcyox1	2.0	0.0004	Prenylcysteine oxidase 1
NM_176920	Lrtm1	2.0	0.0004	Leucine-rich repeats and transmembrane domains 1
NM_001013833	Prkg1	2.0	0.0004	Protein kinase, cGMP-dependent, type 1
NM_019735	Apip	2.0	0.0004	APAF1 interacting protein
NM_011734	Siac	2.0	0.0004	Sialic acid acetylesterase
NM_009022	Aldh1a2	2.0	0.0004	Aldehyde dehydrogenase family 1, subfamily A2
NM_008524	Lum	2.0	0.0004	Lumican
NM_001198790	Ak1	2.0	0.0216	Adenylate kinase 1
NM_178401	Ramp1	2.0	0.0004	Receptor (calcitonin) activity modifying protein 1
NM_172752	Sorbs2	2.0	0.0004	Sorbin and SH3 domain containing 2
NM_013737	Pla2g7	2.0	0.0004	Phospholipase A2, group VII (platelet-activating factor acetylhydrolase, plasma)
NR_027236	AI854703	2.0	0.0004	Expressed sequence AI854703
NM_145602	Ndrg4	2.0	0.0004	N-myc downstream regulated gene 4
NM_011759	Zfp41	2.0	0.0004	Zinc finger protein 41
NM_007506	Atp5gl	2.0	0.0004	ATP synthase, H+ transporting, mitochondrial F0 complex, subunit c (subunit 9), isoform 1
NM_019573	Wwox	2.0	0.0004	WW domain-containing oxidoreductase
NM_009073	Rom1	2.0	0.0004	Rod outer segment membrane protein 1
NM_027289	Nt5dc2	2.0	0.0130	5'-nucleotidase domain containing 2
Downregulated by AR-42				
NM_025994	Efhd2	-2.0	0.0004	Ef hand domain containing 2
NM_016868	Hif3a	-2.0	0.0004	Hypoxia inducible factor 3, alpha subunit

Date Reçue/Date Received 2022-02-22

NM_029936	Ddx10	2.4	0.0008	DEAD (Asp-Glu-Ala-Asp) box polypeptide 10
NM_133769	Cyfip2	2.4	0.0004	Cytoplasmic FMR1 interacting protein 2
NM_153546	Mboat1	2.4	0.0004	Membrane bound O-acyltransferase domain containing 1
NM_173431	Rpgripl1	2.4	0.0032	Rpgrip1-like
NM_138953	Ell2	2.4	0.0107	Elongation factor RNA polymerase II 2
NM_010264	Nr6a1	2.4	0.0420	Nuclear receptor subfamily 6, group A, member 1
NM_001127725	Sec14l5	2.4	0.0004	SEC14-like 5 (S. cerevisiae)
NM_182930	Plekha6	2.4	0.0004	Pleckstrin homology domain containing family A member 6
NM_011331	Ccl12	2.4	0.0116	Chemokine (C-C motif) ligand 12
NM_207278	Tigd4	2.4	0.0004	Tigger transposable element derived 4
NM_177039	A530016L24Rik	2.4	0.0004	RIKEN cDNA A530016L24 gene
NM_178929	Kazald1	2.3	0.0004	Kazal-type serine peptidase inhibitor domain 1
NM_178608	Recp1	2.3	0.0004	Receptor accessory protein 1
NM_001252455	Ptprs	2.3	0.0004	Protein tyrosine phosphatase, receptor type, S
NM_028639	Ttc7	2.3	0.0004	Tetratricopeptide repeat domain 7
NM_013491	Clcn1	2.3	0.0004	Chloride channel 1
NM_025474	Mrps14	2.3	0.0004	Mitochondrial ribosomal protein S14
NM_008305	Hspg2	2.3	0.0004	Perlecan (heparan sulfate proteoglycan 2)
NM_009533	Xrcc5	2.3	0.0353	X-ray repair complementing defective repair in Chinese hamster cells 5
NM_019573	Wwox	2.3	0.0314	WW domain-containing oxidoreductase
NM_025358	Ndufa9	2.3	0.0004	NADH dehydrogenase (ubiquinone) 1 alpha subcomplex, 9
NM_011923	Angptl2	2.3	0.0004	Angiopoietin-like 2
NM_026728	Echdc2	2.3	0.0004	Enoyl Coenzyme A hydratase domain containing 2
NM_177471	Ccdc69	2.3	0.0004	Coiled-coil domain containing 69
NM_001291282	Tm6sf1	2.3	0.0004	Transmembrane 6 superfamily member 1
NM_009396	Tnfaip2	2.3	0.0004	Tumor necrosis factor, alpha-induced protein 2
NM_001007578	Armcx6	2.3	0.0004	Armadillo repeat containing, X-linked 6
NM_133804	Tmem132a	2.3	0.0004	Transmembrane protein 132A
NM_011436	Sorl1	2.3	0.0004	Sortilin-related receptor, LDLR class A repeats-containing
NM_001164225	Fbx116	2.3	0.0004	F-box and leucine-rich repeat protein 16
NM_001007583	Best3	2.3	0.0004	Bestrophin 3
NM_133903	Spon2	2.3	0.0004	Spondin 2, extracellular matrix protein
NM_001243009	Col6a3	2.3	0.0004	Collagen, type VI, alpha 3
NM_025343	Rmnd1	2.3	0.0200	Required for meiotic nuclear division 1 homolog (S. cerevisiae)
NM_0l0272	Gdf11	2.3	0.0004	Growth differentiation factor 11
NM_026219	Uqcrb	2.3	0.0008	Ubiquinol-cytochrome ceductase binding protein
NM_001039562	Ankrd37	2.2	0.0004	Ankyrin repeat domain 37
NM_146188	Kctd15	2.2	0.0004	Potassium channel tetramerisation domain containing 15

Date Reçue/Date Received 2022-02-22

NM_012065	Pde6g	-2.0	0.0004	Phosphodiesterase 6G, cGMP-specific, rod, gamma
NM_023476	Tinag11	-2.0	0.0488	n/a
NM_001042655	Tbcld17	-2.0	0.0004	TBC1 domain family, member 17
NM_007695	Chi311	-2.0	0.0004	Chitinase 3-like 1
NM_026877	Aspscr1	-2.0	0.0004	Alveolar soft part sarcoma chromosome region, candidate 1 (human)
NM_138677	Edcm1	-2.0	0.0004	ER degradation enhancer, mannosidase alpha-like 1
NM_026220	Mfapla	-2.0	0.0004	Microfibrillar-associated protein 1A
NM_001033411	Gm826	-2.0	0.0004	Gene model 826, (NCBI)
NM_153075	Catsper2	-2.0	0.0004	Cation channel sperm associated 2
NM_001163704	Fbxo6	-2.0	0.0004	F-box protein 6
NM_001162465	Dtnb	-2.0	0.0004	Dystrobrevin, beta
NM_011690	Vars	-2.0	0.0004	Valy1-tRNA synthetase
NM_001081349	Slc43al	-2.0	0.0004	Solute carrier family 43 member 1
NM_133765	Fbxo31	-2.1	0.0004	F-box protein 31
NM_029008	4833403115Rik	-2.1	0.0004	RIKEN cDNA 4833403l15 gene
NM_001286498	Tex264	-2.1	0.0004	Testis expressed gene 264
NM_001289917	Rora	-2.1	0.0004	RAR-related orphan receptor alpha
NM_010220	Fkbp5	-2.1	0.0004	FK506 binding protein 5
NM_011724	Xirp1	-2.1	0.0004	Xin actn-binding repeat containing 1
NM_001145858	Sh3bp2	-2.1	0.0004	SH3-domain binding protein 2
NM_001037129	Musk	-2.1	0.0004	Muscle, skeletal receptor tyrosine kinase
NM_025341	Abhd6	-2.1	0.0004	Abhydidase domain containing 6
NM_010176	Fah	-2.1	0.0004	Fumarylacetoacetate hydrolase;
NM_007923	Elk4	-2.1	0.0004	ELK4, member of ETS oncogene family
NM_153136	Nudt18	-2.1	0.0004	Nudix (nucleoside diphosphate linked moiety X)-typc motif 18
NM_016684	Zscan12	-2.1	0.0004	Zinc finger and SCAN domain containing 12
NM_001291014	Zkscan17	-2.1	0.0004	Zinc finger with KRAB and SCAN domains 17
NM_016972	Slc7a8	-2.1	0.0004	Solute carrier family 7 (cationic amino acid transporter, y+ system), member 8
NM_057172	Fubp1	-2.1	0.0112	Far upstream element (FUSE) binding protein 1
NM_022882	Lpin2	-2.1	0.0004	Lipin 2
NM_011663	Zrsr1	-2.1	0.0004	Zinc finger (CCCH type), RNA binding motif and serine/arginine rich 11
NM_016896	Map3k14	-2.1	0.0004	Mitogen-activated protein kinase kinase kinase 14
NM_138950	Wdr81	-2.1	0.0004	WD repeat domain 81
NR_104298	Gn13	-2.1	0.0004	Guanine, nucleotide binding protein-like 3 (nucleolar)
NM_016661	Ahcy	-2.1	0.0004	S-adenosy 1homocysteine hydrolase
NM_010757	Mafk	-2.1	0.0004	V-maf musculoaponeurotic fibrosarcoma oncogene family, protein K (avian)
NM_021897	Trp53inp1	-2.1	0.0004	Transformation related protein 53 inducible nuclear protein 1

Date Reçue/Date Received 2022-02-22

NM_009025	Rasa3	-2.1	0.0004	RAS p21 protein activator 3
NM_133895	Slc15a4	-2.1	0.0004	Solute carrier family 15, member 4
NM_053098	Lmod2	-2.1	0.0004	Leiomodin 2 (cardiac)
NM_052994	Spock2	-2.1	0.0021	Sparc/osteonectin,cwcv and kazal-like domains proteoglycan 2
NM_176968	Nt5dc1	-2.1	0.0004	5'-nucleotidase domain containing 1
NM_027493	Actr8	-2.1	0.0004	ARP8 actin-related protein 8 homolog (S. cerevisiae)
NM_001111099	Cdkn1a	-2.1	0.0004	Cyclin-dependent kinase inhibitor 1A (P21)
NM_001256042	Hsf4	-2.1	0.0004	Heat shock transcription factor 4
NM_0l0l00	Edar	-2.1	0.0062	Ectodysplasin-A receptor
NM_007746	Map3k8	-2.1	0.0004	Mitogen activated protein kinase kinase kinase 8
NM_023913	Ern1	-2.1	0.0004	Endoplasmic retivulum (ER) to nucleus signalling 1
NM_001199733	Daxx	-2.1	0.0004	Death domain-associated protein 6
NM_007570	Btg2	-2.1	0.0004	B-cell translocation gene 2, anti-proliferative
NM_019822	Adrm1	-2.1	0.0004	Adhesion regulating molecule 1
NM_029415	S1c10a6	-2.1	0.0004	Solute carrier family 10 (sodium/bile acid cotransporter family), member 6
NM_001081044	My1k2	-2.1	0.0004	Myosin, light polypeptide kinase 2, skeletal muscle
NM_175133	1110038D17Rik	-2.1	0.0004	RIKEN cDNA 1110038D17 gene
NM_029083	Ddit4	-2.1	0.0004	DNA-damase-inducible transcript 4
NM_145135	Rnh1	-2.1	0.0004	Ribonuclease/angiogenin inhibitor 1
NM_016736	Nub1	-2.1	0.0004	Negative regulator of ubiquitin-like proteins 1
NM_027560	Arrdc2	-2.1	0.0004	Arrestin domain containing 2
NM_025514	Anapcl6	-2.1	0.0004	n/a
NR_044986	4933406C10Rik	-2.2	0.0004	RIKEN cDNA 4933406C10 gene
NM_008407	Itih3	-2.2	0.0004	Inter-alpha trypsin inhibitor, heavy chain 3
NM_010813	Mnt	-2.2	0.0004	Max binding protein
NM_026483	Mphosph10	-2.2	0.0004	M-phase phosphoprotein 10 (U3 small nucleolar ribonucleoprotein)
NM_001081044	Mylk2	-2.2	0.0004	Myosin, light polypeptide kinase 2, skeletal muscle
NM_001290727	Arid5a	-2.2	0.0004	AT rich interactive domain 5A (Mrf1 like)
NM_010115	Klk1b26	-2.2	0.0121	Kallikrein 1-related peptidase b26
NM_015818	Hs6st1	-2.2	0.0240	Heparan sulfate 6-O-sulfotransferase 1
NM_015787	Hist1h1e	-2.2	0.0004	Histone cluster 1, H1e
NM_023422	Hist1h2be	-2.2	0.0004	Histone cluster 1, H2be
NM_177362	Zfp771	-2.2	0.0004	Zinc finger protein 771
NM_172713	Sdad1	-2.2	0.0004	SDA 1 domain containing 1
NM_007582	Cacng1	-2.2	0.0004	Calcium channel, voltage-dependent, gamma subunit 1
NM_020033	Ankrd2	-2.2	0.0004	Ankyrin repeat domain 2 (stretch responsive muscle)
NM_0l 1874	Psmc4	-2.2	0.0004	Proteasome (prosome, macropain) 26S subunit, ATPase,4
NM_172845	Adamts4	-2.2	0.0004	A distintegrin-like and metallopeptidase

Date Reçue/Date Received 2022-02-22

				(reprolysin type) with thrombospondin type 1 motif, 4
NM_025635	Zwint	-2.2	0.0004	ZW10 interactor
NM_009464	Ucp3	-2.2	0.0004	Uncoupling protein 3 (mitochondrial, proton carrier)
NM_026853	Asb11	-2.2	0.0004	Ankyrin repeat and SOCS box-containing protein 11
NM_001290727	Arid5a	-2.2	0.0060	AT rich interactive domain 5A (Mrf1 like)
NM_183270	Chchd8	-2.2	0.0004	Coiled-coil-helix-coiled-coil-helix domain containing 8
NM_153065	Ddx27	-2.2	0.0004	DEAD (Asp-Glu-Ala-Asp) box polypeptide 27
NR_027965	2310061J03Rik	-2.2	0.0155	RIKEN cDNA 2310061J03 gene
NM_133218	Zfp704	-2.2	0.0004	Zinc finger protein 704
NM_008694	Ngp	-2.2	0.0004	Neutrophilic granule protein
NM_001272031	Arvef	-2.2	0.0024	Armadillo repeat gene deleted in velo-cardio-facial syndrome
NM_001164560	Trmt1	-2.2	0.0004	TRM1 tRNA methyltransferase 1 homolog (S. cerevisiae)
NR_028142	Pnp1a2	-2.2	0.0004	Paratin-like phospholipase domain containing 2
NM_023248	Sbds	-2.2	0.0004	Shwachman-Bodian-Diamond syndrome homolog (human)
NM_027460	Slc25a33	-2.2	0.0004	Solute carrier family 25, member 33
NM_025706	Tbcldl5	-2.2	0.0004	TBC1 domain family, member 15
NM_175456	Abra	-2.2	0.0004	Actin-binding Rho activating protein
NM_019930	Ranbp9	-2.2	0.0004	RAN binding protein 9
NM_025324	Zfp524	-2.2	0.0004	Zinc finger protein 524
NM_177325	Tsr1	-2.2	0.0004	TSR1, 20S rRNA accumulation, homolog (yeast)
NM_001290698	Synj2	-2.2	0.0004	Synaptojanin 2
NR_033450	Serpina3h	-2.2	0.0316	Serine (or cysteine) peptidase inhibitor, clade A, member 3H
NM_199469	Np1oc4	-2.2	0.0004	Nuclear protein localization 4 homolog (S. cerevisiae)
NM_026674	Aph1c	-2.2	0.0004	Anterior pharynx defective 1c homolog (C, elegans)
NM_010234	Fos	-2.3	0.0004	FBJ osteosarcoma oncogene
NM_010908	Nfkbib	-2.3	0.0004	Nuclear factor of kappa light chain gene enhancer in B-cells inhibitor, beta
NR_045702	AW549542	-2.3	0.0004	Expressed sequence AW549542
NM_011377	Sim2	-2.3	0.0004	Single-minded homolog 2 (Drosophila)
NM_009349	Inmt	-2.3	0.0004	Indolethylamine N-methyltransferase
NM_026545	Psmd8	-2.3	0.0004	Proteasome (prosome, macropain) 26S subunit, non-ATPase, 8
NM_009272	Srm	-2.3	0.0004	Spermidine synthase
NR_104580	Slc8a1	-2.3	0.0004	Solute carrier family 8 (sodium/calcium exchanger), member 1
NM_001146707	Nap1l1	-2.3	0.0004	Nucleosome assembly protein 1-like 1
NM_008871	Serpine1	-2.3	0.0004	Serine (or cysteine) peptidase inhibitor, clade

Date Reçue/Date Received 2022-02-22

				E, member 1
NM_009963	Cry2	-2.3	0.0004	Cryptochrome 2 (photolyase-like)
NM_001081185	Flnc	-2.3	0.0004	Filamin C, gamma (actin binding protein 280)
NM_009238	Sox4	-2.3	0.0004	SRY-box containing gene 4
NM_172546	Cnksr3	-2.3	0.0049	Cnksr family member 3
NM_008951	Psmd4	-2.3	0.0004	Proteasome(prosome, macropain) 26S subunit, non-ATPsae,4
NM_146251	Pnpla7	-2.3	0.0004	Patatin-like phospholipase domain containing 7
NM_010321	Gnmt	-2.3	0.0004	Glycine N-methyltransferase
NM_001012322	Sctr	-2.3	0.0004	Secretin receptor
NM_178646	Tigd5	-2.3	0.0004	Tigger transposable element derived 5
NM_021462	Mknk2	-2.3	0.0004	MAP kinase-interacting serine/threonine kinase 2
NM_133753	Errfi1	-2.3	0.0004	ERBB receptor feedback inhibitor 1
NM_145604	D230025D16Rik	-2.4	0.0004	RIKEN cDNA D230025D16 gene
NM_017407	Spag5	-2.4	0.0004	Sperm associated antigen 5
NM_001159367	Per1	-2.4	0.0062	Period homolog 1 (Drosophila)
NM_178045	Rassf4	-2.4	0.0004	Ras association (RalGDS/AF-6) domain family 4
NM_001135152	Slc39al4	-2.4	0.0301	Solute carrier family 39 (zinc transporter), member 14
NM_011227	Rab20	-2.4	0.0004	RAB20, member RAS oncogene family
NM_011752	Zfp259	-2.4	0.0004	Zinc finger protein 259
NM_019873	Fkbp1	-2.4	0.0004	FK506 binding protein-like
NM_027154	Tmbim1	-2.4	0.0004	Transmembrane BAX inhibitor motif containing 1
NM_007970	Ezh1	-2.4	0.0004	Enhancer of zeste homolog 1 (Drosophila)
NM_001289716	Bcl211	-2.4	0.0004	Bcl2-like 1
NM_008655	Gadd45b	-2.4	0.0004	Growth arrest and DNA-damage-inducible 45 beta
NM_175164	Arhgap26	-2.4	0.0004	Rho GTPase activating protein 26
NM_00l033335	Serpina3f	-2.4	0.0384	Serine (or cysteine) peptidase inhibitor, clade A, member 3F
NM_009251	Serpina3g	-2.4	0.0384	Serine (or cysteine) peptidacse inhibitor, clade A, member 3G
NM_001165894	Akt1	-2.4	0.0004	Thymoma viral proto-oncogene 1
NM_011728	Xpa	-2.4	0.0004	Xeroderma pigmentosum, complementation group A
NM_028133	Egln3	-2.4	0.0004	EGL nine homolog 3 (C.elegans)
NM_080575	Acss1	-2.4	0.0004	Acyl-CoA synthetase short-chain family member 1
NM_019482	Panx1	-2.4	0.0004	Pannexin 1
NM_007428	Agt	-2.5	0.0004	Angiotensinogen (serpin peptidase inhibitor, clade A, member 8)
NM_030063	Acbd7	-2.5	0.0281	Acyl-Coenzyme A binding domain containing 7
NM_019739	Foxo1	-2.5	0.0004	Forkhead box O1
NM_029836	Tspy12	-2.5	0.0004	TSPY-like 2
NM_001161627	Tmem1 16	-2.5	0.0004	Transmembrane protein 116
NM_013560	Hspb1	-2.5	0.0004	Heat shock protein 1

Date Reçue/Date Received 2022-02-22

NM_001081212	Irs2	-2.5	0.0004	Insulin receptor substrate 2
NM_025525	Rnf113a2	-2.5	0.0052	Ring finger protein 113A2
NM_008416	Junb	-2.5	0.0004	Jun-B oncogene
NM_011969	Psma7	-2.5	0.0004	Proteasome (prosome, macropain) subunit, alpha type 7
NM_001001446	Cyp2c44	-2.5	0.0026	Cytochrome P450, family 2, subfamily c, polypeptide 44
NM_001081024	Setdb2	-2.5	0.0004	SET domain, bifurcated 2
NR_027943	1110038B12Rik	-2.5	0.0004	RIKEN cDNA 1110038B12 gene
NR_027893	BB123696	-2.5	0.0011	Expressed sequence BB123696
NM_016693	Map3k6	-2.6	0.0004	Mitogen-activated protein kinase kinase kinase 6
NM_026538	Ddx56	-2.6	0.0004	DEAD (Asp-Glu-Ala-Asp) box polypeptide 56
NM_001139520	Samhd1	-2.6	0.0004	SAM domain and HD domain, 1
NM_020042	Mocs1	-2.6	0.0004	Molybdenum cofactor synthesis 1
NM_173027	Ip6k3	-2.6	0.0004	n/a
NM_133661	Slc6a12	-2.6	0.0004	Solute carrier family 6 (neurotransmitter transporter, betaine/GABA), member 12
NM_025404	Ar14d	-2.6	0.0004	ADP-ribosylation factor-like 4D
NM_028638	Gad11	-2.6	0.0004	Glutamate decarboxylase-like 1
NR_015530	9530026P05Rik	-2.6	0.0276	RIKEN cDNA 9530026P05 gene
NM_013681	Syn2	-2.6	0.0325	Synapsin II
NM_019432	Tmem37	-2.7	0.0004	Transmembrane protein 37
NM_018737	Ctps2	-2.7	0.0393	Cytidin 5' triphosphate synthase 2
NM_009667	Ampd3	-2.7	0.0004	AMP deaminase 3
NM_001033302	Gm129	-2.7	0.0014	Gene model 129, (NCBI)
NM_029774	Ttll11	-2.7	0.0004	Tubulin tyrosine ligase-like family, member 11
NM_001081005	1500012F01Rik	-2.7	0.0004	RIKEN cDNA 1500012F01 gene
NM_001081432	Ptprq	-2.7	0.0174	Protein tyrosine phosphatase, receptor type, Q
NM_001282071	Sftpb	-2.7	0.0008	Surfactant associated protein B
NM_030210	Aacs	-2.7	0.0004	Acetoacetyl-CoA synthetase
NM_183257	Hamp2	-2.7	0.0004	Hepcidin antimicrobial peptide 2
NM_001164075	Tgif1	-2.8	0.0004	TG interacting factor 1
NM_178909	Wdr92	-2.8	0.0004	WD repeat domain 92
NM_020590	Gabarap11	-2.8	0.0004	Gamma-aminobutyric acid [GABA(A)] receptor-associated protein-like 1
NR_024067	Snhg6	-2.8	0.0004	Small nucleolar RNA host gene (non-protein coding) 6
NM_001166394	4931428F04Rik	-2.8	0.0004	RIKEN cDNA 4931428F04
NM_012017	Zfp346	-2.8	0.0004	Zinc finger protein 346
NM_174989	Ticam1	-2.8	0.0004	Toll-like receptor adaptor molecule 1
NM_001013370	Sesn1	-2.9	0.0004	Sestrin 1
NM_134247	Acot4	-2.9	0.0204	Acyl-CoA thioesterase 4
NM_009052	Bex1	-2.9	0.0004	Brain expressed gene 1
NM_001184710	Tfdp2	-2.9	0.0004	Transcription factor Dp 2
NM_008720	Npc1	-2.9	0.0004	Niemann Pick type C1
NM_009252	Serpina3n	-2.9	0.0004	Serine (or cysteine) peptidase inhibitor, clade A, member 3N
NM_144536	Cdka11	-2.9	0.0004	CDK5 regulatory subunit associated protein

Date Reçue/Date Received 2022-02-22

				1-like 1
NM_007679	Cebpd	-2.9	0.0004	CCAAT/enhancer binding protein (C/EBP), delta
NM_020581	Angpt14	-3.0	0.0004	Angiopoietin-like 4
NM_026346	Fbxo32	-3.0	0.0004	F-box protein 32
NM_028770	Krt80	-3.0	0.0004	Keratin 80
NM_001159324	Gaa	-3.0	0.0004	Glucosidase, alpha, acid
NM_011510	Abcc8	-3.0	0.0004	ATP-binding cassette, sub-family C (CFTR/MRP), member 8
NM_001289632	Itih4	-3.0	0.0004	Inter alpha-trypsin inhibitor. heavy chain 4
NR_038151	2410004N09Rik	-3.1	0.0004	RIKEN cDNA2410004N09 gene
NM_181593	Itpkc	-3.1	0.0004	Inositol 1,4,5-trisphosphate 3-kinase C
NM_010755	Maff	-3.1	0.0004	V-maf musculoaponeurotic fibrosarcoma oncogene family, protein F (avian)
NM_007918	Eif4ebp1	-3.2	0.0155	Eukaryotic translation initiation factor 4E binding protein 1
NM_029799	Arrdc5	-3.2	0.0004	Arrestin domain containing 5
NM_177755	Klh138	-3.2	0.0126	n/a
NM_001282006	Tekt1	-3.2	0.0004	Tektin 1
NM_008252	Hmgb2	-3.2	0.0004	High mobility group box 2
NM_201610	Neil2	-3.2	0.0004	Nei like 2 (E. coli)
NM_029035	Spsb1	-3.2	0.0004	SpIA/ryanodine receptor domain and SOCS box containing 1
NM_025427	1190002H23Rik	-3.3	0.0004	RIKEN cDNA 1190002H23 gene
NM_001081219	Myo1a	-3.3	0.0449	Myosin 1A
NM_009117	Saa1	-3.3	0.0004	Serum amyloid A 1
NM_001287386	Gck	-3.3	0.0004	Glucokinase
NM_008244	Hgs	-3.3	0.0004	HGF-regulated tyrosine kinase substrate
NM_021542	Kcnk5	-3.3	0.0004	Potassium channel, subfamily k, member 5
NM_197980	Cox19	-3.3	0.0004	COX 19 cytochrome c oxidase assembly homolog (S, cerevisiae)
NM_007918	Eif4cbp1	-3.3	0.0004	Eukaryotic translation initiation factor 4E
NM_145980	8430408G22Rik	-3.3	0.0004	RIKEN cDNA 8430408G22 gene
NM_033596	Hist2h4	-3.4	0.0004	Histone cluster 2, H4
NM_146186	Wdr62	-3.4	0.0004	WD repeat domain 62
NM_053110	Gpnmb	-3.4	0.0004	Glycoprotein (transmembrane) nmb
NM_011314	Saa2	-3.4	0.0004	Serum amyloid A 2
NM_001291058	Cd68	-3.4	0.0004	CD68 antigen
NM_012006	Acot1	-3.4	0.0004	Acyl-CoA thioesterase 1
NM_134188	Acot2	-3.4	0.0004	Acyl-CoA thioesterase 2
NM_177093	Lrrc58	-3.4	0.0004	Leucine rich repeat containing 58
NM_026779	Mocos	-3.4	0.0004	Molybdenum cofactor sulfurase
NM_009154	Sema5a	-3.4	0.0004	Sema domain, seven thrombospondin repeats (type 1 and type 1-like). transmembrane domain
NM_146578	Olfr1033	-3.4	0.0004	Olfactory receptor 1033
NM_029290	1700011103Rik	-3.4	0.0176	RIKEN cDNA 1700011103
NM_013468	Ankrd1	-3.6	0.0004	Ankyrin repeat domain 1 (cardiac muscle)
NM_029774	Ttl111	-3.6	0.0198	Tubulin tyrosine ligase-like family, member 11

Date Reçue/Date Received 2022-02-22

NM_010559	Il6ra	-3.6	0.0004	Interleukin 6 receptor, alpha
NM_010559	Il6ra	-3.6	0.0004	Interleukin 6 receptor, alpha
NM_001135152	Slc39a14	-3.7	0.0004	Solute carrier family 39 (zinc transporter), member 14
NM_146578	Olfr1033	-3.8	0.0329	Olfactory receptor 1033
NM_015803	Atp8a2	-3.8	0.0470	ATPase, aminophospholipid transporter-like, class 1, type 8A, member 2
NM_019701	Clcnkb	-3.8	0.0004	Chloride channel Kb
NM_144821	AI317395	-3.9	0.0004	Expressed sequence AI317395
NM_001039048	Trim63	-3.9	0.0004	Tripartite motif-containing 63
NM_181390	Mustn1	-3.9	0.0004	Musculoskeletal, embryonic nuclear protein 1
NM_011315	Saa3	-4.0	0.0004	Serum amyloid A 3
NM_203492	Mrgprg	-4.0	0.0004	MAS-related GPR, member G
NM_177028	5330437I02Rik	-4.1	0.0004	RIKEN cDNA 5330437102 gene
NM_023065	Ifi30	-4.1	0.0004	Interferon gamma inducible protein 30
NM_001081219	Myo1a	-4.1	0.0004	Myosin 1A
NM_001081047	Cnksr1	-4.1	0.0004	Connector enhancer of kinase suppressor of Ras 1
NM_008796	Pctp	-4.1	0.0085	Phosphatidylcholine transfer protein
NM_010100	Edar	-4.2	0.0340	Ectodysplasin-A receptor
NM_001256489	9030624G23Rik	-4.2	0.0004	RIKEN cDNA 9030624G23 gene
NR_030738	2410006H16Rik	-4.2	0.0004	RIKEN cDNA 2410006H16 gene
NM_023557	Slc44a4	-4.3	0.0004	Solute carrier family 44, member 4
NM_011366	Sorbs3	-4.3	0.0004	Sorbin and SH3 domain containing 3
NM_175643	Adamts2	-4.4	0.0004	A distinte grin-like and metallopeptidase (reprolysin type) with thrombospondin type 1 motif, 2
NM_007873	Doc2b	-4.7	0.0004	Double C2, beta
NM_175681	Glp2r	-4.7	0.0004	Glucagon-like peptide 2 receptor
NM_008630	Mt2	-4.8	0.0004	Metallothionein 2
NM_008491	Lcn2	-4.9	0.0004	Lipocalin 2
NM_177028	5330437102Rik	-4.9	0.0004	RIKEN cDNA 5330437102 gene
NM_007873	Doc2b	-5.1	0.0004	Double C2. beta
NR_038011	C730036E19Rik	-5.2	0.0004	RIKEN cDNA C730036E19 gene
NM_013602	Mt1	-5.2	0.0004	Metallothionein 1
NM_027211	Anxa13	-5.4	0.0008	Annexin A13
NM_011104	Prkce	-7.0	0.0004	Protein kinase C, epsilon

[0042] Table 1 shows exemplary sequences of primers used for real-time RT-PCR;

Date Reçue/Date Received 2022-02-22

[0043] Table 2 shows exemplary Ingenuity Pathway Analysis (IPA)(QIAGEN) of differentially expressed genes (≥4-fold) related to muscle disease or functions between AR-42- and vehicle-treated C-26 tumor-bearing mice (n = 6);

[0044] Table 3 shows exemplary cytokine profile analysis of serum samples from tumor-free and C-26 tumor-bearing mice treated with vehicle or AR-42 (means ± S.D.; n = 3 for each group); and

[0045] Table 4 shows exemplary RNA-seq analysis of differentially expressed genes (≥ 4-fold) in muscles from AR-42-treated versus vehicle-treated C-26 tumor-bearing mice (n = 3).

DETAILED DESCRIPTION

[0046] Before describing several exemplary aspects described herein, it is to be understood that the invention is not limited to the details of construction or process steps set forth in the following description. The aspects described herein are capable of being practiced or being carried out in various ways.

[0047] Aspects described herein disclose the effects of oral AR-42 in attenuating cachexia-induced weight loss and skeletal muscle atrophy and prolonging survival in the $CD2F_1$ mouse colon 26 (C-26) tumor model of cancer cachexia. The mouse $CD2F_1$ cachexia model is described, for example, in BMC Cancer. 2010 Jul 8;10:363. The observed anti-cachexia effect was associated with the ability of AR-42 to reprogram cell metabolism and to downregulate IL-6 levels in diseased muscle tissues to suppress muscle wasting and other cachexia-related effects independent of AR-42's effects on reducing tumor load.

[0048] Aspects described herein disclose the effects of oral AR-42 in attenuating cachexia-induced weight loss, skeletal muscle atrophy, and prolonging survival in the Lewis Lung Carcinoma (LLC) tumor model of cancer cachexia. See e.g., Expert Opin Drug Discov. Nov 1, 2009; 4(11): 1145–1155.

[0049] HDAC inhibitors described in U.S. Patent Number 8,318,808 can be used in various methods described herein. These HDAC inhibitors are based on, for example, fatty acids coupled with Zn^{2+}-chelating motifs through aromatic Ω-amino acid linkers. In various aspects, the HDAC inhibitors may have the formula:

Date Reçue/Date Received 2022-02-22

[0050] 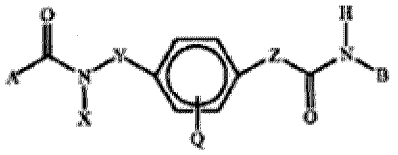

[0051] wherein X is chosen from H and CH3; Y is (CH2)n wherein n is 0-2; Z is chosen from (CH2)m wherein m is 0-3 and (CH)2; A is a hydrocarbyl group; B is o-aminophenyl or hydroxyl group; and Q is a halogen, hydrogen, or methyl.

[0052] In another aspect, methods described herein utilize AR-42, also known as (S)-N-hydroxy-4-(3-methyl-2-phenylbutanamido)benzamide having the following chemical structure:

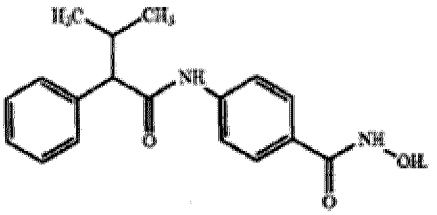

[0053] In yet another aspect, AR-42 includes salts, solvates, hydrates, anhydrous, co-crystalline and other crystalline forms and combinations. AR-42 can be formulated into a variety of dosage forms having increased stability, increased bioavailability, sustained release, and other properties.

[0054] In one aspect, HDAC inhibitors are classified characterized as being zinc dependent or nicotinamide adenine dinucleotide (NAD) dependent (Discov Med 10(54):462-470, November 2010) and are placed into four classes with eighteen family subtypes based on its HDAC substrate: class I (HDACs 1, 2, 3, and 8); class II (HDACs 4, 5, 6, 7, 9, and 10; class III (sirtuins 1-7 (SIRT)); and class IV (HDAC 11). Id. In another aspect, HDAC inhibitors include, but are not limited to, Vorinostat (SAHA) (class I and II inhibitor), Depsipeptide class I inhibitor, and AR-42 (class I and IIb inhibitor). See e.g., Strahl, B.D. and Allis, C.D. (2000) *Nature* 403:41-45. Other HDAC inhibitors (e.g., Trichostatin A or TSA) inhibit class 1 and class 2 HDACs. The substrates for HDAC inhibitors vary among the classes and subtypes.

[0055] In another aspect, the HDAC inhibitor inhibits class 1 and class 2b HDACs. In yet another aspect, the HDAC inhibitor is AR-42.

Date Reçue/Date Received 2022-02-22

[0056] In the colon 26 (C-26) tumor model of cancer cachexia, a fragment of the C26 tumor is grafted in isogenic BALB/c mice and the mice develop an undifferentiated carcinoma. Skeletal muscle atrophy (measured by muscle force and resistance to fatigue) correlated with the observed biochemical changes and the model was described as a "well standardized experimental model for research on cancer cachexia." BMC Cancer. 2010 Jul 8;10:363.

[0057] In one aspect, methods of suppressing cachexia in a mammal with cancer by administering an HDAC class 1 and 2b inhibitor to the mammal in an amount effective to substantially maintain the mammal's weight compared to a mammal that does not receive the HDAC class 1 and 2b inhibitor are provided. In another aspect, the HDAC inhibitor is AR-42.

[0058] In yet another aspect, the mammal's weight is not reduced by more than about 6% after about the first 15 days following treatment with AR-42.

[0059] In another aspect, the cancer is selected from the group consisting of pancreatic, colon, head, neck, gastric, and esophageal. In another aspect, the mammal is a human.

[0060] AR-42 can be administered in an amount of about 1 mg/kg to about 100 mg/kg of the mammal and administered at least once a day. In another aspect, AR-42 is administered twice a day in an amount of about 50 mg/kg of the mammal's weight.

[0061] In yet another aspect, levels of IL-6 are reduced by about 56% compared to a mammal that does not receive AR-42. In another aspect, levels of leukemia inhibitory factor (LIF) are reduced by about 88% compared to a mammal that does not receive AR-42. In another aspect, expression of Atrogin-1 mRNA is restored to basal levels compared to a mammal that does not receive AR-42.

[0062] In one aspect, expression of MuRF1 mRNA is restored to basal levels compared to a mammal that does not receive AR-42. In another aspect, cachexia-induced increase in IL-6Rα mRNA levels is reduced by about 85% compared to a mammal that does not receive AR-42.

[0063] In yet another aspect, cachexia-induced loss of adipose tissue is substantially restored compared to a mammal that does not receive AR-42. In another aspect, cachexia-induced reduction in skeletal muscle fiber size is restored by AR-42 compared to a mammal that does not receive AR-42.

Date Reçue/Date Received 2022-02-22

[0064] Methods of maintaining skeletal muscle weight in a mammal having cancer comprising administering a HDAC class 1 and 2b inhibitor to said mammal in an amount effective to maintain at least about 90% of said mammal's skeletal muscle weight over a period of time of at least fifteen days compared to a mammal that does not receive the HDAC class 1 and 2b inhibitor are also provided.

[0065] In another aspect, methods of prolonging survival of a mammal having cancer comprising administering a HDAC class 1 and 2b inhibitor to the mammal in an amount effective to substantially prolong survival of the mammal compared to a mammal that does not receive the HDAC class 1 and 2b inhibitor are provided. In yet another aspect, the mammal survives at least about 21 days after the administering of AR-42 to the mammal.

[0066] In another aspect, administration of AR-42 attenuated cachexia-induced weight loss and skeletal muscle atrophy and prolonged survival in mammals. Without being bound by theory, it is thought that the anti-cachexia effect is associated with the ability of AR-42 to reprogram cell metabolism and to downregulate IL-6 levels in diseased muscle tissues to suppress muscle wasting and other cachexia-related effects independent of AR-42's effects on reducing tumor load.

[0067] In one aspect, the anti-cachexia effects of AR-42 were measured by variety of techniques including qRT-PCT analysis of the expression of established mediators of muscle atrophy in cancer (e.g., Cancer Cell. 2008 Nov 4;14(5):369-81), measurement of the levels of anti-inflammatory cytokines in serum and gastrocnemius muscle tissues (Am J Pathol. 2011 Mar;178(3):1059-68), metabolomic profiling analysis (J Cachexia Sarcopenia Muscle. 2013 Jun;4(2):145-55), measuring the levels of free amino acids in muscle tissue (J Cachexia Sarcopenia Muscle. 2013 Jun;4(2):145-55; Am J Physiol Endocrinol Metab. 2007 Feb;292(2):E501-12), measuring the "glycolytic signature" of cachectic muscle by measuring levels of biochemical associated with the glycolysis pathway (Cachexia Sarcopenia Muscle. 2013 Jun;4(2):145-55), measuring the level of glycogen storage in cachectic muscle tissue (Cell Death Differ. 2012 Oct;19(10):1698-708), analyzing branched-chain amino acid metabolism in cachectic muscle (Int J Biochem Cell Biol. 2013 Oct;45(10):2163-72), and measuring levels of 2-hydroxybutyrate and ophthalmate in cachectic muscle (PLoS One. 2010 May 28;5(5):e10883; Int J Cancer. 2010 Feb 1;126(3):756-63).

Date Reçue/Date Received 2022-02-22

[0068] HDAC inhibitors, as described herein, can be administered to patient in need of treatment (e.g., a patient having cancer and exhibiting symptoms of cachexia). In one aspect, certain cancers are particularly associated with cachexia including, but not limited to pancreatic, gastric, head, neck, and esophageal ("cachexia-associated cancers"). In another aspect, a class 1, 2b HDAC inhibitor (e.g., AR-42) is administered to a patient in need of treatment.

[0069] As used herein, the term "substantially" refers to "most of," a "majority of," or at least 50%, 60%, 70%, 80%, and 90% of the weight or amount of, for example, of a mammal that does not have cancer.

[0070] The terms "treat," "reduce," "suppress," "inhibit," "prevent," or similar terms, as used herein, do not necessarily mean 100% or complete treatment or prevention. Rather, these terms refer to various degrees of treatment or prevention of a particular disease (e.g., 100%, 90%, 80%, 70%, 60%, 50%, 40%, 30%, 20%, 10%, 5%, or 1%) as recognized in the art as being beneficial.

[0071] The terms "treatment" or "prevention" also refer to delaying onset of a disease for a period of time or delaying onset indefinitely. The term "treatment" or "treating" refers to administering a drug or treatment to a patient or prescribing a drug to a patient (e.g., by a doctor, nurse, or other medical professional) where the patient or a third party (e.g., caretaker, family member, or health care professional) administers the drug or treatment. The term "amount effective" refers to an amount of a drug or treatment (e.g., the HDAC class I and IIb inhibitor AR-42) that will treat, reduce, suppress, inhibit, prevent disease(s) or condition(s) (e.g., cachexia) or prolong survival of a mammal with a disease or condition.

[0072] The term "prolong" or "prolonging" as used herein, refers to increasing time of survival of a mammal receiving treatment compared to a mammal that does not receive treatment. In this aspect, "prolonged survival" can refer to increasing the lifespan of the mammal by, for example, 1%, 5%, 10%, 20%, 30%, 40%, 50%, 60%, 70%, 80% or 90% of the lifespan of mammal that does not have cancer.

[0073] Any of the HDAC inhibitors described herein can be administered orally, parenterally (IV, IM, depot-IM, SQ, and depot-SQ), sublingually, intranasally (inhalation), intrathecally, topically, or rectally. Dosage forms known to those of skill in the art are suitable for delivery of the HDAC inhibitors described herein.

Date Reçue/Date Received 2022-02-22

[0074] In one aspect, exemplary HDAC inhibitors are administered in an oral dosage form (e.g., pill, capsule, caplet, or tablet, etc.) to a patient diagnosed with a cancer associated with cachexia (e.g., pancreatic, bladder, gastric, head and neck).

[0075] HDAC inhibitors can be formulated into suitable pharmaceutical preparations such as tablets, capsules, or elixirs for oral administration or in sterile solutions or suspensions for parenteral administration. HDAC inhibitors described herein can be formulated into pharmaceutical compositions using techniques and procedures well known in the art.

[0076] In one aspect, about 0.1 to 1000 mg, about 5 to about 100 mg, or about 10 to about 50 mg of the HDAC inhibitor (e.g., AR-42), or a physiologically acceptable salt or ester can be compounded with a physiologically acceptable vehicle, carrier, excipient, binder, preservative, stabilizer, flavor, etc., in a unit dosage form as called for by accepted pharmaceutical practice. The amount of active substance in compositions or preparations comprising the HDAC inhibitors is such that a suitable dosage in the range indicated is obtained.

[0077] In another aspect, the compositions can be formulated in a unit dosage form, each dosage containing from about 1 to about 500 mg, or about 10 to about 100 mg of the active ingredient. The term "unit dosage from" refers to physically discrete units suitable as unitary dosages for human subjects and other mammals, each unit containing a predetermined quantity of active material calculated to produce the desired therapeutic effect, in association with a suitable pharmaceutical excipient.

[0078] In one aspect, one or more of the HDAC inhibitors are mixed with a suitable pharmaceutically acceptable carrier to form compositions. Upon mixing or addition of the compound(s), the resulting mixture may be a solution, suspension, emulsion, or the like. Liposomal suspensions may also be used as pharmaceutically acceptable carriers. These may be prepared according to methods known to those skilled in the art. The form of the resulting mixture depends upon a number of factors, including the intended mode of administration and the solubility of the compound in the selected carrier or vehicle. In one aspect, the effective concentration is sufficient for lessening or ameliorating at least one symptom of the disease, disorder, or condition treated and may be empirically determined.

Date Reçue/Date Received 2022-02-22

[0079] In yet another aspect, AR-42 suppresses muscle wasting in cachexia as shown in the C-26 and LLC tumor models of cachexia. The pro-inflammatory cytokines, IL-6 and TNF, represent major pro-cachectic factors in the two models (31, 32). Cytokine profile analysis indicated that, while AR-42 had no effect on serum TNF levels in C-26 tumor-bearing mice, it reduced levels of serum IL-6 and intramuscular IL-6Rα mRNA expression. Nonetheless, these AR-42-treated C-26 tumor-bearing mice still exhibited elevated serum IL-6 levels and IL-6Rα mRNA compared to tumor-free mice, suggesting that decreased IL-6 signaling is not solely responsible for AR-42-mediated suppression of muscle wasting.

[0080] Mechanistically, the anti-cachectic effect of AR-42 is unique as the HDAC inhibitors valproic acid and trichostatin-A could not reverse muscle loss in C-26 tumor-bearing mice despite their ability to modulate the myostatin/follistatin axis (33). Similarly, our findings show that, unlike AR-42, vorinostat and romidepsin were ineffective in attenuating cachexia-induced weight loss in the C-26 model. This discrepancy was attributable to the greater ability of AR-42 to suppress the mRNA expression of the E3 ligases Atrogin-1 and MuRF1 in the muscles of tumor-bearing mice, which may reflect differences in their respective abilities to modulate global gene expression in skeletal muscles. Recent evidence suggests a mechanistic link between aberrant acetylation/expression of transcription factors and muscle wasting in diseased muscles, leading to dysregulated expression of cachexia-associated genes [review: (34)]. It was reported that the histone acetyltransferase activity of p300/CBP differentially regulates transcriptional activity and nuclear localization of Foxo family transcription factors in skeletal muscles (35), and that class I HDACs, especially HDAC1, play a crucial role in mediating nutrient deprivation- or muscle disuse-induced muscle atrophy by regulating expression of Foxo and its targets Atrogin-1 and MuRF1 (22).

[0081] RNA-seq analysis revealed the ability of AR-42 to reverse tumor-induced shift in gene expression. A total of 677 genes were identified that were differentially expressed by 4-fold or greater between AR-42- and vehicle-treated tumor-bearing mice. Conceivably, this large number of differentially expressed genes might arise from the effect of AR-42 on the transcriptional activity and/or expression of multiple transcription factors/regulators. In addition to Foxo1, AR-42 also modulated the expression of many other transcription factors/regulators, including C/EBPδ, Fos, Jun-b, DAXX, ERN1, HIF3α, MAFF, MAFK, and Mef2c (Figure 11).

Date Reçue/Date Received 2022-02-22

Among these transcription factors, the importance of Mef2c in the development of skeletal, cardiac, and smooth muscle is well documented (36), and the AP-1 signaling cascade has been implicated in cancer-associated muscle wasting (37).

[0082] It has been proposed that cachectic muscles in C-26 tumor-bearing mice exhibit tumor Warburg physiology, characterized by a high rate of glycolysis (38). Our metabolomic data reveals a pronounced reprogramming of skeletal muscle metabolism in C-26 tumor-bearing mice, which was completely reversed by AR-42. Moreover, the suppressive effect of AR-42 on the production of 2-hydroxybutyrate and opthalmate, biomarkers for insulin resistance (17) and oxidative stress (18), is noteworthy, as substantial evidence has associated insulin resistance (39, 40) and oxidative stress (41) with cachexia.

[0083] Mechanistically, the ability of AR-42 to maintain the integrity of skeletal muscles in tumor-bearing mice arises from its diverse, cumulative effects on tumor-induced changes in multiple transcriptional programs and metabolic phenotype. It is of therapeutic significance that oral administration of AR-42 at a late stage of tumor growth was still effective in slowing down the progression of muscle wasting in C-26 tumor-bearing mice. Together, these findings show that HDAC inhibitors (e.g., AR-42) can be used as part of a comprehensive therapeutic strategy for cancer cachexia, as described herein.

[0084] Pharmaceutical carriers or vehicles suitable for administration of the HDAC inhibitors described herein include any such carriers suitable for the particular mode of administration. In addition, the active materials can also be mixed with other active materials that do not impair the desired action, or with materials that supplement the desired action, or have another action. The compounds may be formulated as the sole pharmaceutically active ingredient in the composition or may be combined with other active ingredients.

[0085] In another aspect, if the HDAC inhibitors exhibit insufficient solubility, methods for solubilizing may be used. Such methods are known and include, but are not limited to, using co-solvents such as dimethylsulfoxide (DMSO), using surfactants such as TWEEN™, and dissolution in aqueous sodium bicarbonate. Derivatives of the compounds, such as salts or prodrugs, may also be used in formulating effective pharmaceutical compositions.

Date Reçue/Date Received 2022-02-22

[0086] The concentration of the compound is effective for delivery of an amount upon administration that lessens or ameliorates at least one symptom of the disorder for which the compound is administered. Typically, the compositions are formulated for single dosage administration.

[0087] In another aspect, the HDAC inhibitors described herein may be prepared with carriers that protect them against rapid elimination from the body, such as time-release formulations or coatings. Such carriers include controlled release formulations, such as, but not limited to, microencapsulated delivery systems. The active compound can be included in the pharmaceutically acceptable carrier in an amount sufficient to exert a therapeutically useful effect in the absence of undesirable side effects on the patient treated. The therapeutically effective concentration may be determined empirically by testing the compounds in known in vitro and in vivo model systems for the treated disorder.

[0088] In another aspect, the HDAC inhibitors and compositions described herein can be enclosed in multiple or single dose containers. The enclosed compounds and compositions can be provided in kits, for example, including component parts that can be assembled for use. For example, AR-42 in lyophilized form and a suitable diluent may be provided as separated components for combination prior to use. A kit may include AR-42 and a second therapeutic agent for co-administration. AR-42 and a second therapeutic agent may be provided as separate component parts. A kit may include a plurality of containers, each container holding one or more unit dose of the compounds described herein. In one aspect, the containers can be adapted for the desired mode of administration, including, but not limited to tablets, gel capsules, sustained-release capsules, and the like for oral administration; depot products, pre-filled syringes, ampoules, vials, and the like for parenteral administration; and patches, medipads, creams, and the like for topical administration.

[0089] The concentration of the exemplary HDAC inhibitor in the pharmaceutical composition will depend on absorption, inactivation, and excretion rates of the active compound, the dosage schedule, and amount administered as well as other factors known to those of skill in the art.

[0090] In another aspect, the active ingredient may be administered at once, or may be divided into a number of smaller doses to be administered at intervals of time. It is understood

Date Reçue/Date Received 2022-02-22

that the precise dosage and duration of treatment is a function of the disease being treated and may be determined empirically using known testing protocols or by extrapolation from in vivo or in vitro test data. It is to be noted that concentrations and dosage values may also vary with the severity of the condition to be alleviated. It is to be further understood that for any particular subject, specific dosage regimens should be adjusted over time according to the individual need and the professional judgment of the person administering or supervising the administration of the compositions, and that the concentration ranges set forth herein are exemplary only and are not intended to limit the scope or practice of the claimed compositions.

[0091] If oral administration is desired, the compound can be provided in a composition that protects it from the acidic environment of the stomach. For example, the composition can be formulated in an enteric coating that maintains its integrity in the stomach and releases the active compound in the intestine. The composition may also be formulated in combination with an antacid or other such ingredient.

[0092] Oral compositions will generally include an inert diluent or an edible carrier and may be compressed into tablets or enclosed in gelatin capsules. For the purpose of oral therapeutic administration, the active compound or compounds can be incorporated with excipients and used in the form of tablets, capsules, or troches. Pharmaceutically compatible binding agents and adjuvant materials can be included as part of the composition.

[0093] The tablets, pills, capsules, troches, and the like can contain any of the following ingredients or compounds of a similar nature: a binder such as, but not limited to, gum tragacanth, acacia, corn starch, or gelatin; an excipient such as microcrystalline cellulose, starch, or lactose; a disintegrating agent such as, but not limited to, alginic acid and corn starch; a lubricant such as, but not limited to, magnesium stearate; a glidant, such as, but not limited to, colloidal silicon dioxide; a sweetening agent such as sucrose or saccharin; and a flavoring agent such as peppermint, methyl salicylate, or fruit flavoring.

[0094] When the dosage unit form is a capsule, it can contain, in addition to material of the above type, a liquid carrier such as fatty oil. In addition, dosage unit forms can contain various other materials, which modify the physical form of the dosage unit, for example, coatings of sugar and other enteric agents. The compounds can also be administered as a component of an elixir, suspension, syrup, wafer, chewing gum or the like. A syrup may contain, in addition to

Date Reçue/Date Received 2022-02-22

the active compounds, sucrose as a sweetening agent and certain preservatives, dyes and colorings, and flavors.

[0095] The active materials can also be mixed with other active materials that do not impair the desired action, or with materials that supplement the desired action. The HDAC inhibitor AR-42 can be used, for example, in combination with an antitumor agent, a hormone, a steroid, or a retinoid. The antitumor agent may be one of numerous chemotherapy agents such as an alkylating agent, an antimetabolite, a hormonal agent, an antibiotic, colchicine, a vinca alkaloid, L-asparaginase, procarbazine, hydroxyurea, mitotane, nitrosoureas or an imidazole carboxamide. Suitable agents include those agents which promote depolarization of tubulin. Examples include colchicine and vinca alkaloids, including vinblastine and vincristine.

[0096] In another aspect, the HDAC inhibitors described herein can be co-administered or administered before or after immunization of a patient with a vaccine to enhance the immune response to the vaccine. In one aspect the vaccine is a DNA vaccine, for example, and HPV vaccine.

[0097] In one aspect, solutions or suspensions used for parenteral, intradermal, subcutaneous, or topical application can include any of the following components: a sterile diluent such as water for injection, saline solution, fixed oil, a naturally occurring vegetable oil such as sesame oil, coconut oil, peanut oil, cottonseed oil, and the like, or a synthetic fatty vehicle such as ethyl oleate, and the like, polyethylene glycol, glycerin, propylene glycol, or other synthetic solvent; antimicrobial agents such as benzyl alcohol and methyl parabens; antioxidants such as ascorbic acid and sodium bisulfite; chelating agents such as ethylenediaminetetraacetic acid (EDTA); buffers such as acetates, citrates, and phosphates; and agents for the adjustment of tonicity such as sodium chloride and dextrose. Parenteral preparations can be enclosed in ampoules, disposable syringes, or multiple dose vials made of glass, plastic, or other suitable material. Buffers, preservatives, antioxidants, and the like can be incorporated as required.

[0098] Where administered intravenously, suitable carriers include, but are not limited to, physiological saline, phosphate buffered saline (PBS), and solutions containing thickening and solubilizing agents such as glucose, polyethylene glycol, polypropyleneglycol, and mixtures thereof. Liposomal suspensions including tissue-targeted liposomes may also be suitable as

Date Reçue/Date Received 2022-02-22

pharmaceutically acceptable carriers. These may be prepared according to methods known in the art.

[0099] In another aspect, the HDAC inhibitors may be prepared with carriers that protect the compound against rapid elimination from the body, such as time-release formulations or coatings. Such carriers include controlled release formulations, such as, but not limited to, implants and microencapsulated delivery systems, and biodegradable, biocompatible polymers such as collagen, ethylene vinyl acetate, polyanhydrides, polyglycolic acid, polyorthoesters, polylactic acid, and the like. Methods for preparation of such formulations are known to those skilled in the art.

[00100] In yet another aspect, compounds employed in the methods of the disclosure may be administered enterally or parenterally. When administered orally, compounds employed in the methods of the disclosure can be administered in usual dosage forms for oral administration as is well known to those skilled in the art. These dosage forms include the usual solid unit dosage forms of tablets and capsules as well as liquid dosage forms such as solutions, suspensions, and elixirs. When the solid dosage forms are used, they can be of the sustained release type so that the compounds employed in the methods described herein need to be administered only once or twice daily.

[00101] The oral dosage forms can be administered to the patient 1, 2, 3, or 4 times daily. The HDAC inhibitor AR-42 described herein can be administered either three or fewer times, or even once or twice daily. Hence, the HDAC inhibitor compound AR-42 employed in the methods of the disclosure be administered in oral dosage form. Whatever oral dosage form is used, they can be designed so as to protect the compounds employed in the methods described herein from the acidic environment of the stomach. Enteric coated tablets are well known to those skilled in the art. In addition, capsules filled with small spheres each coated to protect from the acidic stomach, are also well known to those skilled in the art.

[00102] The terms "therapeutically effective amount" and "therapeutically effective period of time" are used to denote treatments at dosages and for periods of time effective to reduce neoplastic cell growth. As noted above, such administration can be parenteral, oral, sublingual, transdermal, topical, intranasal, or intrarectal. In one aspect, when administered systemically, the therapeutic composition can be administered at a sufficient dosage to attain a blood level of

Date Reçue/Date Received 2022-02-22

the compounds of from about 0.1 μM to about 100 mM. For localized administration, much lower concentrations than this can be effective, and much higher concentrations may be tolerated. One of skill in the art will appreciate that such therapeutic effect resulting in a lower effective concentration of an HDAC inhibitor or AR-42 may vary considerably depending on the tissue, organ, or the particular animal or patient to be treated. It is also understood that while a patient may be started at one dose, that dose may be varied overtime as the patient's condition changes.

[00103] It should be apparent to one skilled in the art that the exact dosage and frequency of administration will depend on the particular compounds employed in the methods of the disclosure administered, the particular condition being treated, the severity of the condition being treated, the age, weight, general physical condition of the particular patient, and other medication the individual may be taking as is well known to administering physicians who are skilled in this art.

EXAMPLES

[00104] The following non-limiting examples illustrate aspects described herein.

[00105] **Example 1**

[00106] Cancer cachexia models

[00107] C-26 model

[00108] In one aspect, tumors were established by subcutaneous injection of C-26 cells (0.5 x 106 cells in 0.1 ml) into the right flank of male CD2F1 mice (approximately 6 weeks of age; Harlan Laboratories, Indianapolis, IN)(11). Tumor-bearing mice, as well as tumor-free mice serving as non-cachectic controls, were randomized into groups that were treated with either AR-42 (50 mg/kg, p.o. by gavage, every other day; Arno Therapeutics, Inc., Flemington, NJ) or vehicle (0.5% methylcellulose (w/v) and 0.1% Tween-80 (v/v) in sterile water) starting 6 days after cell injection. To investigate the effect of delayed treatment, treatments with drug and/or vehicle were started 6, 10 and 12 days after cancer cell injection.

[00109] In another aspect, the effects of AR-42 were compared to other HDAC inhibitors. In this aspect, additional groups of C-26 tumor-bearing mice were treated with vorinostat (50

Date Reçue/Date Received 2022-02-22

mg/kg, p.o., once daily) and romidepsin (0.6 mg/kg; i.p., twice weekly) (ChemieTek (Indianapolis, IN)).

[00110] LLC model

[00111] In another aspect, subcutaneous tumors were established in male C57BL/6 mice (approximately 6 weeks of age; Harlan) by injection of 0.5 x 106 LLC cells into the right flank. Treatment with AR-42 and vehicle was performed as for the C-26 model beginning 6 days after cell injection. In both models, body weights and food consumption were monitored daily and tumor size was measured no less than every two days. Mice were fasted for 2 hours prior to sacrifice, at which time, hind limb muscles, heart, spleen, epididymal fat, and blood were collected and the weights of the solid tissues were measured. Muscle samples were frozen in liquid nitrogen-chilled 2-methylbutane and then stored at -80ºC until analysis.

[00112] **Example 2**

[00113] Grip strength measurement

[00114] Forelimb grip strength was measured in mice using a Digital Grip Strength Meter (Columbus Instruments, Columbus, OH). Five measurements were taken from each mouse, the average of which was designated as the mouse's grip strength.

[00115] Morphometric analysis of muscle fiber size

[00116] Ten-μm sections were cut from frozen skeletal muscle samples using a cryostat (Leica) and then stained with H&E. Images were captured using an Olympus BX51 microscope (Olympus America, Inc.) and muscle fiber cross-sectional areas were determined using Olympus CellSens 1.11 software. Measurements were obtained from five different sections of muscle from each of five mice from each group.

[00117] RNA isolation, qRT-PCR, and RNA-seq analysis

[00118] Total RNA was isolated from homogenized gastrocnemius muscles (n = 3/group) with TRIzol reagent (Life Technologies, Carlsbad, CA) and then purified using the RNAeasy Mini Kit (Qiagen, Valencia, CA). qRT-PCR was performed as described previously (42) by using the Bio-Rad CFX96 Real-Time PCR Detection System with iQ SYBR Green Supermix (Bio-Rad, Hercules, CA). Primer sequences are listed in Table 1. RNA-seq library generation

Date Reçue/Date Received 2022-02-22

and data analysis were performed at The Ohio State University Comprehensive Cancer Center (OSUCCC) Nucleic Acid Shared Resource.

[00119] Metabolomic and cytokine profiling

[00120] Gastrocnemius muscles and sera were collected at day 17 post-cell injection from each treatment group (n = 8/group). Muscle was submitted to Metabolon, Inc. (Durham, NC) for metabolomic analysis of 270 metabolic intermediates via proprietary mass spectrometry platforms. Serum was submitted to Eve Technologies (Alberta, Canada) for analysis of 32 cytokines using a mouse cytokine array (32-plex panel).

[00121] Statistical analysis

[00122] Data analysis was conducted by using SAS 9.3 software (SAS, Inc; Cary, NC). For the experiments with repeated measures, data were analyzed by mixed effect models, incorporating observational dependencies across each subject. For other experiments involving independent groups, data were analyzed by ANOVA. For the time-to-event experiment (Fig. 2B), the difference in survival functions were compared by log-rank tests. Multiplicities were adjusted by Holm's method to control the overall family-wise error rate at 0.05. RNA-seq data were analyzed by using Ingenuity Pathway Analysis (IPA) software (Ingenuity Systems, Redwood City, CA). Only genes with >4-fold change and $P<0.05$ were selected for pathway analysis.

[00123] **Example 3**

[00124] AR-42 suppresses cancer cachexia in the C-26 colon adenocarcinoma model

[00125] In one aspect, mice were treated orally by gavage with AR-42 (50mg/kg) or vehicle every other day starting 6 days after injection C-26 cells, when palpable tumors had formed. While the vehicle group showed a large drop in body weight starting at day 12, AR-42-treated mice maintained their weight at levels comparable to that of tumor-free controls (Fig. 1A, left). By the study endpoint (day 15), the magnitude of the weight loss, after deducting the mass of the tumors ($1cm^3$ volume = 1gram mass), reached >20% for the vehicle-treated group, and 6% for AR-42-treated mice (center). This effect cannot be attributed to decreased tumor burden, since AR-42 did not alter tumor growth relative to vehicle (right), or to increased food intake, since average daily consumption was comparable in the AR-42-treated and vehicle-treated

Date Reçue/Date Received 2022-02-22

groups, and less than that in tumor-free mice (Fig. 1C). The AR-42-treated mice, despite their large tumor burden, were alert, responsive, active, and lacked the hunched posture and rough haircoat observed in vehicle-treated counterparts by the end point of this study (Fig. 1B).

[00126] **Example 4**

[00127] AR-42 protects muscle against cachexia-induced atrophy

[00128] Consistent with the preservation of body weight, skeletal muscle mass was preserved in AR-42-treated tumor-bearing mice. Indicative of cachexia, the weights of gastrocnemius, tibialis anterior and quadriceps from vehicle-treated tumor-bearing (tumor-bearing/vehicle) mice were reduced by 20.6%, 10.5%, and 18.1%, respectively, relative to corresponding muscles from tumor-free control mice, while those in AR-42-treated tumor-bearing (tumor-bearing/AR-42) mice were reduced by 9.6%, 0.8%, and 5.8%, respectively (Fig. 1D).

[00129] Tumor-bearing/vehicle mice exhibited other hallmarks of cachexia, including significant losses of cardiac and, particularly, adipose tissue mass (29.3±6.0% of tumor-free control), which were ameliorated by AR-42 treatment (Fig. 1E, upper). Interestingly, AR-42 significantly reduced the mass of adipose tissue by approximately 50% in tumor-free mice yet restored the loss of adipose tissue mass in tumor-bearing mice to a level comparable to that of tumor-free/AR-42 mice, a dichotomous effect suggesting its ability to maintain lipid homeostasis.

[00130] In another aspect, C-26 tumor-bearing mice exhibited grossly enlarged spleens relative to tumor-free control mice (11), which were not improved by AR-42 (Fig. 1E, lower). As splenomegaly in C-26 tumor-bearing mice results from expansion of myeloid-derived suppressor cells and other immune cells in the spleen (12), this finding suggests AR-42 was acting predominantly on the muscle rather than through an immunologic mechanism.

[00131] The protective effect of AR-42 against muscle wasting was manifested by the abrogation of cachexia-induced reduction in skeletal muscle fiber size. Tumor-bearing/vehicle mice exhibited a 48.2% decrease relative to the tumor-free control in mean cross-sectional area of muscle fibers at day 15 (1297.6±638.8 versus 2503.5±917.5 μm^2), which was restored by AR-42 (2146.3±923.4 μm^2)(Fig. 2A, left). The prominent shift in fiber size distribution to smaller

Date Reçue/Date Received 2022-02-22

cross-sectional area in cachectic muscles of tumor-bearing/vehicle mice was reversed by AR-42 (Fig. 2A, right)

[00132] AR-42 prolongs the survival of C-26 tumor-bearing mice

[00133] The effects of AR-42 were compared to other HDAC inhibitors (i.e., vorinostat and romidepsin) in C-26 tumor-bearing mice. Starting on day 6 after tumor cell injection, mice were treated continuously with AR-42 (50 mg/kg every other day, orally), vorinostat [50 mg/kg once daily, orally (13)], romidepsin [0.6 mg/kg twice weekly, i.p. (14)], or vehicle, until weight loss, as determined by daily body weight measurements and subtraction of tumor mass, reached 20% of starting weight. As shown, oral AR-42 was effective in protecting these mice from tumor-associated wasting, with 100% cumulative survival at day 21 when tumor volume reached the threshold for euthanasia (Fig. 2B). In contrast, vorinostat and romidepsin showed limited or no appreciable protective effects on body weight. Moreover, tumor-bearing/AR-42 mice were alert, responsive, active, and appeared healthy at 21 days after tumor cell injection, in contrast to vehicle- (Day 15), romidepsin- (Day 16), and vorinostat-treated mice (Day 18)(Fig. 2C).

[00134] **Example 5**

[00135] Differential effects on the regulation of skeletal muscle protein turnover

[00136] Skeletal muscle mass is regulated by a balance between protein synthesis and degradation. Without being bound by theory, it is believed that the differential anti-cachectic effect of AR-42 versus vorinostat and romidepsin may be attributable to differences in their ability to regulate pathways governing protein turnover. This was supported by the suppressive effect of AR-42 on the mRNA expression of Atrogin-1/MAFbx and, MuRF1, two E3 ligases involved in ubiquitin-mediated skeletal muscle protein degradation (15, 16) (Fig. 2D).

[00137] qPCR analysis of gastrocnemius muscles revealed a significant increase in Atrogin-1 and MuRF1 mRNA levels (29.4±3.5-fold and 25.8±3.9-fold, respectively) in cachectic muscle (tumor-bearing/vehicle; n=8) relative to the tumor-free/vehicle control (n=6). AR-42 was able to restore expression of Atrogin-1 (2.7±0.7-fold) and MuRF1 (1.1 ± 0.2-fold) mRNA to basal levels (n=8). Vorinostat (n=8) and romidepsin (n=5) also significantly reduced the mRNA expression of these two E3 ligases in cachectic muscles, but to a lesser extent than AR-42

Date Reçue/Date Received 2022-02-22

(Atrogin-1/MuRF1: vorinostat, 9.6±1.8/5.5±1.1-fold; romidepsin, 19.6±3.1/14.6±3.3-fold)(Fig. 2D).

[00138] To confirm that the anti-cachectic activity of AR-42 was not specific to the C-26 model, it was also evaluated in the LLC model. C57BL/6 mice bearing subcutaneous LLC tumors were treated with AR-42 (50 mg/kg, p.o., every other day) starting on day 6 after tumor cell injection, and continuing until day 20 when hind limb muscles were harvested at sacrifice. As shown in Fig. 7, AR-42 protected LLC tumor-bearing C57Bl/6 mice from loss of muscle mass (gastrocnemius: vehicle, 81.7±3.7% of non-cachectic control; AR-42, 92.2±3.5%; tibialis anterior: vehicle, 80.3±4.0%; AR-42, 93.4±3.9%; quadriceps: vehicle, 84.4±4.6%; AR-42, 93.4±4.8%; all *P* values <0.05, n=8).

[00139] **Example 6**

[00140] AR-42 maintains metabolic integrity of muscle in tumor-bearing mice

[00141] With cachexia, skeletal muscles undergo complex metabolic changes in response to tumor/host-derived inflammatory and neuroendocrine stressors (1). Accordingly, we conducted metabolic profiling analysis to investigate the effect of AR-42 on cachexia-induced shifts in metabolic phenotype in skeletal muscle. Tumor-free and C-26 tumor-bearing mice were treated with vehicle or AR-42 as aforementioned, and gastrocnemius muscles were collected at day 17 for metabolomic analysis. Comparison of muscle biochemical profiles among the four groups (n=8/group) revealed the ability of AR-42 to restore cachexia-induced metabolic changes in skeletal muscles, which are summarized as follows.

[00142] **Glycolysis**. Cachectic muscles from tumor-bearing/vehicle mice showed significantly lower levels of glucose and key glycolytic intermediates than tumor-free controls (Fig. 3A). AR-42 reversed these metabolic changes, restoring the intramuscular levels of glucose and intermediates to or, in some cases, above baseline levels detected in tumor-free/vehicle mice. Moreover, elevated glucose was shunted into sorbitol-fructose biosynthesis and pentose phosphate pathways, leading to increased production of sorbitol, fructose, and ribose, a metabolite derived from the pentose phosphate pathway.

[00143] **Glycogen stores**. Muscle from tumor-bearing/vehicle mice showed significant decreases in short-chain malto-oligosaccharides and glucose 1-phosphate (Fig. 3B), suggesting

Date Reçue/Date Received 2022-02-22

the depletion of glycogen stores in cachectic muscles. AR-42 treatment significantly replenished these glycogen metabolic intermediates.

[00144] **Free amino acids**. Consistent with the increased protein degradation that characterizes muscle wasting, a large number of free amino acids were significantly elevated in cachectic muscles from tumor-bearing/vehicle mice relative to that in tumor-free/vehicle mice (Fig. 4), indicative of a cachectic phenotype. Similarly, several amino acid derivatives/metabolites that function as neurotransmitters, including kynurenin, *N*-acetyl-aspartyl-glutamate, and γ-aminobutyrate, were elevated. In contrast, alanine, which is released from muscles to support liver gluconeogenesis, was reduced in cachectic muscles. This cachectic phenotype was reversed by AR-42 treatment, indicating its ability to block muscle protein degradation.

[00145] **Organic acids**. The amino acid metabolites 2-hydroxybutyrate and ophthalmate are biomarkers for insulin resistance (17) and oxidative stress (18), respectively. The increase in these two organic acids in muscles of tumor-bearing/vehicle mice (Fig. 4) suggests that cachexia promotes insulin resistance and oxidative stress, which, in turn, exacerbates muscle wasting. AR-42 dramatically reduced the two biomarkers to levels comparable to those measured in tumor-free mice.

[00146] **Example 7**

[00147] AR-42 suppresses cancer cachexia by targeting multiple pro-cachexia drivers

[00148] To shed light onto the mechanism by which AR-42 mediated its anti-cachectic effect, sera and gastrocnemius muscle from vehicle- or AR-42-treated tumor-free and C-26 tumor-bearing mice were used for cytokine profiling analysis and whole transcriptome shotgun sequencing (RNA-seq), respectively.

[00149] Cytokine profiles. Of 32 cytokines examined (Table 3), IL-6 and leukemia inhibitory factor (LIF), two well-recognized cachexia drivers (19), were significantly increased in the sera of tumor-bearing/vehicle mice relative to that of tumor-free/vehicle mice (IL-6; 230±105 versus 2.9±1.3 pg/ml; LIF, 19.7±9.3 versus 1.7±1.5 pg/ml) (Fig. 5A, upper), while no significant differences were noted with other cytokines. AR-42 reduced IL-6 and LIF levels by 56% and 88%, respectively, in tumor-bearing mice (IL-6, 102±38 pg/ml; LIF, 3.8±1.6 pg/ml)

Date Reçue/Date Received 2022-02-22

compared to the vehicle-treated counterparts. In light of the ability of AR-42 to blunt cachexia-associated increases in IL-6, we examined the effect of AR-42 on intramuscular mRNA levels of IL-6 receptor alpha chain (IL-6Rα). IL-6Rα mRNA was significantly elevated (13±1.4-fold) in muscle of tumor-bearing/vehicle mice (n=9) compared to that of tumor-free mice (n=6). AR-42 reduced this cachexia-induced increase by 85% (2.0±0.2-fold; n=10)(Fig. 5, lower). These findings suggest that AR-42 inhibits muscle wasting, in part, by blocking IL-6 signaling.

[00150] **RNA-seq analysis**. Principal component analysis of the RNA-seq data revealed a pronounced effect of the C-26 tumor on the global gene expression pattern in the muscle of tumor-bearing/vehicle mice relative to tumor-free/vehicle counterparts (Fig. 5B, left). While AR-42 had no appreciable effect on the pattern of gene expression in the non-cachectic muscle of tumor-free mice, it reversed the tumor-induced shift in gene expression in cachectic muscle to a state close to that in tumor-free mice. Pursuant to this, we conducted pairwise analysis of differentially expressed genes between tumor-bearing/vehicle mice and the other three treatment groups, the results of which are represented in a Venn diagram (Fig. 5B, right). The largely overlapping areas among paired analyses suggest that AR-42 restores, to a great extent, tumor-induced changes in global gene expression.

[00151] Pairwise comparison of gene expression in muscles from vehicle- and AR-42-treated tumor-bearing mice revealed a total of 677 genes with 4-fold or greater differential expression (376 upregulated and 301 downregulated) (Table 3). Analysis of these genomic data for their functional and disease associations using Ingenuity Pathway Analysis (IPA) revealed that 66 of these differentially expressed genes were annotated to categories of atrophy, contractility, development, and muscle morphology, and skeletal muscle cell size, muscle cell death, and protein catabolism (Table 4).

[00152] Of these muscle function- and disease-associated genes, the effects of AR-42 on the following six genes are noteworthy in light of their demonstrated links with cancer-induced cachexia. These include *Foxo1* (encoding Forkhead box protein O1) (20-23) and its target genes *Trim63* (MuRF1) and *Fbxo32* (Atrogin-1) (24, 25), *PNPLA2* [adipose triglyceride lipase (ATGL)] (26, 27), *UCP3* (uncoupling protein 3) (28, 29), and *Mef2c* [myogenic transcription factor myocyte enhancer factor] (30) (Fig. 5C). Validation of the RNA-seq data for these six

Date Reçue/Date Received 2022-02-22

genes by qRT-PCR showed a high correlation between the data sets for the relative mRNA expression levels among the four treatment groups (Fig. 5D).

[00153] **Example 8**

[00154] Delayed treatment with AR-42 remains effective in suppressing muscle wasting

[00155] The above findings demonstrate the efficacy of oral AR-42 in suppressing cancer-associated muscle wasting by restoring metabolic and gene expression profiles in skeletal muscle. In those experiments, treatment was initiated early in the progression of cachexia when overt signs of wasting were undetectable. To investigate whether later initiation of AR-42 treatment remains protective against cachexia, C-26 tumor-bearing mice were treated with AR-42 (50 mg/kg, p.o., every other day) starting at 6, 10 and 12 days after tumor cell injection.

[00156] Consistent with our earlier data (Fig. 1), tumor-bearing/vehicle mice lost 19% of body weight (tumor excluded) by day 17. In contrast, treatment with AR-42 starting at day 6 (D6), 10 (D10), or 12 (D12) limited weight loss to 6%, 11%, and 12%, respectively (n=8)(Fig. 6A, left), without appreciable effects on tumor growth (right). Moreover, AR-42-treated mice exhibited signs better health than their vehicle-treated counterparts (Fig. 6B). This protective effect of AR-42 was reflected in the preservation of gastrocnemius weight and, to a lesser extent, that of tibialis anterior and quadriceps muscles (Fig. 6C). Consistent with the protective effect on muscle mass, handgrip dynamometry indicated that AR-42 helped preserve forelimb muscle strength in all drug-treated groups relative to the vehicle-treated control at day 15 and 16 (Fig. 6D).

[00157] **Example 9**

[00158] Tumor-bearing/vehicle mice exhibited other hallmarks of cachexia, including significant losses of cardiac and, particularly, adipose tissue mass (29.3±6.0% of tumor free control), which were ameliorated by AR-42 treatment (Fig. 1E, upper). Interestingly, AR-42 significantly reduced the mass of adipose tissue by approximately 50% in tumor free mice yet restored the loss of adipose tissue mass in tumor-bearing mice to a level comparable to that of tumor-free/AR-42 mice, a dichotomous effect suggesting its ability to maintain lipid homeostasis.

Date Reçue/Date Received 2022-02-22

[00159] C-26 tumor-bearing mice exhibited grossly enlarged spleens relative to tumor-free control mice (11), which was not improved by AR-42 (Fig. 1E, lower). As splenomegaly in C-26 tumor-bearing mice results from expansion of myeloid-derived suppressor cells and other immune cells in the spleen (12), this finding suggests AR-42 was acting predominantly on the muscle rather than through an immunologic mechanism.

[00160] The protective effect of AR-42 against muscle wasting was manifested by the abrogation of cachexia-induced reduction in skeletal muscle fiber size. Tumor-bearing/vehicle mice exhibited a 48.2% decrease relative to the tumor-free control in mean cross-sectional area of muscle fibers at day 15 (1297.6±638.8 versus 2503.5±917.5 μm^2), which was restored by AR-42 (2146.3±923.4 μm^2)(Fig. 2A, left). The prominent shift in fiber size distribution to smaller cross-sectional area in cachectic muscles of tumor-bearing/vehicle mice was reversed by AR-42 (Fig. 2A, right).

[00161] **Example 10**

[00162] Differential effects on the regulation of skeletal muscle protein turnover

[00163] As skeletal muscle mass is regulated by a balance between protein synthesis and degradation, the differential anti-cachectic effect of AR-42 versus vorinostat and romidepsin may be attributable to differences in their ability to regulate pathways governing protein turnover. This was supported by the suppressive effect of AR-42 on the mRNA expression of Atrogin-1/MAFbx and, MuRF1, two E3 ligases involved in ubiquitin-mediated skeletal muscle protein degradation (15, 16) (Fig. 2D). As expected, qPCR analysis of gastrocnemius muscles revealed a significant increase in Atrogin-1 and MuRF1 mRNA levels (29.4±3.5-fold and 25.8±3.9-fold, respectively) in cachectic muscle (tumor-bearing/vehicle; n=8) relative to the tumor-free/vehicle control (n=6). AR-42 was able to restore expression of Atrogin-1 (2.7±0.7-fold) and MuRF1 (1.1 ± 0.2-fold) mRNA to basal levels (n=8). Vorinostat (n=8) and romidepsin (n=5) also significantly reduced the mRNA expression of these two E3 ligases in cachectic muscles, but to a lesser extent than AR-42 (Atrogin-1/MuRF1: vorinostat, 9.6±1.8/5.5±1.1-fold; romidepsin, 19.6±3.1/14.6±3.3-fold) (Fig. 2D).

[00164] **Example 11**

[00165] Cells

Date Reçue/Date Received 2022-02-22

[00166] Cultured C-26 and LLC cells were maintained in fetal bovine serum (FBS)-supplemented (10%) RPMI 1640 medium and DMEM medium (Invitrogen, Carlsbad, CA), respectively, at 37°C in a humidified incubator with 5% CO_2. For injection into mice for cancer cachexia models, cells were harvested by trypsinization, pelleted in the FBS-supplemented culture medium, and then resuspended in sterile PBS at a concentration of 5×10^6 cells/ml.

[00167] Mice

[00168] CD2F1 and C57BL/6 mice were group-housed under conditions of constant photoperiod (12-hour light/12-hour dark), temperature and humidity with *ad libitum* access to water and standard diet. Mice were briefly anesthetized (isoflurane, 3-4%) during administration of drugs (AR-42, vorinostat, vehicle) by oral gavage. Food consumption was estimated by weighing food in each cage daily and dividing the daily decrease in food by the number of mice in the cage. Tumor volumes were calculated from caliper measurements using a standard formula (length x width^2 x $\pi/6$).

[00169] Grip strength measurement

[00170] To measure forelimb grip strength, each mouse was held by the base of its tail and lowered over the apparatus until its forepaws grasped the pull bar. The mouse was then gently pulled horizontally in a straight line away from the grip meter until the mouse released the bar, and the maximum force attained was recorded. Five measurements were taken from each mouse, the average of which was designated as the mouse's grip strength.

[00171] RNA-seq library generation and data analysis pipeline

[00172] RNA quality was assessed on an Agilent 2100 Bioanalyzer using a Pico RNA chip and the input total RNA amount was assessed using Agilent Qubit RNA assay. Transcriptome libraries were prepared using the Illumina TruSeq RNA Sample Preparation Kit V2. The resultant libraries were assessed for quantity and quality using Agilent Qubit DNA assay and with PerkinElmer Labchip DNA GX analysis, respectively. All libraries were mixed in equal proportions generating pools of samples that would yield approximately 40 million passed filter reads when sequenced on Illumina HiSeq 2500 sequencer. The raw sequencing data from the Illumina HiSeq CASAVA pipeline were assessed for quality using FastQC, RNASeQC and RSeQC software. Subsequent analyses were as follows: demultiplexed passed filter sequencing

Date Reçue/Date Received 2022-02-22

reads were aligned to GRCm38/mm10 using TopHat 2 (v2.0.7) RNAseq aligner; CuffLinks 2 (c2.1.1) was used for assembling the aligned reads to UCSC mm10 gene annotation; CuffCompare and CuffMerge was used to compile aligned reads to mm10 genes and merge assembled transcripts into a custom gene annotation; CuffDiff was used to compare differential gene expression associated with each treatment group.

[00173] **Example 12**

[00174] To confirm that the anti-cachectic activity of AR-42 was not specific to the C-26 model, it was also evaluated in the LLC model. C57BL/6 mice bearing subcutaneous 11 LLC tumors were treated with AR-42 (50 mg/kg, p.o., every other day) starting on day 6 after tumor cell injection, and continuing until day 20 when hind limb muscles were harvested at sacrifice.

[00175] As shown in Figure 7, AR-42 protects against cancer-induced muscle wasting in the LLC mouse model of cachexia. Effects of AR-42 versus vehicle on the mass of hindlimb muscles, including gastrocnemius, tibialis anterior, and quadriceps, in both tumor-free and tumor-bearing mice were compared to that of vehicle-treated tumor-bearing mice. Mice were treated in the same manner as described in Fig. 1A, except that mice were sacrificed at day 20 after tumor cell injection. Data are presented as means ± S.D. (n = 8); (gastrocnemius: vehicle, 81.7±3.7% of non-cachectic control; AR-42, 92.2±3.5%; tibialis anterior: vehicle, 80.3±4.0%; AR-42, 93.4±3.9%; quadriceps: vehicle, 84.4±4.6%; AR-42, 93.4±4.8%; all P values <0.05, n=8).

Date Reçue/Date Received 2022-02-22

REFERENCES

[00176] 1. Fearon KC, Glass DJ, Guttridge DC. Cancer cachexia: mediators, signaling, and metabolic pathways. Cell Metab 2012; 16: 153-66.

[00177] 2. Tisdale MJ. Cachexia in cancer patients. Nat Rev Cancer 2002; 2: 862-71.

[00178] 3. von Haehling S, Anker SD. Cachexia as a major underestimated and unmet medical need: facts and numbers. J Cachexia Sarcopenia Muscle 2010; 1: 1-5.

[00179] 4. Tisdale MJ. Mechanisms of cancer cachexia. Physiol Rev 2009; 89: 381-410.

[00180] 5. Lee SJ, Glass DJ. Treating cancer cachexia to treat cancer. Skelet Muscle 2011; 1: 2.

[00181] 6. Maccio A, Madeddu C, Mantovani G. Current pharmacotherapy options for cancer anorexia and cachexia. Expert Opin Pharmacother 2012; 13: 2453-72.

[00182] 7. Kulp SK, Chen CS, Wang DS, Chen CY, Chen CS. Antitumor effects of a novel phenylbutyrate-based histone deacetylase inhibitor, (S)-HDAC-42, in prostate cancer. Clin Cancer Res 2006; 12: 5199-206.

[00183] 8. Lu YS, Kashida Y, Kulp SK, Wang YC, Wang D, Hung JH, et al. Efficacy of a novel histone deacetylase inhibitor in murine models of hepatocellular carcinoma. Hepatology 2007; 46: 1119-30.

[00184] 9. Sargeant AM, Rengel RC, Kulp SK, Klein RD, Clinton SK, Wang YC, et al. OSU-HDAC42, a histone deacetylase inhibitor, blocks prostate tumor progression in the transgenic adenocarcinoma of the mouse prostate model. Cancer Res 2008; 68: 3999-4009.

[00185] 10. Yang YT, Balch C, Kulp SK, Mand MR, Nephew KP, Chen CS. A rationally designed histone deacetylase inhibitor with distinct antitumor activity against ovarian cancer. Neoplasia 2009; 11: 552-63, 3 p following 63.

[00186] 11. Acharyya S, Ladner KJ, Nelsen LL, Damrauer J, Reiser PJ, Swoap S, et al. Cancer cachexia is regulated by selective targeting of skeletal muscle gene products. J Clin Invest 2004; 114: 370-8.

Date Reçue/Date Received 2022-02-22

[00187] 12. Mundy-Bosse BL, Lesinski GB, Jaime-Ramirez AC, Benninger K, Khan M, Kuppusamy P, et al. Myeloid-derived suppressor cell inhibition of the IFN response in tumor-bearing mice. Cancer Res 2011; 71: 5101-10.

[00188] 13. Lucas DM, Alinari L, West DA, Davis ME, Edwards RB, Johnson AJ, et al. The novel deacetylase inhibitor AR-42 demonstrates pre-clinical activity in B-cell malignancies in vitro and in vivo. PLoS One 2010; 5: e10941.

[00189] 14. Sasakawa Y, Naoe Y, Inoue T, Sasakawa T, Matsuo M, Manda T, et al. Effects of FK228, a novel histone deacetylase inhibitor, on human lymphoma U-937 cells in vitro and in vivo. Biochem Pharmacol 2002; 64: 1079-90.

[00190] 15. Bodine SC, Latres E, Baumhueter S, Lai VK, Nunez L, Clarke BA, et al. Identification of ubiquitin ligases required for skeletal muscle atrophy. Science 2001; 294: 1704-8.

[00191] 16. Lecker SH, Jagoe RT, Gilbert A, Gomes M, Baracos V, Bailey J, et al. Multiple types of skeletal muscle atrophy involve a common program of changes in gene expression. FASEB J 2004; 18: 39-51.

[00192] 17. Gall WE, Beebe K, Lawton KA, Adam KP, Mitchell MW, Nakhle PJ, et al. alpha-hydroxybutyrate is an early biomarker of insulin resistance and glucose intolerance in a nondiabetic population. PLoS One 2010; 5: e10883.

[00193] 18. Soga T, Baran R, Suematsu M, Ueno Y, Ikeda S, Sakurakawa T, et al. Differential metabolomics reveals ophthalmic acid as an oxidative stress biomarker indicating hepatic glutathione consumption. J Biol Chem 2006; 281: 16768-76.

[00194] 19. Tisdale MJ. Biology of cachexia. J Natl Cancer Inst 1997; 89: 1763-73.

[00195] 20. Kamei Y, Miura S, Suzuki M, Kai Y, Mizukami J, Taniguchi T, et al. Skeletal muscle FOXO1 (FKHR) transgenic mice have less skeletal muscle mass, down-regulated Type I (slow twitch/red muscle) fiber genes, and impaired glycemic control. J Biol Chem 2004; 279: 41114-23.

Date Reçue/Date Received 2022-02-22

[00196] 21. Reed SA, Sandesara PB, Senf SM, Judge AR. Inhibition of FoxO transcriptional activity prevents muscle fiber atrophy during cachexia and induces hypertrophy. FASEB J 2012; 26: 987-1000.

[00197] 22. Beharry AW, Sandesara PB, Roberts BM, Ferreira LF, Senf SM, Judge AR. HDAC1 activates FoxO and is both sufficient and required for skeletal muscle atrophy. J Cell Sci 2014; 127: 1441-53.

[00198] 23. Sandri M, Sandri C, Gilbert A, Skurk C, Calabria E, Picard A, et al. Foxo transcription factors induce the atrophy-related ubiquitin ligase atrogin-1 and cause skeletal muscle atrophy. Cell 2004; 117: 399-412.

[00199] 24. Gumucio JP, Mendias CL. Atrogin-1, MuRF-1, and sarcopenia. Endocrine 2013; 43: 12-21.

[00200] 25. Bonaldo P, Sandri M. Cellular and molecular mechanisms of muscle atrophy. Dis Model Mech 2013; 6: 25-39.

[00201] 26. Das SK, Hoefler G. The role of triglyceride lipases in cancer associated cachexia. Trends Mol Med 2013; 19: 292-301.

[00202] 27. Young SG, Zechner R. Biochemistry and pathophysiology of intravascular and intracellular lipolysis. Genes Dev 2013; 27: 459-84.

[00203] 28. Collins P, Bing C, McCulloch P, Williams G. Muscle UCP-3 mRNA levels are elevated in weight loss associated with gastrointestinal adenocarcinoma in humans. Br J Cancer 2002; 86: 372-5.

[00204] 29. Constantinou C, Fontes de Oliveira CC, Mintzopoulos D, Busquets S, He J, Kesarwani M, et al. Nuclear magnetic resonance in conjunction with functional genomics suggests mitochondrial dysfunction in a murine model of cancer cachexia. Int J Mol Med 2011; 27: 15-24.

[00205] 30. Shum AM, Mahendradatta T, Taylor RJ, Painter AB, Moore MM, Tsoli M, et al. Disruption of MEF2C signaling and loss of sarcomeric and mitochondrial integrity in cancer-induced skeletal muscle wasting. Aging (Albany NY) 2012; 4: 133-43.

Date Reçue/Date Received 2022-02-22

[00206] 31. Sherry BA, Gelin J, Fong Y, Marano M, Wei H, Cerami A, et al. Anticachectin/tumor necrosis factor-alpha antibodies attenuate development of cachexia in tumor models. FASEB J 1989; 3: 1956-62.

[00207] 32. Strassmann G, Fong M, Kenney JS, Jacob CO. Evidence for the involvement of interleukin 6 in experimental cancer cachexia. J Clin Invest 1992; 89: 1681-4.

[00208] 33. Bonetto A, Penna F, Minero VG, Reffo P, Bonelli G, Baccino FM, et al. Deacetylase inhibitors modulate the myostatin/follistatin axis without improving cachexia in tumor-bearing mice. Curr Cancer Drug Targets 2009; 9: 608-16.

[00209] 34. Alamdari N, Aversa Z, Castillero E, Hasselgren PO. Acetylation and deacetylation--novel factors in muscle wasting. Metabolism 2013; 62: 1-11.

[00210] 35. Senf SM, Sandesara PB, Reed SA, Judge AR. p300 Acetyltransferase activity differentially regulates the localization and activity of the FOXO homologues in skeletal muscle. Am J Physiol Cell Physiol 2011; 300: C1490-501.

[00211] 36. Black BL, Olson EN. Transcriptional control of muscle development by myocyte enhancer factor-2 (MEF2) proteins. Annu Rev Cell Dev Biol 1998; 14: 167-96.

[00212] 37. Moore-Carrasco R, Garcia-Martinez C, Busquets S, Ametller E, Barreiro E, Lopez-Soriano FJ, et al. The AP-1/CJUN signaling cascade is involved in muscle differentiation: implications in muscle wasting during cancer cachexia. FEBS Lett 2006; 580: 691-6.

[00213] 38. Der-Torossian H, Wysong A, Shadfar S, Willis MS, McDunn J, Couch ME. Metabolic derangements in the gastrocnemius and the effect of Compound A therapy in a murine model of cancer cachexia. J Cachexia Sarcopenia Muscle 2013; 4: 145-55.

[00214] 39. Asp ML, Tian M, Wendel AA, Belury MA. Evidence for the contribution of insulin resistance to the development of cachexia in tumor-bearing mice. Int J Cancer 2010; 126: 756-63.

[00215] 40. Honors MA, Kinzig KP. The role of insulin resistance in the development of muscle wasting during cancer cachexia. J Cachexia Sarcopenia Muscle 2012; 3: 5-11.

Date Reçue/Date Received 2022-02-22

[00216] 41. Moylan JS, Reid MB. Oxidative stress, chronic disease, and muscle wasting. Muscle Nerve 2007; 35: 411-29.

[00217] 42. Chu PC, Kulp SK, Chen CS. Insulin-like growth factor-I receptor is suppressed through transcriptional repression and mRNA destabilization by a novel energy restriction-mimetic agent. Carcinogenesis 2013; 34: 2694-705.

[00218] Although the above description refers to particular aspects, it is to be understood that these aspects are merely illustrative. It will be apparent to those skilled in the art that various modifications and variations can be made to the methods described herein. Thus, it is intended that the present description include modifications and variations that are within the scope of the appended claims and their equivalents.

Date Reçue/Date Received 2022-02-22

CLAIMS

What is claimed is:

1. Histone deacetyl-transferase (HDAC) class 1 and 2b inhibitor for use in prolonging survival of a mammal having cancer, wherein the HDAC class 1 and 2b inhibitor is used to substantially prolong survival of the mammal compared to a mammal that does not receive the HDAC class 1 and 2b inhibitor.

2. Histone deacetyl-transferase (HDAC) class 1 and 2b inhibitor for use in the manufacture of a medicament useful for prolonging survival of a mammal having cancer, wherein the medicament is useful for substantially prolonging survival of the mammal compared to a mammal that does not receive the medicament.

3. The use of claim 1 or 2, wherein the HDAC class 1 and 2b inhibitor is AR-42.

4. The use of claim 3, wherein the mammal survives at least about 21 days after an administration of AR-42 to the mammal.

Date Reçue/Date Received 2022-02-22

Figure 1A

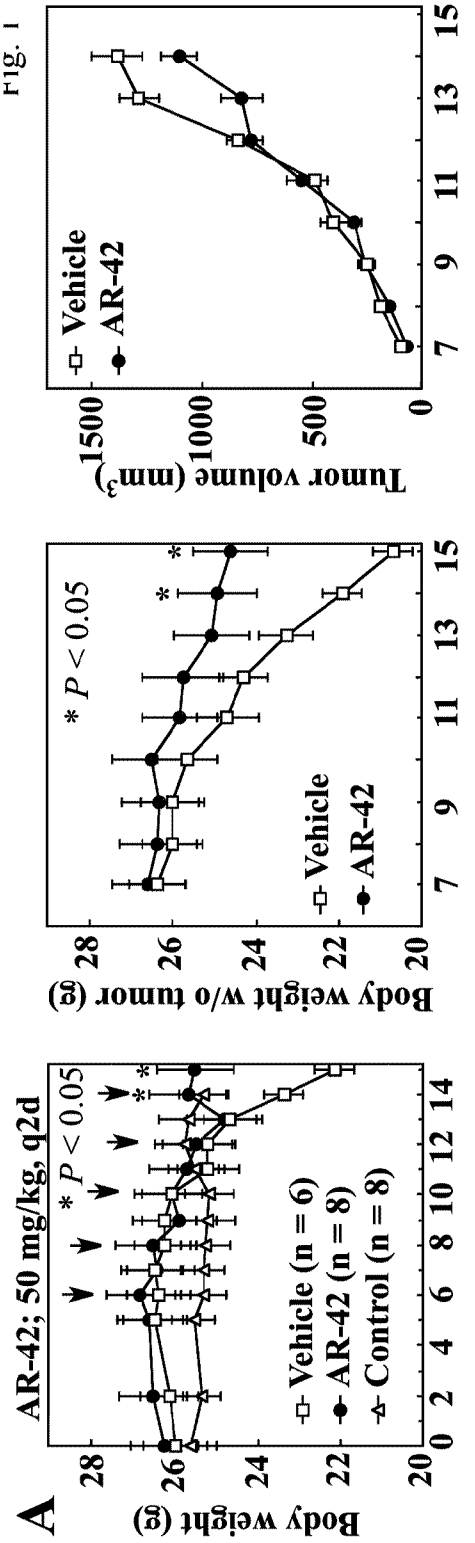
Fig. 1
A
Body weight (g)
AR-42; 50 mg/kg, q2d
* P < 0.05
Vehicle (n = 6)
AR-42 (n = 8)
Control (n = 8)
Body weight w/o tumor (g)
* P < 0.05
Vehicle
AR-42
Tumor volume (mm3)
Vehicle
AR-42

Figure 1B

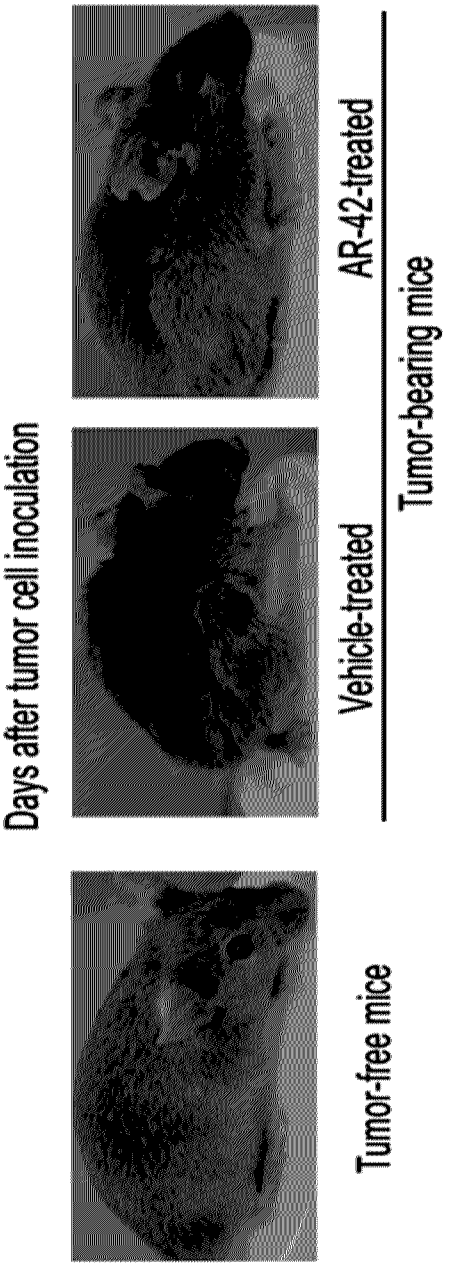
Days after tumor cell inoculation
Tumor-free mice
Vehicle-treated
AR-42-treated
Tumor-bearing mice

Figure 1C

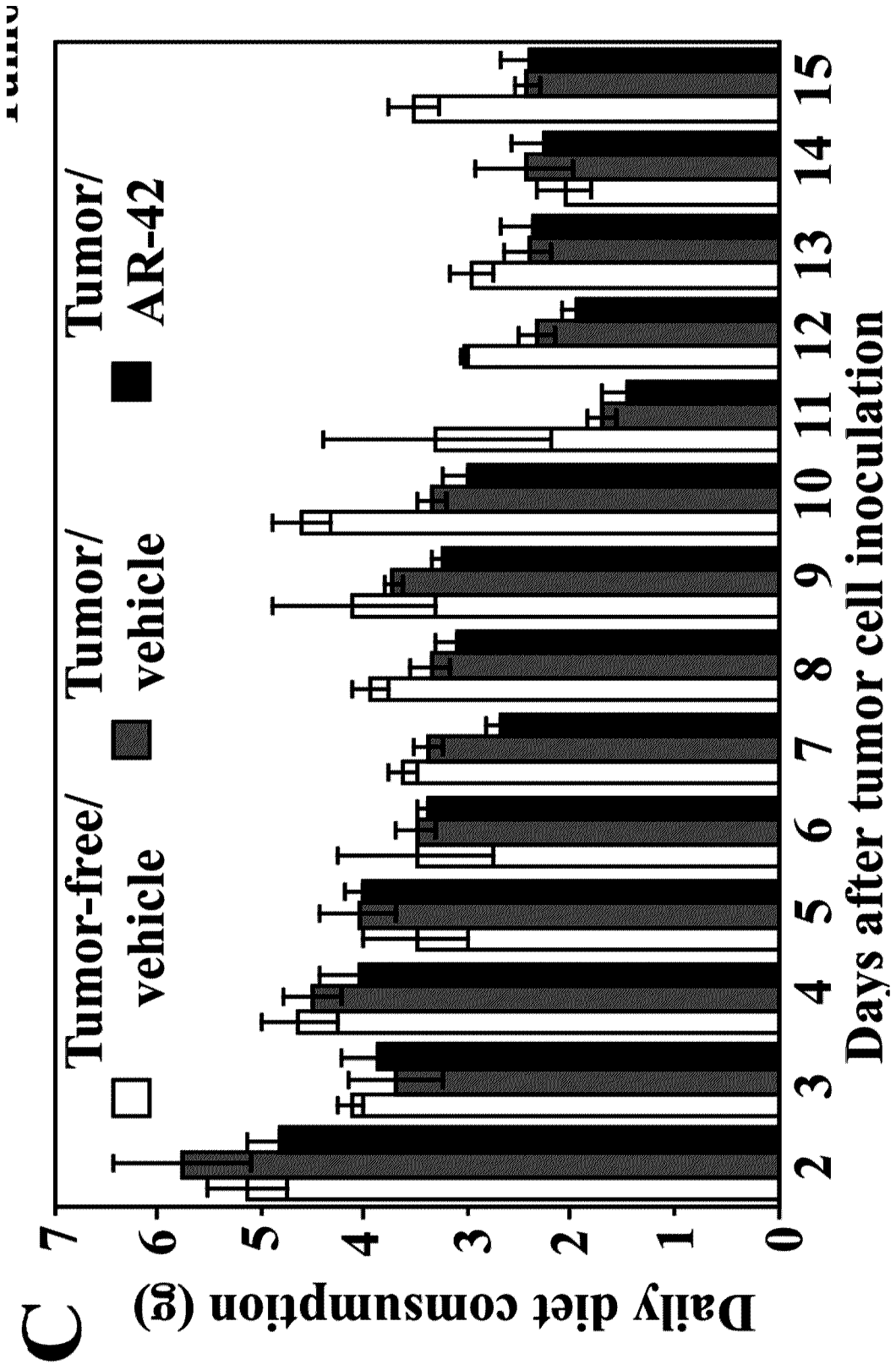

Date Reçue/Date Received 2022-02-22

Figure 1D

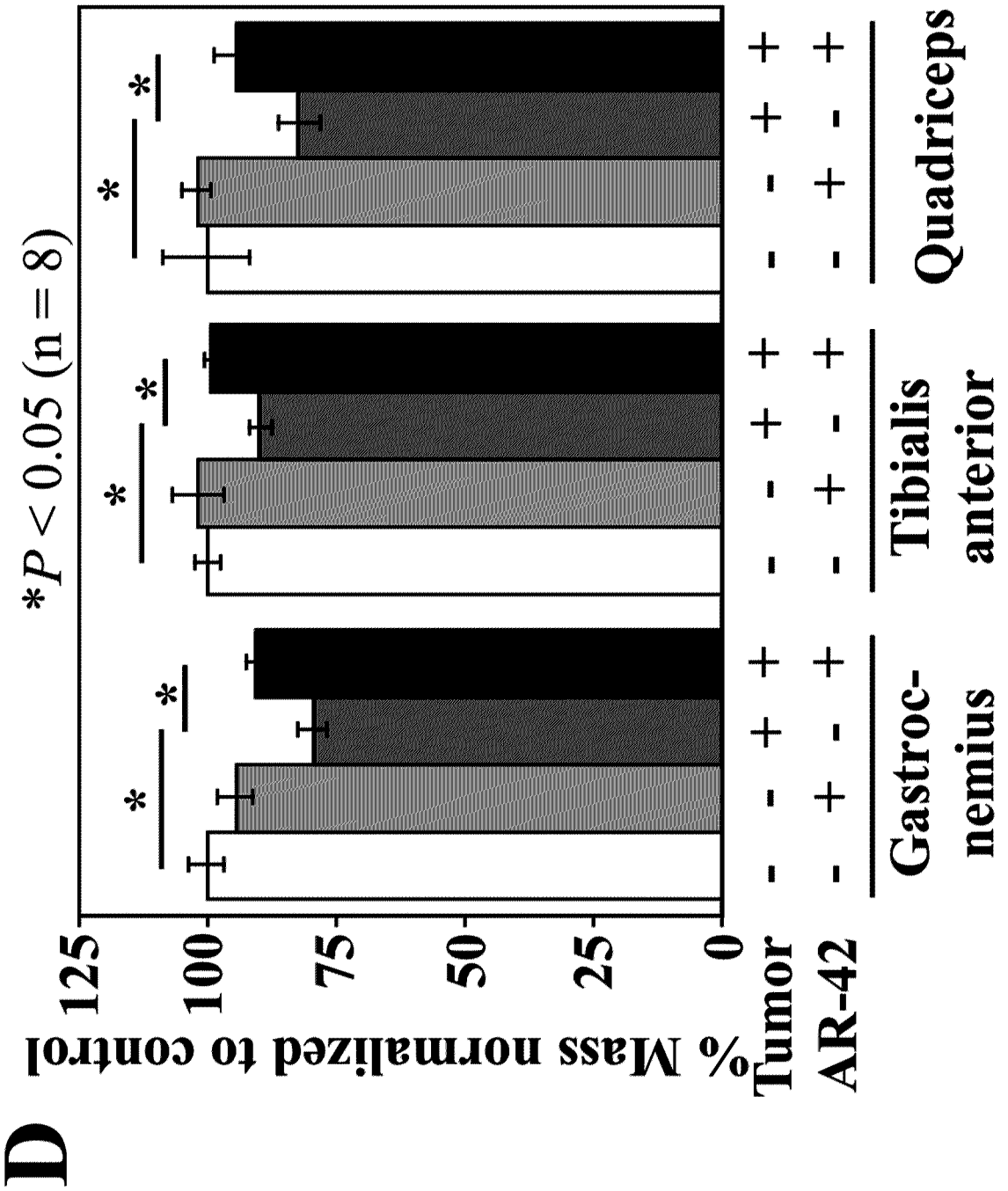

Date Reçue/Date Received 2022-02-22

Figure 1E

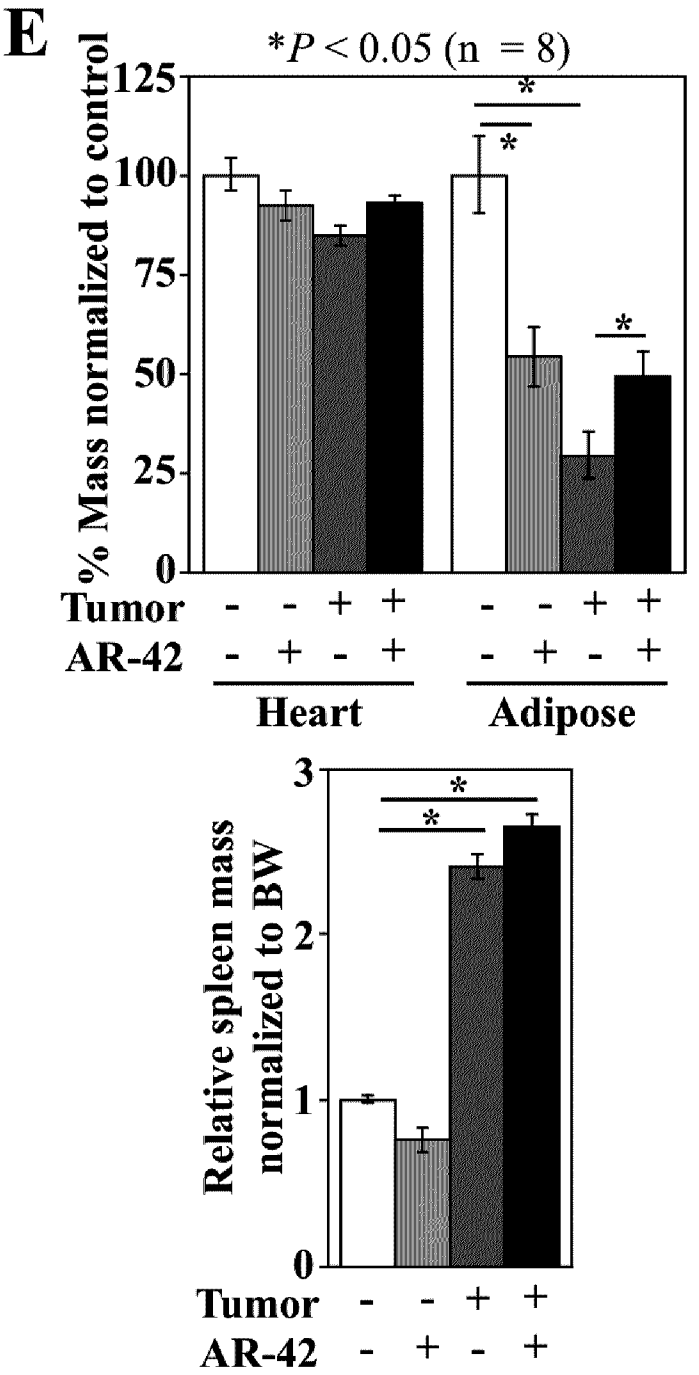
E
*P < 0.05 (n = 8)
% Mass normalized to control
125
100
75
50
25
0
*
*
*
Tumor - - + + - - + +
AR-42 - + - + - + - +
Heart
Adipose
Relative spleen mass normalized to BW
3
2
1
0
*
*
Tumor - - + +
AR-42 - + - +

Figure 2A

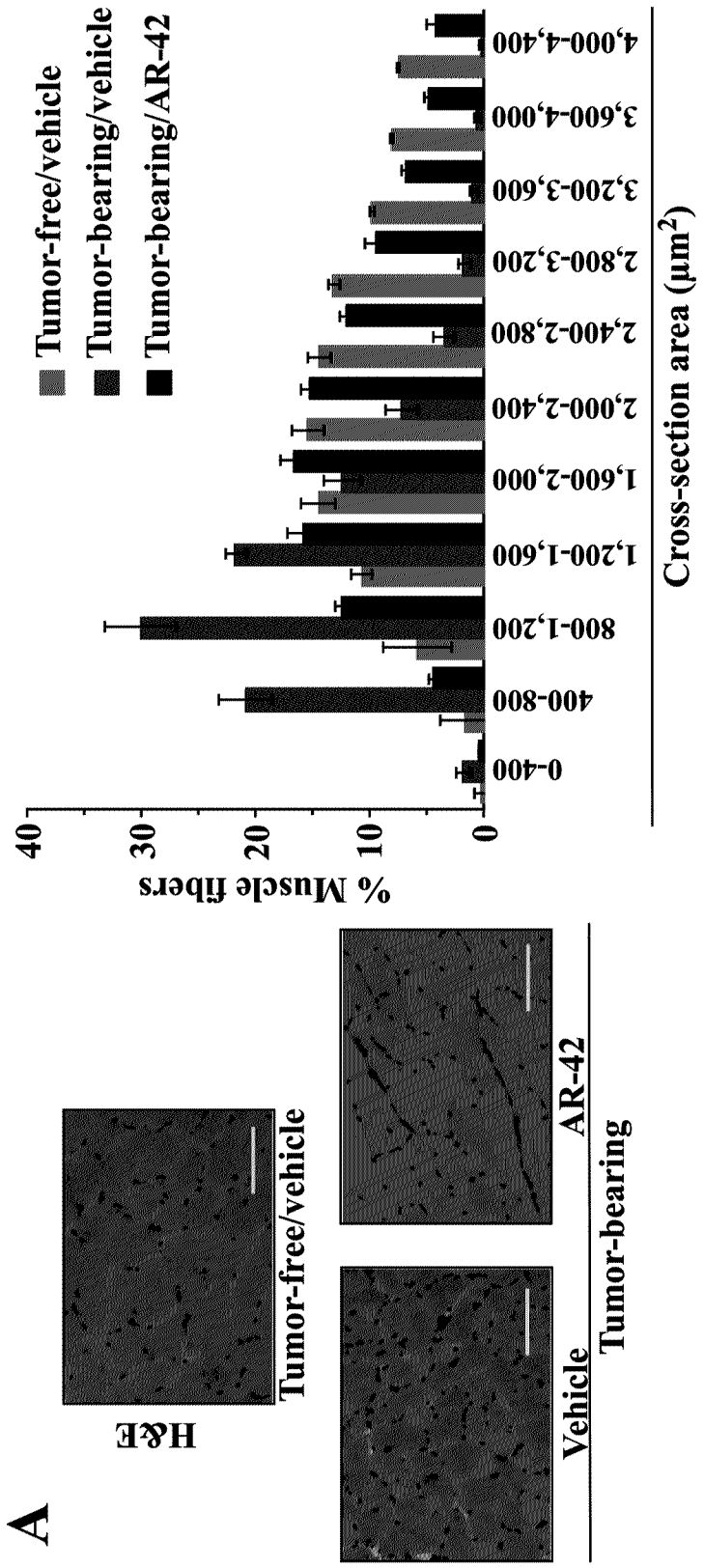
A
H&E
Tumor-free/vehicle
Vehicle
AR-42
Tumor-bearing
Tumor-free/vehicle
Tumor-bearing/vehicle
Tumor-bearing/AR-42
% Muscle fibers
0
10
20
30
40
0-400
400-800
800-1,200
1,200-1,600
1,600-2,000
2,000-2,400
2,400-2,800
2,800-3,200
3,200-3,600
3,600-4,000
4,000-4,400
Cross-section area (μm2)

Figure 2B

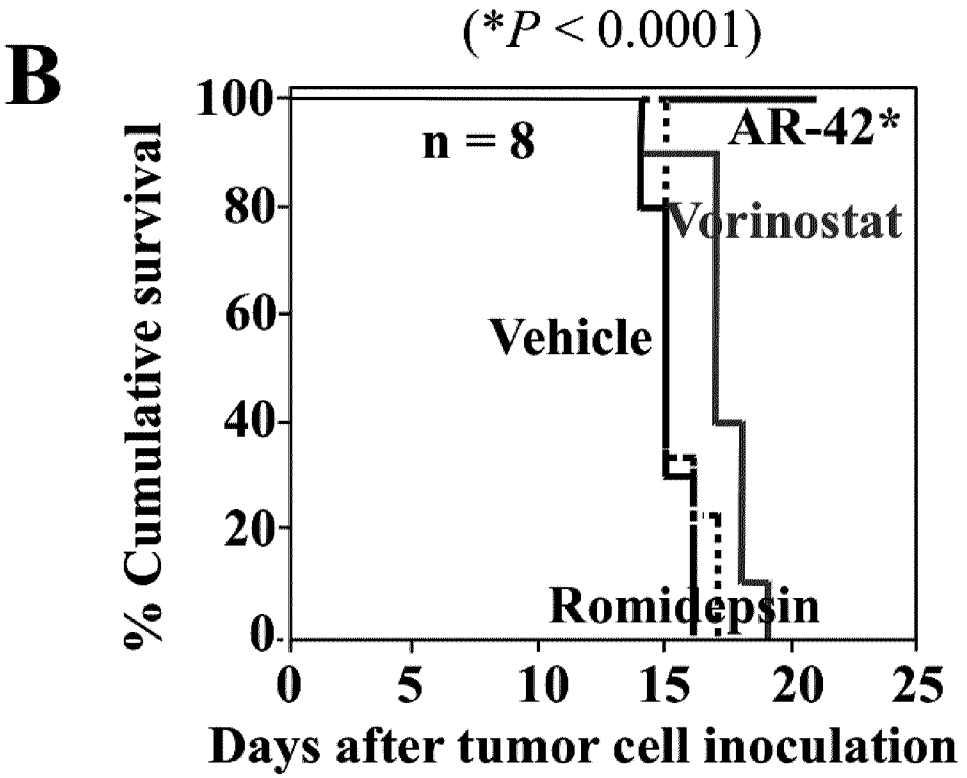

Date Reçue/Date Received 2022-02-22

Figure 2C

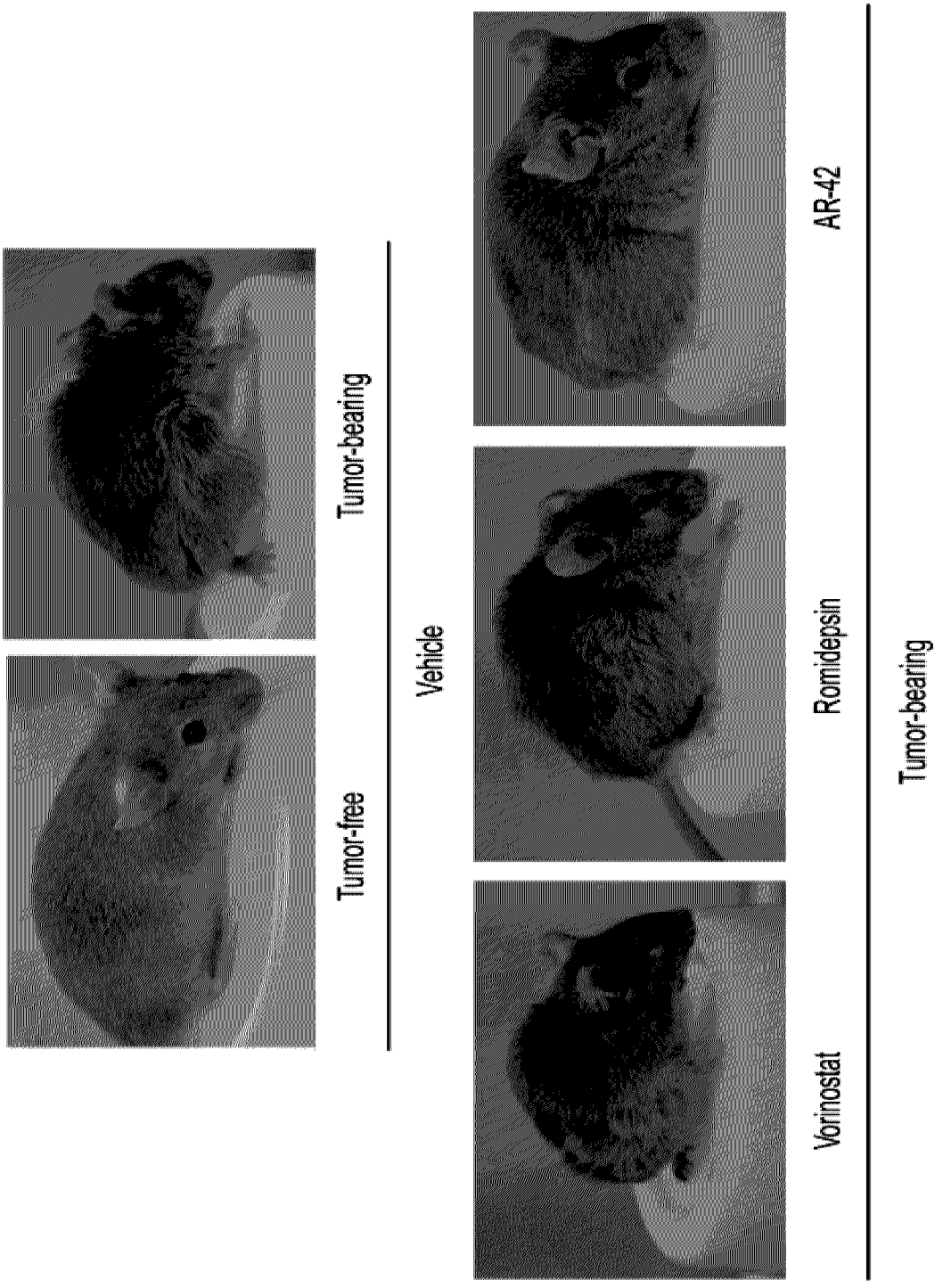
Tumor-bearing
Tumor-free
Vehicle
AR-42
Romidepsin
Vorinostat
Tumor-bearing

Figure 2D

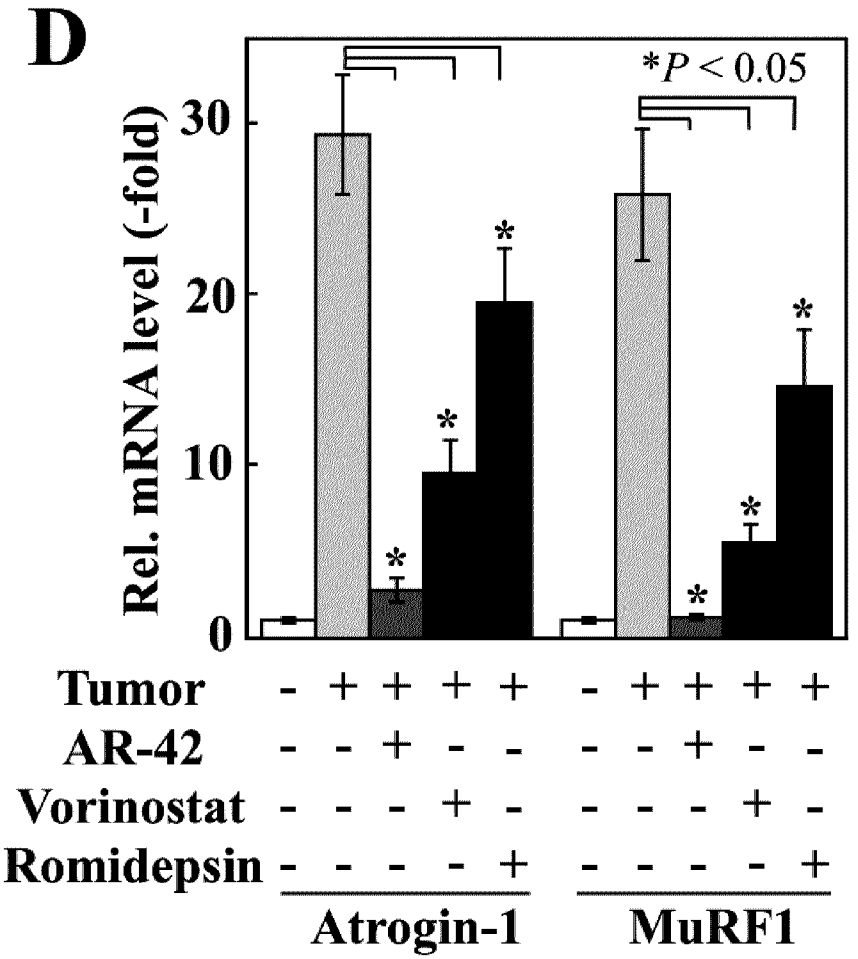
D
*P < 0.05
Rel. mRNA level (-fold)
30
20
10
0
Tumor - + + + + - + + + +
AR-42 - - + - - - - + - -
Vorinostat - - - + - - - - + -
Romidepsin - - - - + - - - - +
Atrogin-1
MuRF1

Figure 3

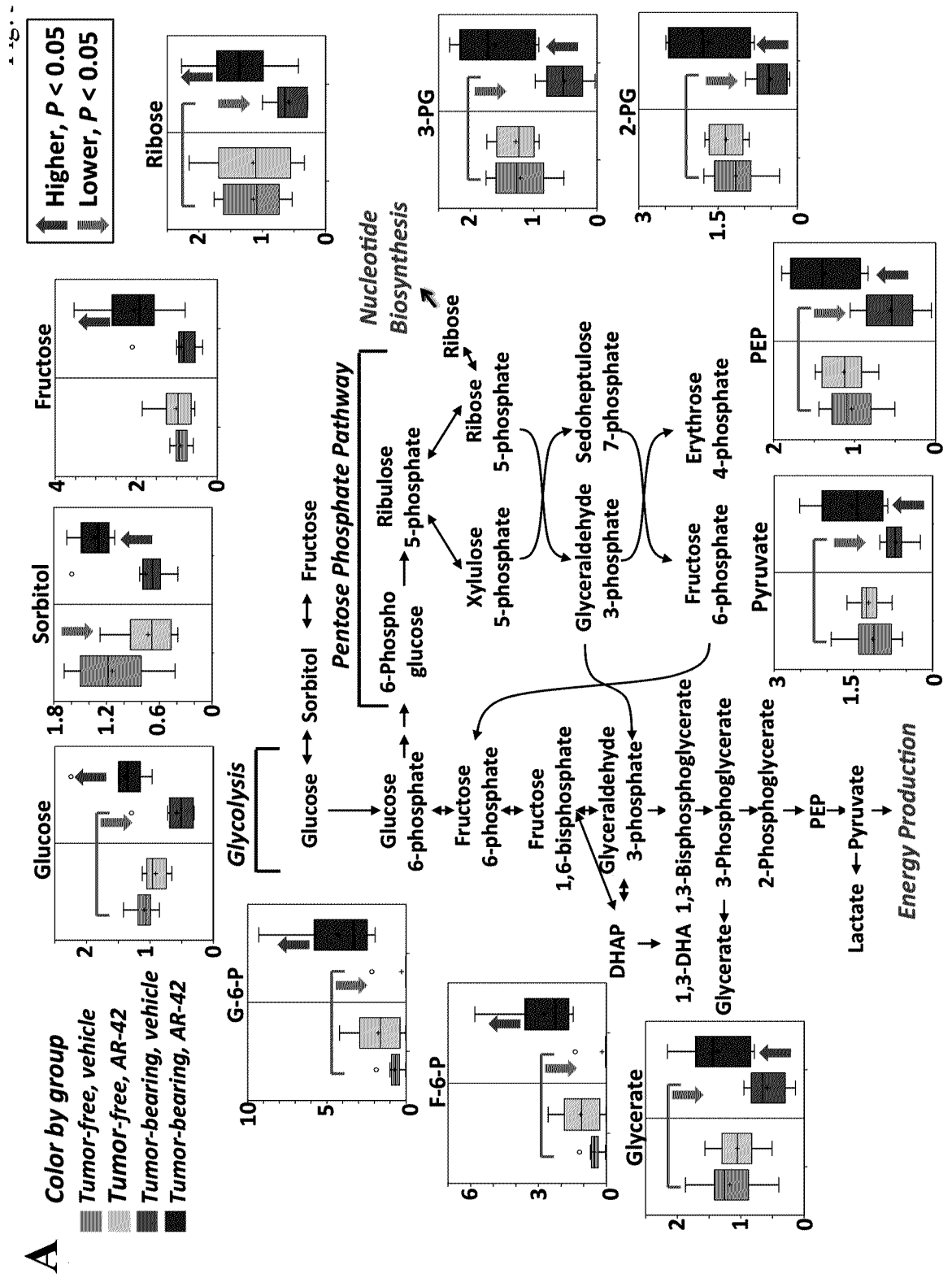
A
Color by group
Tumor-free, vehicle
Tumor-free, AR-42
Tumor-bearing, vehicle
Tumor-bearing, AR-42
Higher, P < 0.05
Lower, P < 0.05
Glucose
Sorbitol
Fructose
Ribose
3-PG
2-PG
PEP
Pyruvate
G-6-P
F-6-P
Glycerate
Glycolysis
Glucose
Sorbitol
Fructose
Pentose Phosphate Pathway
Nucleotide Biosynthesis
6-Phospho glucose
Ribulose 5-phosphate
Ribose
Ribose 5-phosphate
Xylulose 5-phosphate
Sedoheptulose 7-phosphate
Glyceraldehyde 3-phosphate
Erythrose 4-phosphate
Fructose 6-phosphate
Glucose 6-phosphate
Fructose 6-phosphate
Fructose 1,6-bisphosphate
Glyceraldehyde 3-phosphate
DHAP
1,3-DHA
1,3-Bisphosphoglycerate
Glycerate
3-Phosphoglycerate
2-Phosphoglycerate
PEP
Lactate
Pyruvate
Energy Production

Figure 3B

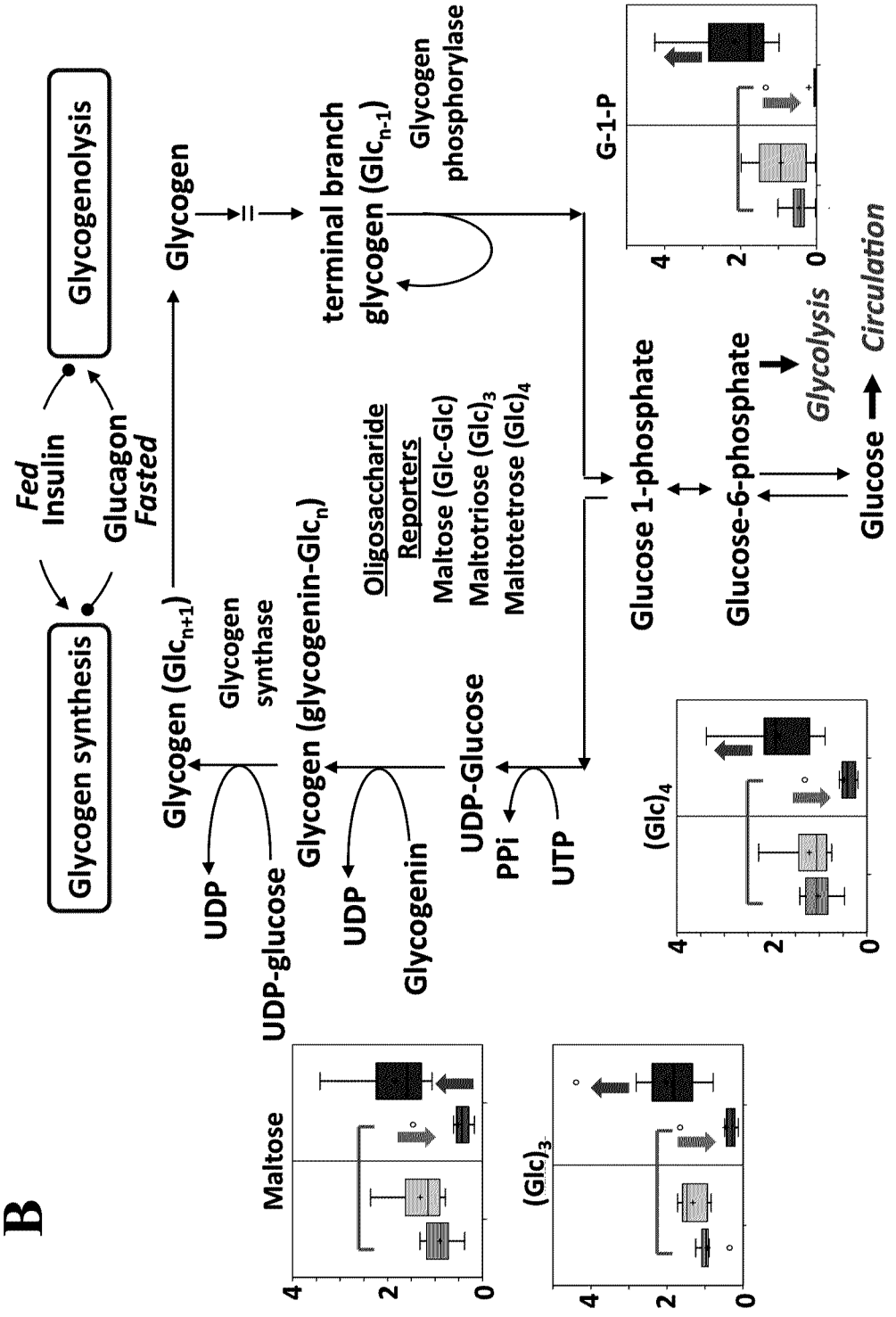
B
Glycogenolysis
Glycogen synthesis
Fed
Insulin
Glucagon
Fasted
Glycogen
terminal branch
glycogen (Glc$_{n-1}$)
Glycogen
phosphorylase
G-1-P
Glycogen (Glc$_{n+1}$)
Glycogen
synthase
Glycogen (glycogenin-Glc$_n$)
Oligosaccharide
Reporters
Maltose (Glc-Glc)
Maltotriose (Glc)$_3$
Maltotetrose (Glc)$_4$
Glucose 1-phosphate
Glucose-6-phosphate
Glycolysis
Glucose
Circulation
UDP
UDP-glucose
UDP
Glycogenin
UDP-Glucose
PPi
UTP
Maltose
(Glc)$_3$
(Glc)$_4$
4
2
0

Figure 4

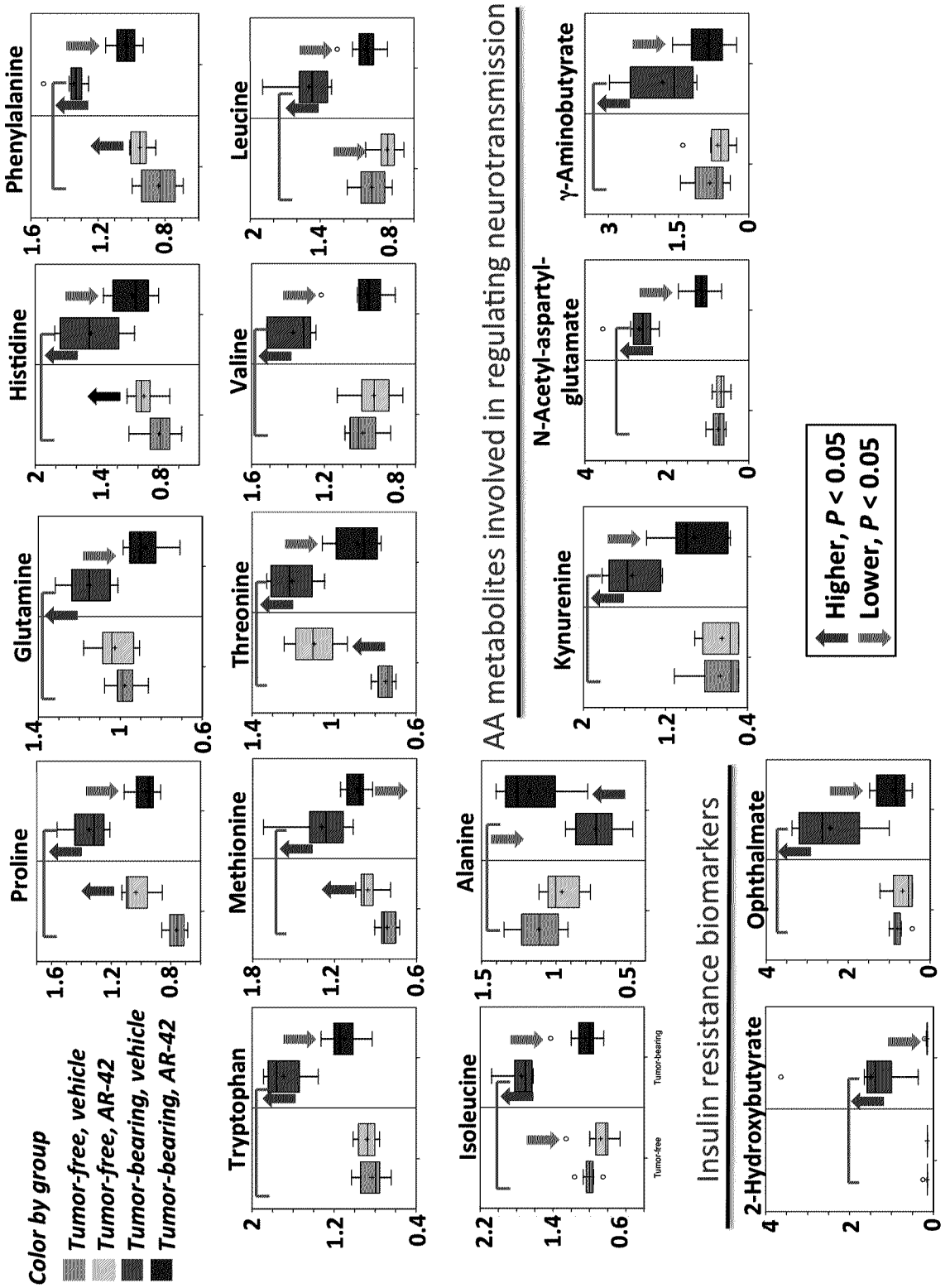
Color by group
Tumor-free, vehicle
Tumor-free, AR-42
Tumor-bearing, vehicle
Tumor-bearing, AR-42
Proline
Glutamine
Histidine
Phenylalanine
Tryptophan
Methionine
Valine
Leucine
Isoleucine
Alanine
Threonine
Kynurenine
N-Acetyl-aspartyl-glutamate
γ-Aminobutyrate
AA metabolites involved in regulating neurotransmission
Insulin resistance biomarkers
2-Hydroxybutyrate
Ophthalmate
Tumor-free
Tumor-bearing
Higher, P < 0.05
Lower, P < 0.05

Figure 5A

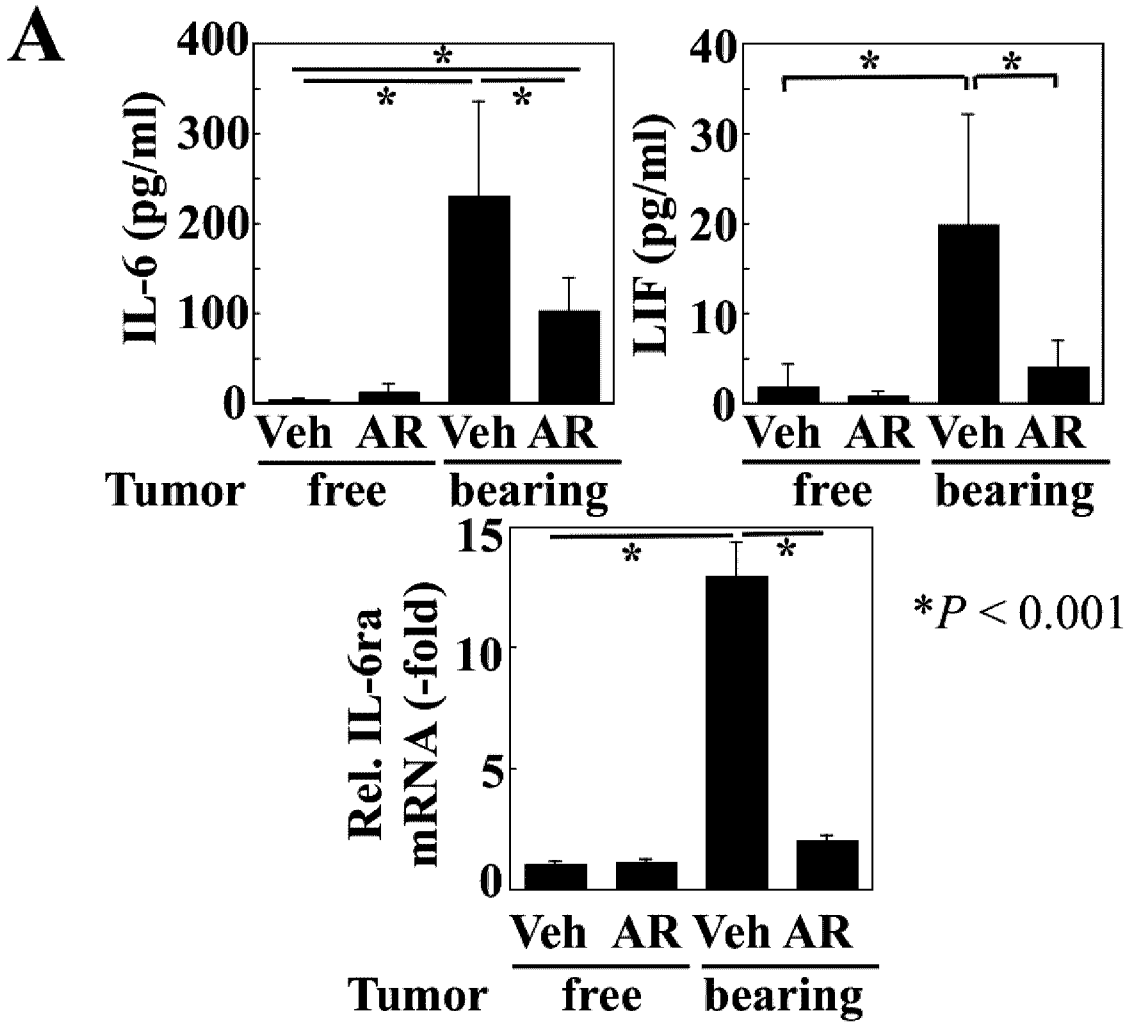
A
IL-6 (pg/ml)
400
300
200
100
0
LIF (pg/ml)
40
30
20
10
0
Rel. IL-6ra mRNA (-fold)
15
10
5
0
*
Veh AR Veh AR
Tumor free bearing
*P < 0.001

Figure 5B

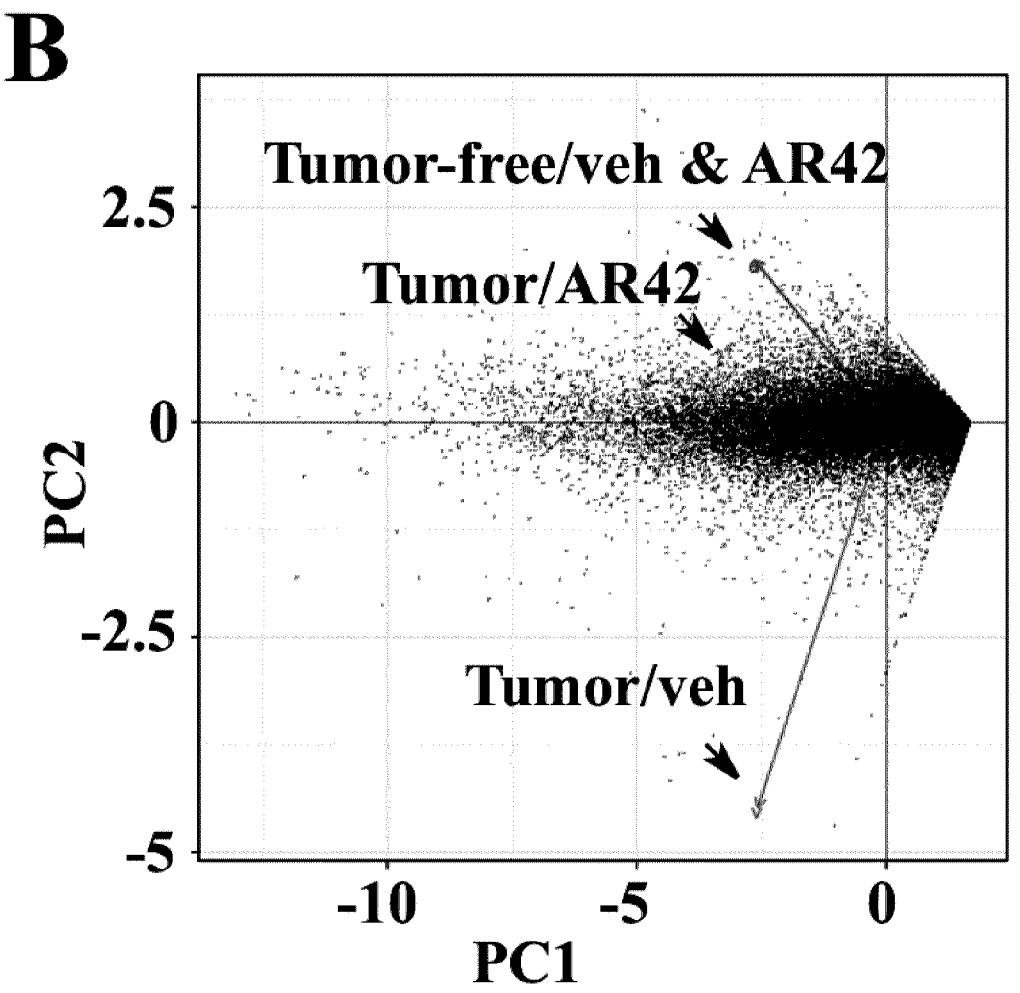

Date Reçue/Date Received 2022-02-22

Figure 5C

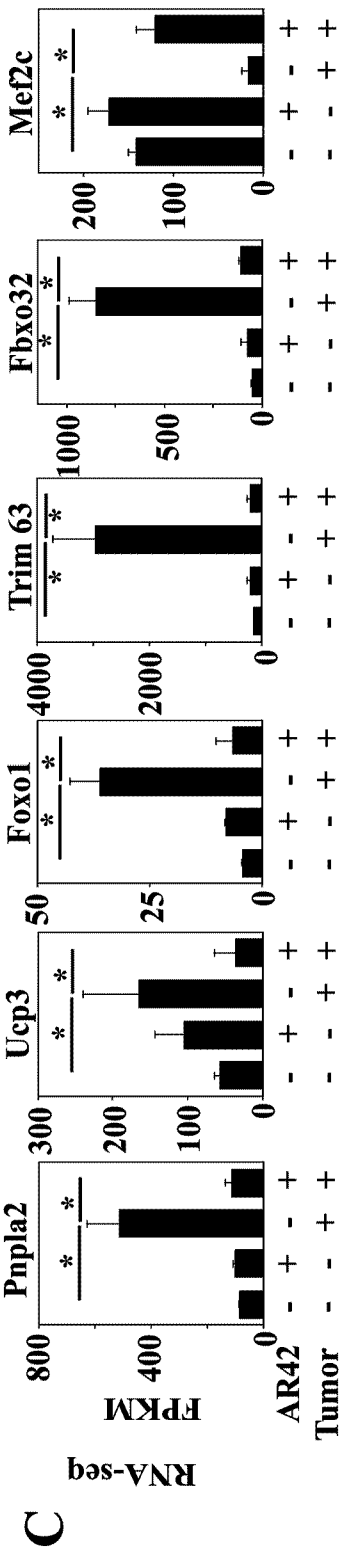

Date Reçue/Date Received 2022-02-22

Figure 5D

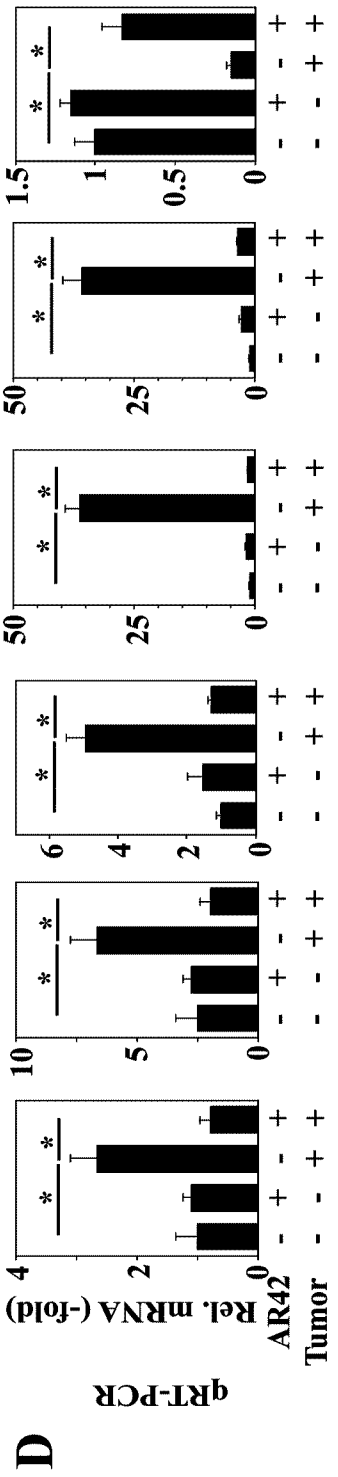

Date Reçue/Date Received 2022-02-22

Figure 6A

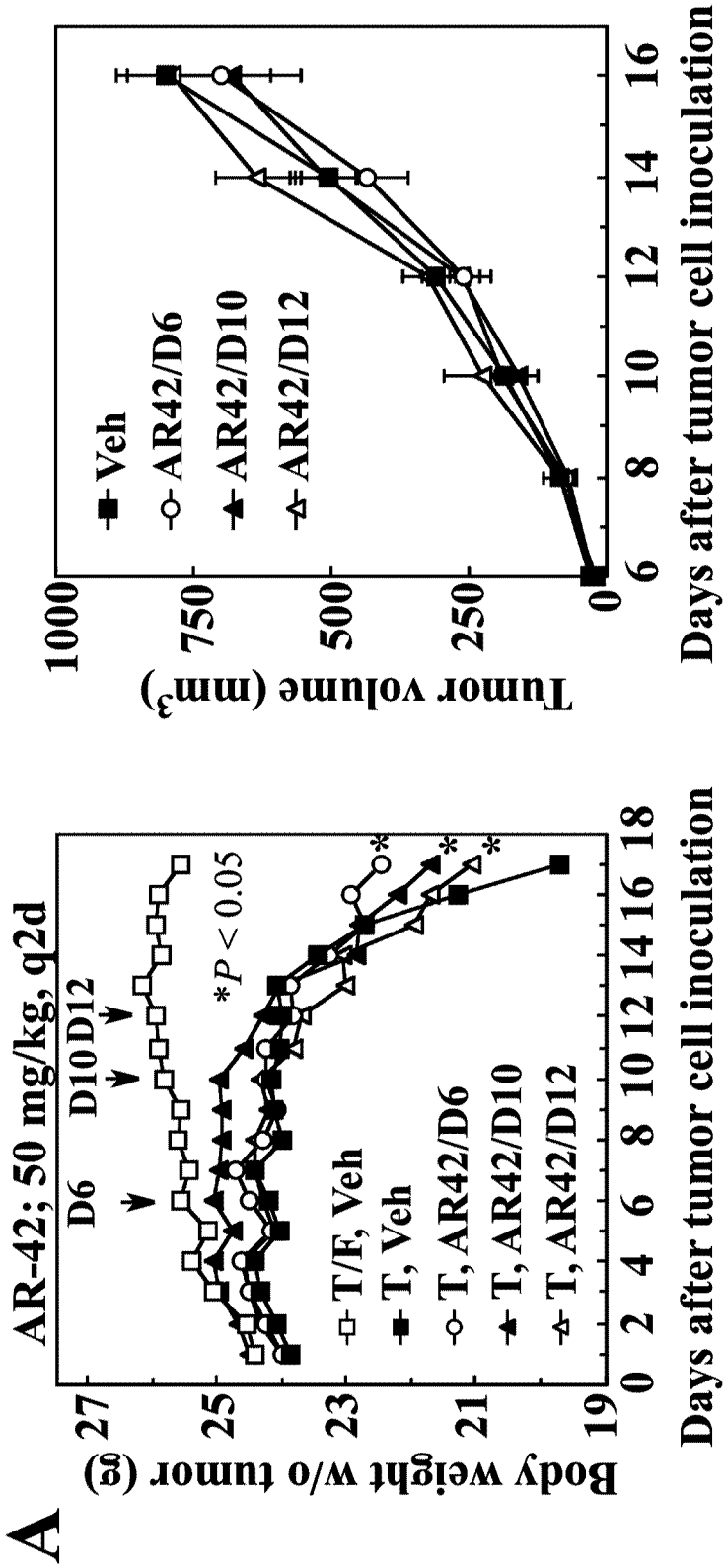
A
AR-42; 50 mg/kg, q2d
D6
D10
D12
*P < 0.05
T/F, Veh
T, Veh
T, AR42/D6
T, AR42/D10
T, AR42/D12
Body weight w/o tumor (g)
Days after tumor cell inoculation
Veh
AR42/D6
AR42/D10
AR42/D12
Tumor volume (mm3)
Days after tumor cell inoculation

Figure 6B

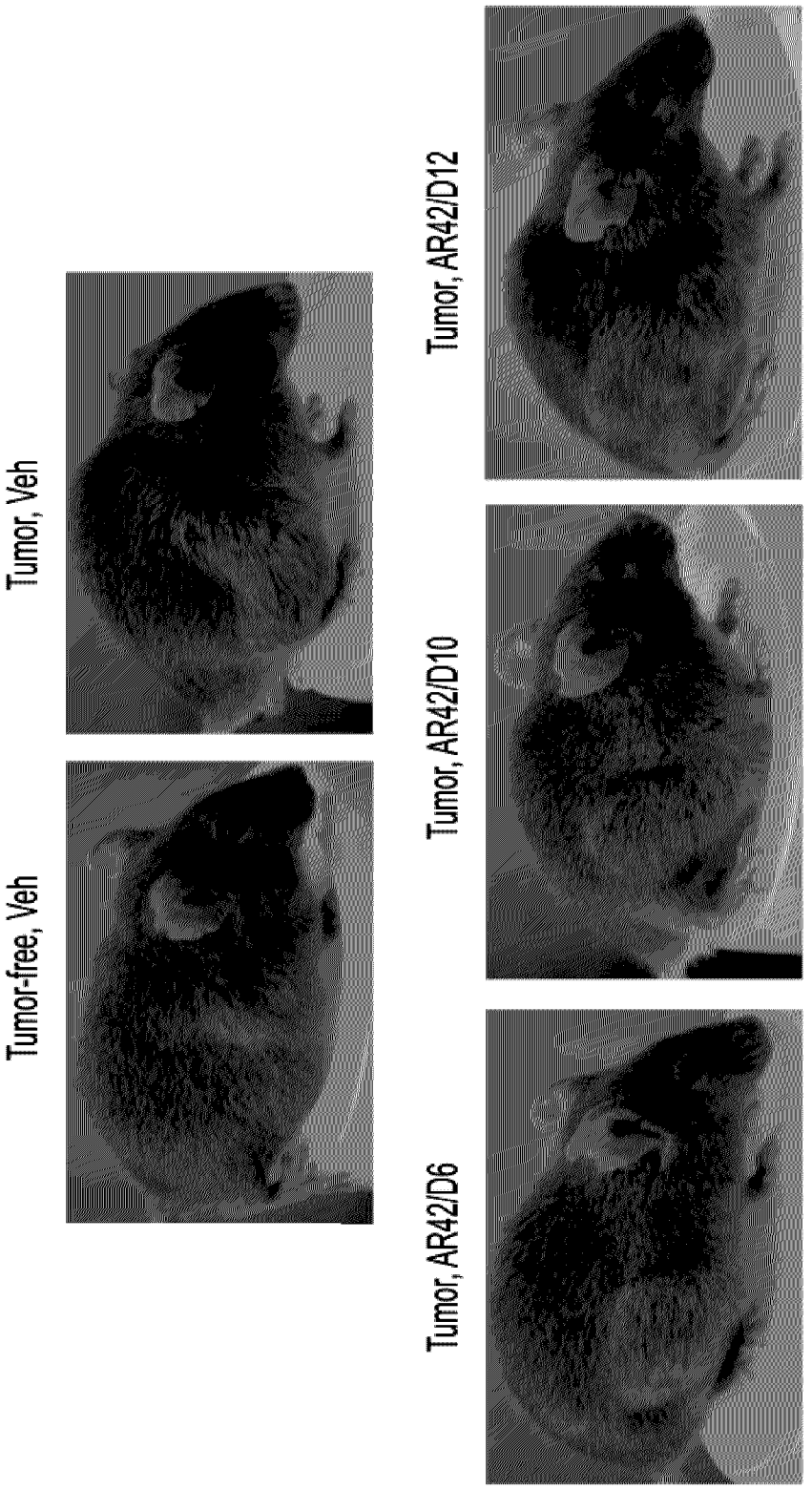

Date Reçue/Date Received 2022-02-22

Figure 6C

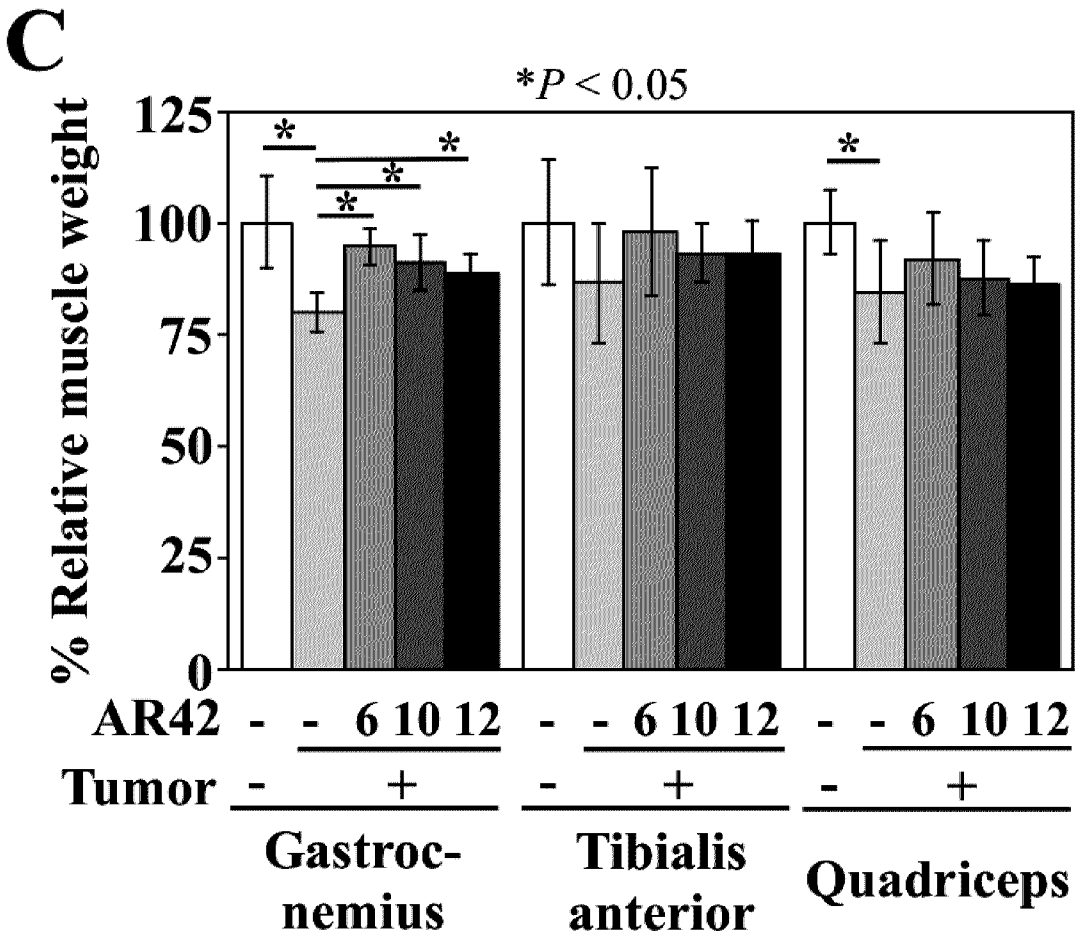

Date Reçue/Date Received 2022-02-22

Figure 6D

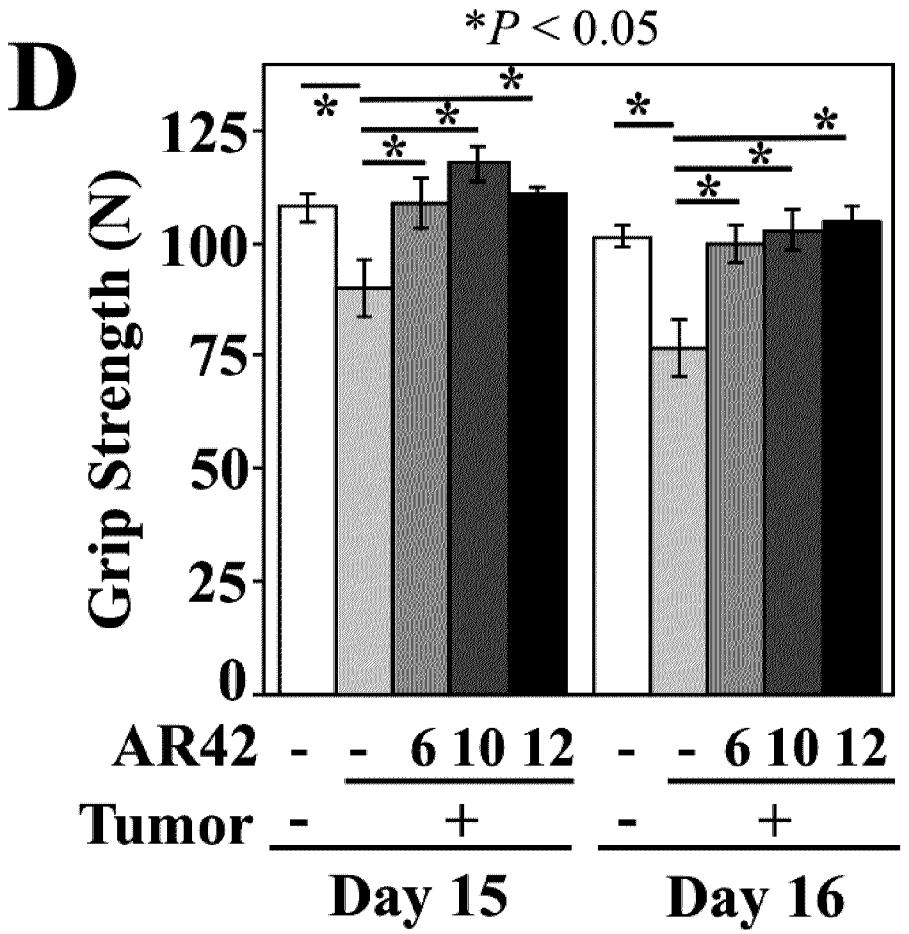

Date Reçue/Date Received 2022-02-22

Figure 7

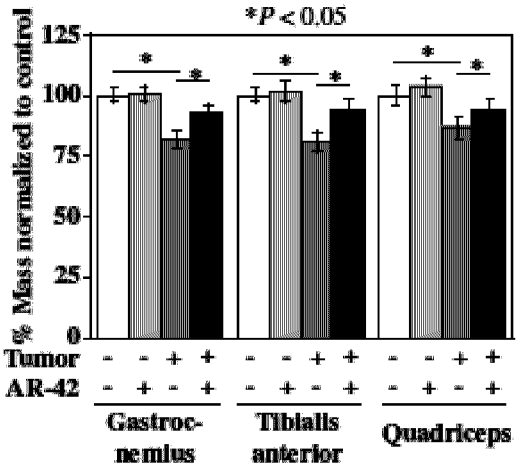

Date Reçue/Date Received 2022-02-22